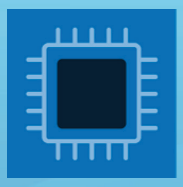

computer sciences and mathematics forum

The 5th Mexican Workshop on Fractional Calculus

Edited by

Jorge M. Cruz-Duarte and Porfirio Toledo-Hernández

Printed Edition of the Proceedings Published in Computer *Sciences & Mathematics Forum*

www.mdpi.com/journal/csmf

MDPI

The 5th Mexican Workshop on Fractional Calculus

The 5th Mexican Workshop on Fractional Calculus

Editors

Jorge Mario Cruz-Duarte
Porfirio Toledo-Hernández

MDPI • Basel • Beijing • Wuhan • Barcelona • Belgrade • Manchester • Tokyo • Cluj • Tianjin

Editors
Jorge Mario Cruz-Duarte
Tecnólogico de Monterrey
México

Porfirio Toledo-Hernández
University of Veracruz
México

Editorial Office
MDPI
St. Alban-Anlage 66
4052 Basel, Switzerland

This is a reprint of Proceedings published online in the open access journal *Computer Sciences & Mathematics Forum* (ISSN 2813-0324) (available at: https://www.mdpi.com/2813-0324/4/1).

For citation purposes, cite each article independently as indicated on the article page online and as indicated below:

LastName, A.A.; LastName, B.B.; LastName, C.C. Article Title. *Journal Name* **Year**, *Volume Number*, Page Range.

ISBN 978-3-0365-6694-8 (Hbk)
ISBN 978-3-0365-6695-5 (PDF)

Contents

About the Editors

Jorge M. Cruz-Duarte

Jorge M. Cruz-Duarte (PhD) is a research professor (since 2021) in the Research Group on Advanced Artificial Intelligence at the Tecnológico de Monterrey (TEC) and a member of the Mexican National System of Researchers (SNI-CONACyT), IEEE, the Mexican Mathematical Society (SMM), and the Mexican Academy in Computer Sciences (AMEXCOMP). Jorge received his B.Sc. and M.Sc. degrees in Electronic Engineering from the Universidad Industrial de Santander (UIS) and his Ph.D. in Electrical Engineering from the Universidad de Guanajuato (UGto). He was on a Short Research Stay at the University POLITEHNICA of Bucharest (UPB). From 2019 to 2021, he was on a Postdoctoral Stay at TEC in collaboration with the Chinese Academy of Sciences (CAS). His research interests include automatic algorithm design, heuristic methods, data science, optimization, mathematical methods, thermodynamics, digital signal processing, electronic thermal management, and fractional calculus.

Porfirio Toledo-Hernández

Porfirio Toledo-Hernández (Ph.D.) is a professor in the Faculty of Mathematics at the University of Veracruz. He is a member of the Mexican National System of Researchers (SNI-CONACyT) and the Mexican Mathematical Society (SMM). Porfirio obtained his Ph.D. in basic mathematics at the Center for Research in Mathematics (CIMAT) in 2011. He has developed research work in mathematical modeling and optimization in topics such as game theory, differential equations, dynamical systems, biological models, and behavior analysis.

Preface to ”The 5th Mexican Workshop on Fractional Calculus”

The Mexican Workshop on Fractional Calculus (MWFC), which originated in the Irapuato-Salamanca Campus Engineering Division of the University of Guanajuato in 2012, has an international scope. Its main objective is to present the latest theoretical advances and applications of fractional calculus to different areas of Science and Engineering. It is also an opportunity for free scientific discussion among young people and experts. Indisputable personalities in the area of fractional calculus have participated in these workshops and have stimulated young scientists. The workshops are aimed at high-level and postgraduate students, as well as young researchers and consolidated researchers. These workshops are held every two years at different universities around the country.

Prefaced by
Prof. J. Juan Rosales-García
Department of Electrical Engineering, DICIS-UG

computer sciences and mathematics forum

MDPI

Editorial

Fractional Calculus in Mexico: The 5th Mexican Workshop on Fractional Calculus (MWFC) †

Jorge M. Cruz-Duarte [1,*] and Porfirio Toledo-Hernández [2]

[1] School of Engineering and Sciences, Tecnologico de Monterrey, Av. Eugenio Garza Sada 2501, Col. Tecnológico, Monterrey 64849, Nuevo León, Mexico
[2] Faculty of Mathematics, University of Veracruz, Paseo 112, Sección 2 S/N, Col. Nuevo Xalapa, Xalapa-Enríquez 91097, Veracruz, Mexico
* Correspondence: jorge.cruz@tec.mx
† All the papers in this proceedings volume were Presented at the 5th Mexican Workshop on Fractional Calculus (MWFC), Monterrey, Mexico, 5–7 October 2022.

The Mexican Workshop on Fractional Calculus (MWFC) is a bi-annual international workshop and the largest Latin American technical event in the field of fractional calculus in Mexico. The focus of MWFC is to motivate critical discussions of ideas about abstract and non-integer operators, chaotic systems, complex behavior, and their applications in several areas. MWFC offers an ideal forum for intellectuals and curious people to present their latest research insights. In its 5th version, MWFC was held in Monterrey, one of the most influential cities in México and home of the Tecnológico de Monterrey (TEC), where MWFC was hosted in a hybrid format. During the 5th MWFC, we attended six plenary talks from distinguished international scientists, as well as two tutorials, a poster session, and four panels of accepted papers.

In submitting conference proceedings to *Computer Sciences and Mathematics Forum*, we certify to the publisher that all papers published in this volume have been subjected to peer review administered by the volume editors. Expert referees conducted reviews to the professional and scientific standards expected of a proceedings journal.

- Type of peer review: Double-blind.
- Conference submission management system: EasyChair via https://www.easychair.org/conferences/overview?a=29473298 (accessed on 10 November 2022).
- Number of submissions sent for review: 22.
- Number of submissions accepted: 16 submissions were accepted to be presented at the 5th MWFC, and 8 of those 16 submissions were considered for inclusion in this conference proceedings and encouraged to submit to MDPI for publication; 2 of those 8 manuscripts were withdrawn by the authors.
- Acceptance rate (number of submissions accepted/number of submissions received): ∼73% for the submissions presented at the 5th MWFC; ∼36% for the submissions considered to be in this conference proceedings and encouraged to further submit to MDPI for publication.
- Average number of reviews per paper: 2.
- Total number of reviewers involved: 16.
- Any additional information on the review process: The average number of papers assigned to each reviewer was about 2–3 to ensure review quality.

Conflicts of Interest: The authors declare no conflict of interest.

Disclaimer/Publisher's Note: The statements, opinions and data contained in all publications are solely those of the individual author(s) and contributor(s) and not of MDPI and/or the editor(s). MDPI and/or the editor(s) disclaim responsibility for any injury to people or property resulting from any ideas, methods, instructions or products referred to in the content.

Citation: Cruz-Duarte, J.M.; Toledo-Hernández, P. Fractional Calculus in Mexico: The 5th Mexican Workshop on Fractional Calculus (MWFC). *Comput. Sci. Math. Forum* **2022**, *4*, 4007. https://doi.org/10.3390/cmsf2022004007

Published: 3 February 2023

computer sciences and mathematics forum

MDPI

Proceeding Paper

Further Remarks on Irrational Systems and Their Applications †

Adrián-Josué Guel-Cortez [1,*], César-Fernando Méndez-Barrios [2], Diego Torres-García [2] and Liliana Félix [2]

[1] Centre for Fluid and Complex Systems, Coventry University, Coventry CV1 5FB, UK
[2] Faculty of Engineering, Autonomous University of San Luis Potosi, San Luis Potosi 78210, Mexico
* Correspondence: adrianjguelc@gmail.com
† Presented at the 5th Mexican Workshop on Fractional Calculus (MWFC), Monterrey, Mexico, 5–7 October 2022.

Abstract: Irrational Systems (ISs) are transfer functions that include terms with irrational exponents. Since such systems are ubiquitous and can be seen when solving partial differential equations, fractional-order differential equations, or non-linear differential equations; their nature seems to be strongly linked with a low-order description of distributed parameter systems. This makes ISs an appealing option for model-reduction applications and controls. In this work, we review some of the fundamental concepts behind a set of ISs that are of core importance in their stability analysis and control design. Specifically, we introduce the notion of multivalued functions, branch points, time response, and stability regions, as well as some practical applications where these systems can be encountered. The theory is accompanied by some numerical examples or simulations.

Keywords: irrational systems; fractional-order control; model-reduction methods

Citation: Guel-Cortez, A.-J.; Méndez-Barrios, C.-F.; Torres-García, D.; Félix, L. Further Remarks on Irrational Systems and Their Applications. *Comput. Sci. Math. Forum* **2022**, *4*, 5. https://doi.org/10.3390/cmsf2022004005

Academic Editors: Jorge M. Cruz-Duarte and Porfirio Toledo-Hernández

Published: 22 December 2022

1. Introduction

Irrational Systems (ISs) can be found when solving partial differential equations, fractional-order differential equations, or non-linear differential equations [1]. ISs have also been called implicit operators since they often come from solving a second-order polynomial whose solution describes the total impedance of infinite linear lumped-element networks (for further details, see [2]). In addition, fractional behavior or non-exponential decay can also be associated with ISs due to their time-response, often related to special functions such as Bessel or error functions [3]. Hence, ISs' nature is strongly linked to a low-order description of distributed parameter systems, making ISs an appealing option for control and model-reduction applications.

In the literature, ISs have been applied as mathematical models in different scenarios. For instance, ref. [4] uses fractances in a lumped model of the cardiovascular system, leading to the description of different types of heart anomalous behaviors. In [3,5,6], ISs are introduced to describe robotic formations in the form of tree-like networks and ladder-like networks. Ref. [7] models pipeline-infinite networks that converge to an IS. Similarly, ref. [8] shows an application of ISs to model electrical line transmissions.

When talking about control applications, in our previous work [9], we discuss the stability and control for a type of IS driven by fractional-order controls. Then, in [10], we formalize our analysis and apply the fractional-order controls of the type proportional-integral (PI) and proportional-derivative (PD), including their fragility analysis.

As the conceptualisation and application of ISs to engineering are still under development, in this work, we summarize the fundamental concepts, assumptions, and limits of ISs. The summary aims to briefly explain IS stability analysis and control based on our previous and undergoing investigations. The work is organized as follows: Section 2 defines the fundamental concepts and details the origins of ISs. It also discusses the intrinsic connection between fractional calculus and ISs. Furthermore, it states the fundamental hypothesis when applying ISs in system modeling. Section 3 describes the conditions of

stability for ISs. Section 4 briefly explains how to design low-order controllers of the type PD-μ (i.e., fractional-order proportional-derivative controls) for the kind of ISs that the paper focuses on. Section 5 gives some examples of ISs' control. Finally, Section 6 provides concluding remarks and outlines future work.

2. Preliminaries

Before formally describing the set of ISs that this work will discuss, we need to introduce the following concepts:

Definition 1 (Multivalued function [11,12])**.** *A multivalued function is any complex function* $F : \mathbb{C} \to \mathbb{C}$ *satisfying*

$$F[z(r, \theta + 2\pi)] \neq F[z(r, \theta)], \tag{1}$$

where r *and* θ *are the magnitude and argument of the complex variable* $z \in \mathbb{C}$*.*

Definition 2 (Branch points and branch cuts [13])**.** *The Branch point (BP) or point of accumulation is defined as the point with the smallest magnitude for which a function is multivalued. Another definition would be: a branch point is a point such that the function is discontinuous when going around an arbitrarily small circuit around this point.*

It is now easier to understand the following definition of an IS:

Definition 3 (Irrational system)**.** *An irrational system is a multi-valued transfer function* $G(s)$ *with one or more terms raised to the power* $\alpha \in \mathbb{Q}$*.*

In this work, we consider ISs described by

$$G(s) = \frac{N(s) + \sqrt{P(s)}}{D(s) + \sqrt{Q(s)}}, \tag{2}$$

where $N(s) = \sum_{k=0}^{m} b_k s^k$, $D(s) = \sum_{k=0}^{n} a_k s^k$, a_i, b_i, $a_n \neq 0$ are arbitrary real numbers, and $n \geq m$. Moreover, $P(s)$ and $Q(s)$ are second-order polynomials with positive real coefficients defined as $P(s) = \sum_{k=0}^{N} \beta_k s^N$ and $Q(s) = \sum_{k=0}^{N} \gamma_k s^N$, respectively.

Clearly, according to Definition 3, the open-loop system (2) and IS with $\alpha = \frac{1}{2}$, and branch points are located at the roots of $P(s)$ and $Q(s)$.

Origins and Connection with Fractional Calculus

Irrational transfer functions such as (2) are proven to appear when modeling infinite networks of lumped elements (for a complete description, see [1,7]). The proof of such a statement, omitted here for brevity, requires the following assumptions:

- The network should contain only linear lumped elements. For instance, viscous dampers, springs, capacitors, or inductors.
- All initial conditions should be equal to zero.
- Elements in the network should have equal impedance value. For example, the tree-like network shown in Figure 1 contains only two linear operators $\mathcal{L}_1$ and $\mathcal{L}_2$, which have the same value throughout all the layers of the network.
- The network is one-dimensional and infinite.

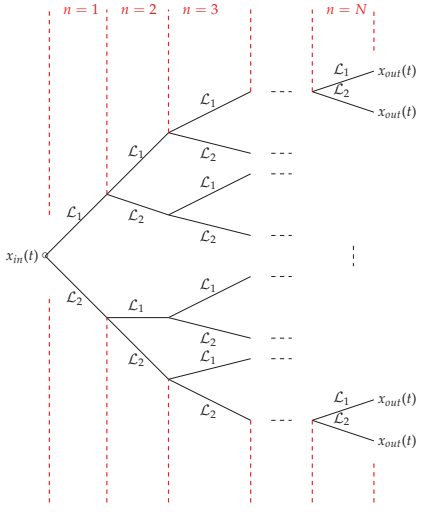

Figure 1. Tree-like network of N layers that can be described by an ISs transfer function. In the network, it is necessary to have $\mathcal{L}_\infty$ and $\mathcal{L}_\in$ to be linear operators. Note that all end-points x_{out} are in the same position. The movement is in one-dimension.

In spite of such necessary conditions, ISs can still be applied in many scenarios, epecially when the following hypotheses are considered:

Hypothesis 1. *The accuracy of 0-dimensional models of complex dynamical systems can increase by adding "networks" as lumped elements in the model.*

Hypothesis 2. *ISs can be used as model reductions for large-scale dynamical systems.*

The validity of Hypothesis 1 has been proved in scenarios such as the cardiovascular system [4,14] or muscle/joint modeling [15].

On the other hand, Hypothesis 2 has been explored in robot formations and transmission lines (for further details, see [6,16–18]). Furthermore, in some cases the ISs description leads to basic fractional-order transfer functions (for instance, see [18]).

For a better understanding of Hypotheses 1 and 2, consider the circuit-like description of the cardiovascular system shown in Figure 2a and the graphical description of a formation of mobile robots in one dimension in Figure 2b. In the case of Figure 2a, we can assume that one of the elements is itself an infinite network of linear elements with an impedance equal to $\frac{1}{C_F^\alpha s^\alpha}$ (i.e., of fractional-order); then, its mathematical model is given by

$$ {}_0\mathcal{D}_t^\alpha P_a = \frac{Q_a}{C_F^\alpha} - \frac{P_a}{RC_F^\alpha}. \tag{3} $$

Furthermore, by using the Caputo definition of the fractional derivative operator ${}_0\mathcal{D}_t^\alpha$ of order $0 < \alpha < 1$, the time response of system (3) is given by

$$ P_a(t) = P_a(0)t^{\alpha-1}\mathbf{E}_{\alpha,\alpha}(-\frac{1}{RC_F^\alpha}t^\alpha) + \frac{1}{C_F^\alpha}\int_0^t Q_a(t-\tau)\tau^{\alpha-1}\mathbf{E}_{\alpha,\alpha}(-\frac{1}{RC_F^\alpha}\tau^\alpha)d\tau, \tag{4} $$

where $\mathbf{E}_{\alpha,\alpha}(z)$ is the Mittag–Leffler function of the complex value z [19]. Equation (4) describes the arterial pressure as a power law equation with a diffusive term. Even though this kind of representation implies some physical challenges that have been recently discussed through various works (for instance, see [20,21] and the references therein), it

is clear that we can substitute any IS's impedance instead of a simple lumped element to expand the capabilities of 0-dimensional models, as discussed in Hypothesis 1.

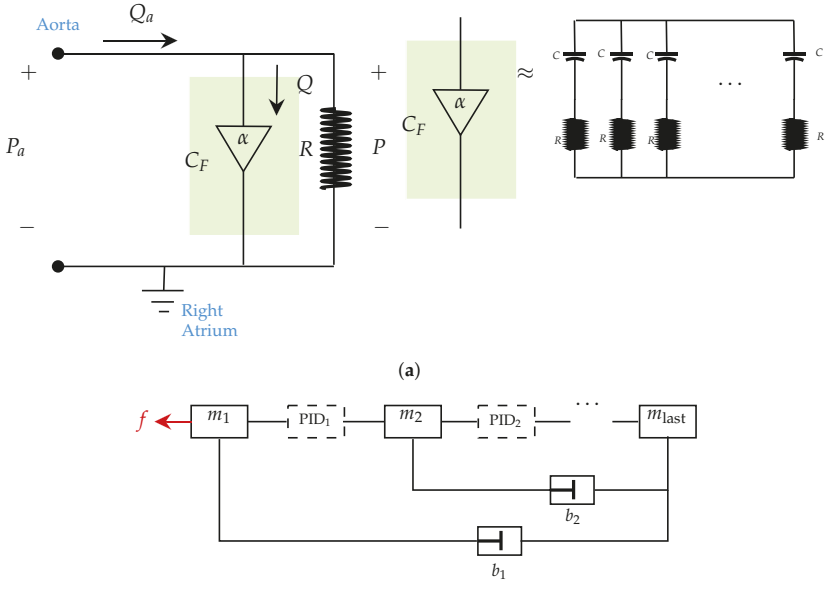

Figure 2. Examples of the application of Hypothesis 1 and 2 in realistic scenarios. (**a**) Model reduction of the cardiovascular system by an electrical system using a fractance. (**b**) Ladder network description of mobile robots described by mechanical elements and driven by PID controls [6].

Regarding Hypothesis 2, Figure 2b shows a PID-driven robotic formation in one-dimension (for example, see [22]) where all robots are described as simple mechanical elements. If we regard the network as infinite, the transfer function relating the leader's position and the last robot in the formation would be an IS [6]. Is this representation a good approximation of the actual transfer function when the number of robots in the network is finite? The answer is still not conclusive and requires further investigation (a preliminary analysis is given in [3]).

3. Stability Analysis

One of the great advantages of ISs mathematical models is that we can easily study their stability if the following Theorem is considered:

Theorem 1 ([8]). *A given multivalued transfer function is stable if and only if it has no pole in* $\mathbb{C}_+$ *and no branch points in* $\mathbb{C}_-$. *Here,* $\mathbb{C}_+$ *and* $\mathbb{C}_-$ *stand for the closed right half plane (RHP) and the open RHP of the first Riemann sheet in the complex plane, respectively.*

Briefly, Theorem 1 states that the BPs should not be located in the right-hand side of the complex plane to achieve the IS's stability. To grasp this conclusion, let us consider the following simple examples:

Example 1. *Consider the multivalued transfer function*

$$G(s) = \frac{1}{\sqrt{s+k}}, \tag{5}$$

where $k \in \mathbb{R}$. *The impulse response of* (5) *is given by (proof given in Appendix A)*

$$y(t) = \mathscr{L}^{-1}\left[\frac{1}{\sqrt{s+k}}\right] = \begin{cases} \frac{e^{-kt}}{\sqrt{\pi t}} & k > 0 \\ \frac{e^{kt}}{\sqrt{\pi t}} & k < 0 \\ \frac{1}{\sqrt{\pi t}} & k = 0 \end{cases}. \tag{6}$$

In Example 1, the IS (5) is stable iff $k > 0$. Note that as mentioned earlier, the BP is located at the root of the radicand $s + k$.

Example 2. *Consider the multivalued transfer function*

$$G(s) = \frac{1}{\sqrt{s^2 + k}}, \tag{7}$$

where $k \in \mathbb{R}$. The impulse response of (7) is given by (see Appendix B)

$$y(t) = \mathscr{L}^{-1}\left[\frac{1}{\sqrt{s^2+k}}\right] = \begin{cases} J_0(\sqrt{k}t) & k > 0 \\ J_0(\boldsymbol{i}\sqrt{k}t) & k < 0 \\ 1 & k = 0 \end{cases}. \tag{8}$$

Equation (7) is an example where the open-loop IS is stable as the BPs are located in the imaginary-axis and not in the right-hand side of the complex plane.

4. Control Design

PD$^\mu$ Control

Once the stability conditions for ISs are established, it is possible to design stabilising low-order controllers by following the *D*-composition method [23]. The following summarizes the procedure, but a complete guide can be found at references [10,24,25].

First, consider a low-order controller, for instance, the fractional-order PD control whose transfer function is well-known to be [9]

$$C(s) = k_p + k_d s^\mu. \tag{9}$$

Then, compute the characteristic polynomial of (2). In this case defined as

$$\Delta(s) := D(s) + \sqrt{Q(s)} + \left(N(s) + \sqrt{P(s)}\right)\left(k_p + k_d s^\mu\right). \tag{10}$$

Now, substitute the stability boundary of the complex plane $s = \boldsymbol{i}\omega$ in the characteristic polynomial and solve for the control gains.

Remark 1. *Note that the substitution of $s = \boldsymbol{i}\omega$ requires one to consider the cases $\omega = 0$, $\omega \to \infty$ and $\omega \neq 0$ separately [25]. In this manner, we create various sets of stability boundaries in the controller's parameter plane that permit us to enclose a stability region (See Figure 3).*

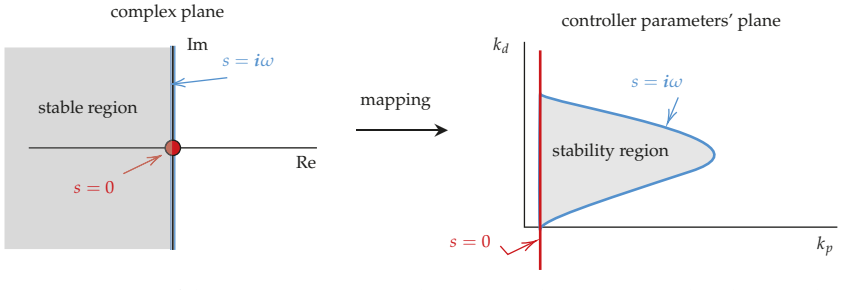

Figure 3. Example of the D-composition method. The method maps the complex plane stability region to the controller parameters' plane. In this case, the plane has not stability boundary at $s \to \infty$.

5. Applications

5.1. Control of IS

We now apply the D-composition method to some specific ISs. Note that, in all examples, the time response of the ISs closed-loop is obtained numerically using the inverse numerical Laplace transform proposed in [26]. Furthermore, fixed parameters have been selected randomly as the example's purpose is to prove the results' validity.

5.2. Bessel

Consider the Laplace transform of the Bessel function of order zero described as

$$\frac{1}{\sqrt{s^2+1}}. \tag{11}$$

Therefore, the characteristic function is given by

$$\Delta(s) = \sqrt{s^2+1} + k_p + k_d s^\mu. \tag{12}$$

Setting $\mu = 0.3$ and solving (12) for k_p and k_d, we obtain two stability boundaries shown in red and blue in Figure 4a. The red curve corresponds to the case where $\omega = 0$ before solving $\Delta(i\omega) = 0$, while the blue corresponds to the case where $\omega \neq 0$. Figure 4b shows the closed-loop response of a set of controller gains inside and outside of what is found to be the IS's stability region.

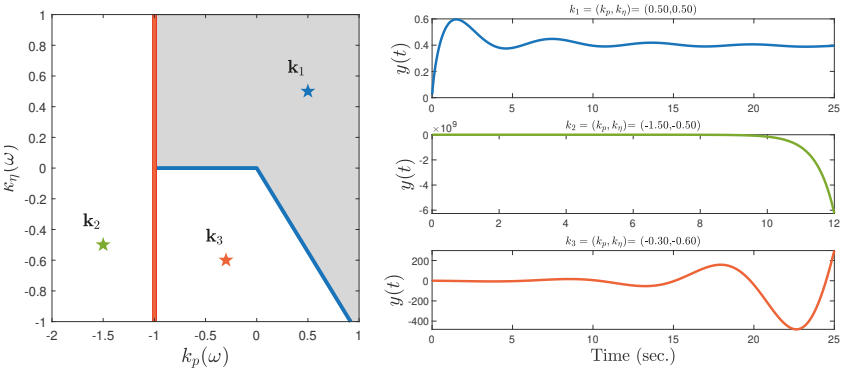

(**a**) (**b**)

Figure 4. Stability analysis of system (11). (**a**) Stability region (gray) of the closed-loop system with $\mu = 0.3$. (**b**) Time response for control gains inside different regions on the parameter's plane.

5.3. First Order IS

Another example of an IS that can be controlled by a fractional-order PD control is

$$\frac{\sqrt{3s+1}}{s+\sqrt{2s+1}}. \tag{13}$$

In this case, the characteristic equation is

$$\Delta(s) = s + \sqrt{2s+1} + \sqrt{3s+1}. \tag{14}$$

Likewise, in the previous application we set $\mu = 0.4$ and solved (14) for k_p and k_d to obtain the stability boundaries shown in Figure 5a. Again, the red curve corresponds to the case where $\omega = 0$ before solving $\Delta(i\omega) = 0$, while the blue corresponds to the case where

$\omega \neq 0$. Figure 5b shows the closed-loop response of a set of controller gains inside and outside of what is found to be the IS's stability region.

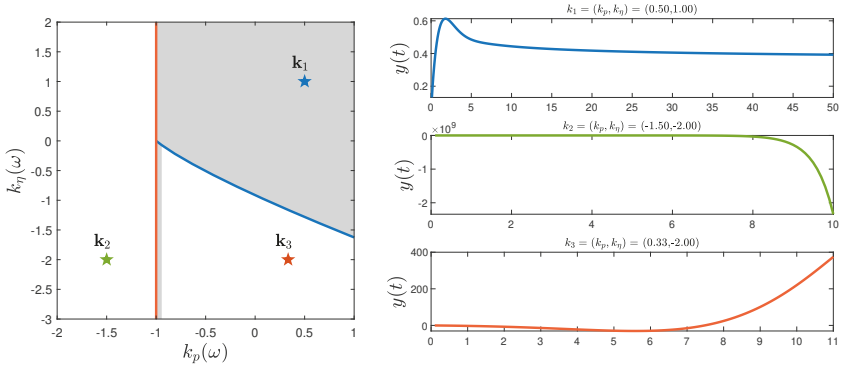

(**a**) (**b**)

Figure 5. Stability analysis of system (13). (**a**) Stability region (gray) of the closed-loop system with $\mu = 0.4$. (**b**) Time response for control gains inside different regions on the parameter's plane.

6. Conclusions

In this work, we have briefly described the concepts, hypotheses, and assumptions behind the use of ISs. In addition, in our applications, we present the stability analysis and control of ISs. As can be seen by the reader, future work may take various paths, including the design of different low-order controls for ISs, the application of ISs to model other complex phenomena, or the creation of irrational controls that could stabilize ISs whose BPs are in the right-hand side of the complex plane.

Author Contributions: Conceptualization, A.-J.G.-C. and C.-F.M.-B.; methodology, A.-J.G.-C.; software, A.-J.G.-C. and D.T.-G.; validation, A.-J.G.-C., C.-F.M.-B., and D.T.-G.; formal analysis, A.-J.G.-C. and C.-F.M.-B.; investigation, A.-J.G.-C.; resources, A.-J.G.-C. and L.F.; data curation, A.-J.G.-C., D.T.-G., and L.F.; writing—original draft preparation, A.-J.G.-C. and D.T.-G.; writing—review and editing, C.-F.M.-B. and L.F.; visualization, A.-J.G.-C.; supervision, A.-J.G.-C. and C.-F.M.-B.; project administration, A.-J.G.-C. and C.-F.M.-B.; and funding acquisition, L.F. All authors have read and agreed to the published version of the manuscript.

Funding: This research was funded by Faculty of Engineering, Autonomous University of San Luis Potosi grant number POA-AME-IMT2022.

Institutional Review Board Statement: Not applicable.

Informed Consent Statement: Not applicable.

Data Availability Statement: Not applicable.

Conflicts of Interest: The authors declare no conflict of interest.

Abbreviations

The following abbreviations are used in this manuscript:

IS	Irrational system
PD	Proportional derivative
PI	Proportional integral
BP	Branch point
PID	Proportional integral derivative

Appendix A. Example 1

To compute the time-response of the multivalued transfer function in (5), we consider the following definition of the inverse Laplace transform:

$$y(t) = \mathscr{L}^{-1}\left[\frac{1}{\sqrt{s+k}}\right] = \frac{1}{2i\pi}\int_{c-\infty}^{c+\infty} G(s)e^{st}ds. \tag{A1}$$

To solve (A1), let the contour C be defined as the sum of C_i, $i \in [1,6]$, as shown in Figure A1. Note that the election of the integration path should be one which avoids branch points, namely, point $-k$ in this scenario.

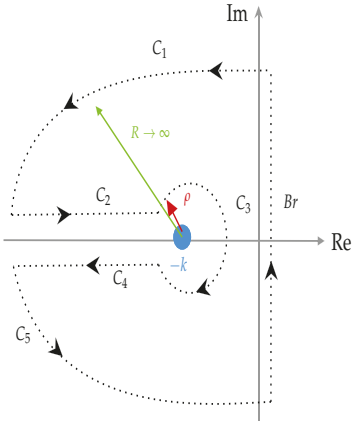

Figure A1. Integration path of Example 1.

According to the residue theorem

$$\int_C G(s)e^{st}ds = 0. \tag{A2}$$

Then, we can express (A1) as

$$\int_{Br} G(s)e^{st}ds = -\sum_{i=1}^{5}\int_{C_i} G(s)e^{st}ds. \tag{A3}$$

Observe that, for $R \to \infty$

$$\int_{C_1} = \int_{C_5} = 0, \tag{A4}$$

and, on the other hand, for $\rho \to 0$ we have

$$\int_{C_3} = 0. \tag{A5}$$

Thus, it suffices to compute the integration along C_2 and C_4 to obtain $y(t)$. In order to perform such an operation, consider the parameterisation $s + k = -r$, which in polar form can be rewritten as $re^{\pm i\pi}$, where the positive sign corresponds to C_2 and the negative sign corresponds to C_4. This permits us describe the path $r \in (k+\rho, \infty)$, with $\delta, \rho \to 0$, i.e.,

$$\int_{C_2+C_4} = \int_{\infty}^{\rho} \frac{e^{-(r+k)t}e^{i\pi}}{\sqrt{r}e^{i\pi/2}}dr + \int_{\rho}^{\infty} \frac{e^{-(r+k)t}e^{-i\pi}}{\sqrt{r}e^{-i\pi/2}}dr, \tag{A6}$$

since $\rho \to 0$

$$\begin{aligned}\int_{C_2+C_4} &= (e^{i\pi} + e^{-i\pi}) \int_0^\infty \frac{e^{-(r+k)t}}{\sqrt{r}} dr \\ &= -2i \sin(\pi/2) e^{-kt} \int_0^\infty \frac{e^{-rt}}{\sqrt{r}} dr \\ &= -2i \sin(\pi/2) e^{-kt} t^{-1/2} \Gamma(1/2).\end{aligned}$$

Now, as we know that

$$\Gamma(x)\Gamma(1-x) = \frac{\pi}{\sin(\pi x)},$$

with $x = 1/2$, from (A1) we have,

$$\mathscr{L}^{-1}\left[\frac{1}{\sqrt{s+k}}\right] = \frac{e^{-kt}}{\sqrt{t\pi}}. \tag{A7}$$

This finishes the proof of statement (6).

Appendix B. Example 2

Following the ideas used to find the inverse Laplace Transform of $\frac{1}{\sqrt{s+k}}$ shown in Appendix A, we now perform the time-response of (7) (given in Equation (8)) by computing

$$y(t) = \mathscr{L}^{-1}\left[\frac{1}{\sqrt{s^2+k}}\right] = \frac{1}{2i\pi} \int_{c-\infty}^{c+\infty} G(s) e^{st} ds. \tag{A8}$$

Observe that for $k > 0$, we have a complex conjugate branch point, while for $k < 0$ we have two real points. Under these observations, we consider two different integration paths, shown in Figure A2, where Figure A2a and Figure A2b correspond to the case of k negative and positive, respectively.

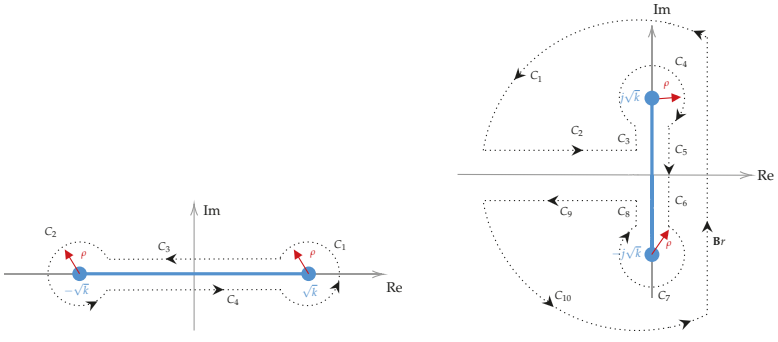

Figure A2. Integration path of Example 2. (**a**) $k < 0$. (**b**) $k > 0$.

We first consider the case $k < 0$; thus, we shall consider the path shown in Figure A2a and create a path such that

$$\int_C G(s) e^{st} ds = 0.$$

Under the assumption that $\rho \to 0$,

$$\int_{C_1+C_2} = 0. \tag{A9}$$

Now, C_3 and C_4 s vary from $\sqrt{k}-\rho$ to $-\sqrt{k}+\rho$, and then we have

$$\int_{C_2+C_3} \frac{e^{st}}{\sqrt{s^2-k}} = -\boldsymbol{i}\int_{-\sqrt{k}+\rho}^{\sqrt{k}-\rho} \frac{e^{st}}{\sqrt{k-s^2}} + \boldsymbol{i}\int_{\sqrt{k}-\rho}^{-\sqrt{k}+\rho} \frac{e^{st}}{\sqrt{k-s^2}} = -2\boldsymbol{i}\int_{-\sqrt{k}+\rho}^{\sqrt{k}-\rho} \frac{e^{st}}{\sqrt{k-s^2}}. \tag{A10}$$

Since $\rho \to 0$,

$$y(t) = \frac{1}{2\pi\boldsymbol{i}}\int_{Br} G(s)e^{st}ds = \frac{1}{\pi}\int_{-\sqrt{k}}^{\sqrt{k}} \frac{e^{st}}{\sqrt{k-s^2}}. \tag{A11}$$

Then, making $s = a\cos(u)$, the integral becomes

$$\frac{1}{\pi}\int_0^{\pi} e^{kt\cos(u)}du = I_0(\sqrt{k}t). \tag{A12}$$

We can express the modified first Bessel function in terms of the first Bessel function if $-\pi < \arg(\sqrt{k}t) \leq \frac{\pi}{2}$:

$$J_\alpha(\boldsymbol{i}\sqrt{k}t) = e^{\alpha\frac{\pi}{2}}I_\alpha(\sqrt{k}t)$$

with $\alpha = 0$:

$$J_0(\boldsymbol{i}\sqrt{k}t) = I_0(\sqrt{k}t).$$

Now, we consider the case where $k > 0$. The inverse Laplace transform of $G(s)$ can be written in two different forms (see for instance [27]):

$$y(t) = \frac{2}{\pi}\int_{\sqrt{k}}^{\infty} \sin(st)\frac{1}{\sqrt{s^2-k}}ds, \tag{A13}$$

$$y(t) = \frac{2}{\pi}\int_0^{\sqrt{k}} \cos(st)\frac{1}{\sqrt{k-s^2}}ds. \tag{A14}$$

The first Bessel function is given as

$$J_0(x) = \frac{1}{\pi}\int_0^{\pi} \cos(-x\sin(\tau))d\tau.$$

Thus, by taking $s = \sqrt{k}\sin(\theta)$ in (A14), with $\theta \in (0, \frac{\pi}{2})$ we have

$$y(t) = \frac{2}{\pi}\int_0^{\frac{\pi}{2}} \cos\left(\sqrt{k}t\sin(\theta)\right)d\theta = \frac{2}{\pi}\frac{\pi}{2}J_0(\sqrt{k}t). \tag{A15}$$

References

1. Guel-Cortez, A.J. Modeling and Control of Fractional-Order Systems. The Linear Systems Case. Ph.D. Thesis, CIEP-UASLP, San Luis, Mexico, 2018.
2. Sen, M.; Hollkamp, J.P.; Semperlotti, F.; Goodwine, B. Implicit and fractional-derivative operators in infinite networks of integer-order components. *Chaos Solitons Fractals* **2018**, *114*, 186–192. [CrossRef]
3. Guel-Cortez, A.J.; Sen, M.; Goodwine, B. Closed form time response of an infinite tree of mechanical components described by an irrational transfer function. In Proceedings of the 2019 American Control Conference (ACC), Philadelphia, PA, USA, 10–12 July 2019; pp. 5828–5833.
4. Guel-Cortez, A.J.; Kim, E. A Fractional-Order Model of the Cardiac Function. In Proceedings of the 13th Chaotic Modeling and Simulation International Conference, Florence, Italy, 9–12 June 2020; Springer: Berlin/Heidelberg, Germany, 2020; pp. 273–285.
5. Leyden, K.; Sen, M.; Goodwine, B. Large and infinite mass–spring–damper networks. *J. Dyn. Syst. Meas. Control* **2019**, *141*, 061005. [CrossRef]
6. Ni, X.; Goodwine, B. Frequency Response and Transfer Functions of Large Self-similar Networks. *arXiv* **2020**, arXiv:2010.11015.
7. Mayes, J.; Sen, M. Approximation of potential-driven flow dynamics in large-scale self-similar tree networks. *Proc. R. Soc. A Math. Phys. Eng. Sci.* **2011**, *467*, 2810–2824. [CrossRef]
8. Merrikh-Bayat, F.; Karimi-Ghartemani, M. On the essential instabilities caused by fractional-order transfer functions. *Math. Probl. Eng.* **2008**, *2008*, 419046. [CrossRef]
9. Guel-Cortez, A.J.; Sen, M.; Goodwine, B. Fractional- PD$^{\mu}$ Controllers for Irrational Systems. In Proceedings of the 2019 International Conference on Control, Decision and Information Technologies, Paris, France, 23–26 April 2019.

10. Guel-Cortez, A.J.; Méndez-Barrios, C.F.; Kim, E.j.; Sen, M. Fractional-order controllers for irrational systems. *IET Control Theory Appl.* **2021**, *15*, 965–977. [CrossRef]
11. Cohen, H. *Complex Analysis with Applications in Science and Engineering*; Springer Science & Business Media: Berlin/Heidelberg, Germany, 2007.
12. Harvey, C. *Conformal mapping on Riemann Surfaces*; Dover Publications, Inc.: New York, NY, USA, 1980.
13. Needham, T. *Complex Visual Analysis*; Oxford University Press, Inc.: New York, NY, USA, 1997.
14. Capoccia, M. Development and characterization of the arterial W indkessel and its role during left ventricular assist device assistance. *Artif. Organs* **2015**, *39*, E138–E153. [CrossRef] [PubMed]
15. Piovesan, D.; Pierobon, A.; DiZio, P.; Lackner, J.R. Measuring multi-joint stiffness during single movements: Numerical validation of a novel time-frequency approach. *PLoS ONE* **2012**, *7*, e33086. [CrossRef]
16. Ni, X.; Goodwine, B. Frequency Response of Transmission Lines with Unevenly Distributed Properties with Application to Railway Safety Monitoring. *arXiv* **2020**, arXiv:2012.09247.
17. Leyden, K.; Goodwine, B. Using fractional-order differential equations for health monitoring of a system of cooperating robots. In Proceedings of the 2016 IEEE International Conference on Robotics and Automation (ICRA), Stockholm, Sweden, 16–21 May 2016; pp. 366–371.
18. Leyden, K.; Sen, M.; Goodwine, B. Models from an implicit operator describing a large mass-spring-damper network. *IFAC-PapersOnLine* **2018**, *51*, 831–836. [CrossRef]
19. Shukla, A.; Prajapati, J. On a generalization of Mittag-Leffler function and its properties. *J. Math. Anal. Appl.* **2007**, *336*, 797–811. [CrossRef]
20. Sabatier, J.; Farges, C.; Tartaglione, V. Some alternative solutions to fractional models for modelling power law type long memory behaviors. *Mathematics* **2020**, *8*, 196. [CrossRef]
21. Sabatier, J. Some Proposals for a Renewal in the Field of Fractional behavior Analysis and Modelling. In *Proceedings of the International Conference on Fractional Differentiation and its Applications (ICFDA'21)*; Springer: Berlin/Heidelberg, Germany, 2022, pp. 1–25.
22. Ramos-Avila, D.; Rodrıguez, C.; Hernández-Carrillo, J.; Guel-Cortez, A.; Sen, M.; Méndez-Barrios, C.; González-Galván, E.; Goodwine, B. Experiments with PD-controlled robots in ring formation. In Proceedings of the XXI Congreso Mexicano de Robótica–COMRob, Ciudad de Manzanillo, Colima, Mexico, 13–15 November 2019.
23. Gryazina, E.N. The D-decomposition theory. *Autom. Remote Control* **2004**, *65*, 1872–1884. [CrossRef]
24. Hernández-Díez, J.E.; Méndez-Barrios, C.F.; Mondié, S.; Niculescu, S.I.; González-Galván, E.J. Proportional-delayed controllers design for LTI-systems: A geometric approach. *Int. J. Control* **2018**, *91*, 907–925. [CrossRef]
25. Barrios, C.F.M. Low-Order Controllers for Time-Delay Systems: An Analytical Approach. Ph.D. Thesis, Université Paris Sud-Paris XI, Bures-sur-Yvette, France, 2011.
26. Abate, J.; Whitt, W. A unified framework for numerically inverting Laplace transforms. *INFORMS J. Comput.* **2006**, *18*, 408–421. [CrossRef]
27. Moslehi, L.; Ansari, A. Some remarks on inverse Laplace transforms involving conjugate branch points with applications. *UPB Sci. Bull. Ser. A-Appl. Math. Phys.* **2016**, *78*, 107–118.

computer sciences and mathematics forum

MDPI

Proceeding Paper

Patterns in a Time-Fractional Predator–Prey System with Finite Interaction Range †

Guillermo Chacón-Acosta [1,2,*] and Mayra Núñez-López [3]

[1] Applied Mathematics and Systems Department, Universidad Autónoma Metropolitana-Cuajimalpa, Vasco de Quiroga 4871, Ciudad de México 05348, Mexico
[2] Institute of Physics and Astronomy, University of Potsdam, 14476 Potsdam-Golm, Germany
[3] Department of Mathematics, Instituto Tecnológico Autónomo de México Río Hondo 1, Col. Progreso Tizapán Ciudad de México 01080, Mexico
* Correspondence: gchacon@cua.uam.mx
† Presented at the 5th Mexican Workshop on Fractional Calculus (MWFC), Monterrey, Mexico, 5–7 October 2022.

Abstract: Diffusive predator–prey systems are well known to exhibit spatial patterns obtained by using the Turing instability mechanism. reaction–diffusion systems were already studied by replacing the time derivative with a fractional order derivative, finding the conditions under which spatial patterns could be formed in such systems. The recent interest in fractional operators is due to the fact that many biological, chemical, physical, engineering, and financial systems can be well described using these tools. This contribution presents a diffusive predator–prey model with a finite interaction scale between species and introduces temporal fractional derivatives associated with species behaviors. We show that the spatial scale of the species interaction affects the range of unstable modes in which patterns can appear. Additionally, the temporal fractional derivatives further modify the emergence of spatial patterns.

Keywords: pattern formation; predator–prey systems; fractional derivatives

Citation: Chacón-Acosta, G.; Núñez-López, M. Patterns in a Time-Fractional Predator–Prey System with Finite Interaction Range. *Comput. Sci. Math. Forum* **2022**, *4*, 3. https://doi.org/10.3390/cmsf2022004003

Academic Editors: Jorge M. Cruz-Duarte and Porfirio Toledo-Hernández

Published: 7 December 2022

1. Introduction

In population dynamics, Lotka–Volterra equations describe a system of two coexisting species whose densities oscillate in time [1]. These systems can exhibit diffusion-driven instabilities, which are explained by the Turing mechanism for diffusion-reaction systems [2,3], through extensions or modifications of the original model [4–6]. Predator–prey interaction is a multi-factor dependent process. For instance, some studies consider hunting cooperation, prey defense mechanisms, limited localized resources, and cross-diffusion terms for studying the influence of movements on both species [7].

It has been proposed that the relative distance between a predator and prey can influence the probability of an encounter between them. The latter is modeled through a nonlinear reactive term that considers the mean of the possible interactions within a fixed radius centered on one of the two species. [8,9]. These finite-range interaction models show that the emergence of patterns is not only driven by diffusion but also there are regions where the instability is driven by the interaction range [8]. Recently, this model has been extended by introducing a constant drift and constraining the system to a large and narrow environment [10]. In such an analysis, the geometry of the boundaries induces an effect that couples with the drift. Thus, the corresponding dispersion relation has three parameters: the ratio of diffusivities, a dimensionless drift, and the ratio of interaction lengths, which enlarge the parameter space and, therefore, the possibilities of obtaining different kinds of spatio-temporal patterns.

On the other hand, many processes, not only in ecology but in many other areas, have been adequately described through models that include equations with fractional time derivatives, which are well-known to model memory and non-local effects [11]. Including

such effects, beyond just modifying the nonlinear interaction terms, brings the model closer to a more realistic situation [12]. For reaction–diffusion models with anomalous diffusion, it has been seen that the parameter that drives the instability is modified by the anomalous diffusion exponent [13]. The inclusion of temporal fractional derivatives in predator–prey systems has been shown to help control the stability of patterns for species coexistence [14]; memory effects can also shift the bifurcation threshold in such systems [15]. It has also been shown that in systems where patterns do not naturally emerge, fractional derivatives can induce diffusion-driven instability and thus pattern formation, hence the importance of using this kind of model [16,17].

In general, the changes induced by fractional time derivatives in reaction–diffusion systems have been extensively studied in the literature [18–22]. In almost all cases, it was found that the nonlinearity of the functions describing the kinetics had an essential role in the generation of spatial and temporal patterns.

In this work, we are interested in finding a relationship between the fractional derivative and the Turing instability, that is, if the temporal fractional derivative induces Turing instability and produces spatial patterns. We present the stability analysis of the model that considers the mean number of interspecies interactions in a given region defined by the interaction distance. This distance is one of the parameters guiding the system towards the instability leading to pattern formation. We consider whether replacing the time derivative by a fractional operator accounts for memory effects in a predator–prey diffusive model with a finite interaction scale between species.

The manuscript is structured as follows. Section 2 analyzes the predator–prey model with a finite interaction length. We find the steady state and the corresponding dispersion relation that depends on three parameters. The instability curve for the control parameter is found when the ratio of the characteristic lengths of each species is larger than two, which is the set value in previous studies. Section 3 presents the system's stability analysis when a fractional operator replaces the time derivative to account for memory effects, and its consequences are discussed. Section 4 summarizes the obtained results.

2. Predator–Prey Model with Finite Interaction Length

Let us consider a model characterized by a system of two equations: one for the prey $N(x,t)$ and one for the predator $P(x,t)$. They describe diffusion in the physical space, and the strength of the interaction (nonlinear term) is a function of individuals' proximity. These reaction–diffusion models with the spatial interaction scale have been widely applied to model the competition of species' coevolution in an ecology community. We introduce two different length scales to consider different effective interaction ranges, the region where prey and predators interact may have different relevance to predator growth and prey death. These scales have an important role in pattern formation. The model is as follows:

$$\frac{\partial N(x,t)}{\partial t} = D_N \frac{\partial^2 N(x,t)}{\partial x^2} + rN(x,t) - \alpha N(x,t) \int_{x-L_1}^{x+L_1} P(s,t)ds, \quad (1)$$

$$\frac{\partial P(x,t)}{\partial t} = D_P \frac{\partial^2 P(x,t)}{\partial x^2} - mP(x,t) + \beta P(x,t) \int_{x-L_2}^{x+L_2} N(s,t)ds. \quad (2)$$

Predators consume the prey with an intrinsic rate α and reproduce with the rate β; r is the growth rate of prey, and predators are assumed to die spontaneously with rate m. D_N and D_P are the constant diffusion coefficients of prey and predators, respectively. The conditions under which the spatio-temporal patterns occur are first studied considering the stationary case with no diffusion. This gives us the stationary state $(\bar{N}, \bar{P}) = (m/(2\beta L_2), r/(2\alpha L_1))$. By considering now small harmonic perturbations for both species, we pbtain the following dispersion relation of the system with diffusion

$$\widehat{\lambda}(K) = -K^2 + \frac{\sqrt{rm}L_1^2}{DK}\sqrt{-\sin^2 K \cos K}. \quad (3)$$

where $D_N = D_P = D$, $L_2 = 2L_1$, $K = kL_1$, and $\widehat{\lambda} = \lambda \frac{L_1^2}{D}$. The system was further studied in [10], and it was found that a general dispersion relation is the following:

$$\widehat{\lambda} = -\frac{(1+d)}{2}(K^2) \pm \frac{1}{2}\left[(1-d)^2K^4 - 4\mu^2\frac{\sin(K)\sin(K\ell)}{K^2\ell}\right]^{1/2}, \tag{4}$$

from now on $\widehat{\lambda} = \lambda \frac{L_1^2}{D_N}$, and the parameters $d = D_P/D_N$, $\mu = \sqrt{rm}L_1^2/D_N$, and $\ell = L_2/L_1$ were introduced. Certainly if $d = 1$ and $\ell = 2$, this reduces to the above expression.

The system (1) and (2) linearized around the stationary point, with no diffusion, leads to a characteristic equation $\widehat{\lambda} = \pm i\mu$, two conjugate imaginary eigenvalues, which is the limiting case for the instability condition since it has no real part. As the eigenvalues are purely imaginary and conjugate to each other, this fixed point must be a center for closed orbits in the local vicinity, i.e., an attractive or repulsive spiral in the phase space.

Turing Instability Parameter Space

For several values of μ, it has been seen that the critical value d_c is reached for values close to 1; therefore, when increasing, there will be no pattern formation. For ℓ, something similar happens; it has been seen that to guarantee pattern formation, $\ell \neq 1$ must be fulfilled, and usually it is just considered $\ell = 2$, as in Equation (3). However, it is not the only possible value.

In Figure 1, we plot the dispersion relation (4) with $d = 1$, as a function of K, varying the parameter μ and for different values of ℓ indicated with different colors. This figure shows that as ℓ increases, different ranges of unstable modes appear for each fixed μ value. The choice of values $\ell > 2$ increases the space of possibilities that meet the instability condition and pattern formation.

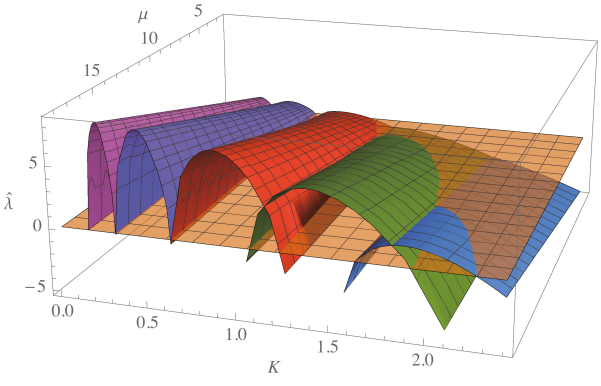

Figure 1. Dispersion relation $\widehat{\lambda}(K)$ varying the parameter μ. Several values of the ratio between the interaction lengths are presented with different color plots; values increase to the left of $\ell = 2$ (blue), $\ell = 3$ (green), $\ell = 5$ (red), $\ell = 10$ (dark purple), and $\ell = 20$ (purple).

To satisfy the instability condition $\mathrm{Re}(\lambda(K)) < 0$ for pattern formation, it is usually necessary to verify the so-called Turing conditions [2], a number of inequalities that come from the analysis of the dispersion relation. This is equivalent to considering the instability threshold when $\widehat{\lambda}_c = 0$ in the characteristic equation, imposing a relation among the system parameters and the critical value K_c, which determines such a threshold. For Equation (4), we find that the parameters to study the instability of the system will be (μ, ℓ). Remember that μ measures the competition of time scales given by the species' growth, death, and

diffusion rates, while ℓ is the ratio between the characteristic lengths. Choosing μ^2 as the control parameter [23], it is possible to obtain the following relation, having fixed $d = 1$,

$$\mu^2(K, \ell) = -\frac{\ell K^6}{\sin(K)\sin(K\ell)}. \tag{5}$$

This expression has a minimum in K_c obtained by deriving and equaling zero; this reduces to solving the next equation, and as we can see it will depend on the choice of ℓ,

$$K_c(\cot(K_c) + \ell \cot(K_c\ell)) = 0. \tag{6}$$

We can construct the stability curve $\mu_c(\ell)$ in parameter space, which satisfies the above equations, such that patterns will emerge for values greater than the critical value of the control parameter $\mu > \mu_c$. See the orange dots and curve in Figure 2.

The ratio of the interaction lengths of the two species ℓ, as mentioned in [8], is an important parameter since it drives the instability together with d. As we can see in Figure 2, as ℓ increases, the parameter μ decreases but does not vanish.

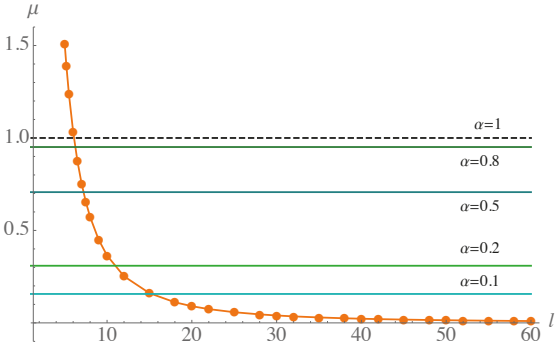

Figure 2. Stability curve μ_c as a function of ℓ with different fractional order values α. To guarantee pattern formation μ must take values above the orange curve.

3. Fractional-Order System Stability Analysis

Let us now consider a reaction–diffusion system of fractional order in the temporal derivative

$$\frac{\partial^\alpha N(x,t)}{\partial t^\alpha} = D_N \frac{\partial^2 N(x,t)}{\partial x^2} + f(N,P), \tag{7}$$

$$\frac{\partial^\alpha P(x,t)}{\partial t^\alpha} = D_P \frac{\partial^2 P(x,t)}{\partial x^2} + g(N,P), \tag{8}$$

where f, g are usually nonlinear functions, and in this case we will consider the same dynamics as in (1) and (2). The fractional time derivative is defined in Caputo's sense as

$$\frac{\partial^\alpha F(t)}{\partial t^\alpha} := \frac{1}{\Gamma(1-\alpha)} \int_0^t \frac{\partial F(t')}{\partial t'} \frac{dt'}{(t-t')^\alpha}, \tag{9}$$

with $0 < \alpha < 1$, which is defined by its Laplace transform as follows:

$$\hat{\mathcal{L}}\left\{\frac{\partial^\alpha F(t)}{\partial t^\alpha}\right\} = s^\alpha \tilde{F}(s) - s^{\alpha-1} F(0+),$$

where $\tilde{F}(s) = \hat{\mathcal{L}}\{F(t)\}$, and $0 < \alpha < 1$.

To study the stability of the system, we first consider the diffusionless case. Let $\mathcal{P} = (\bar{N}, \bar{P})$ be an equilibrium point of the system; its the stability of can be determined by linearizing the system (7) and (8) around it, which leads to the following linear system:

$$\begin{pmatrix} \frac{\partial^\alpha \bar{N}(x,t)}{\partial t^\alpha} \\ \\ \frac{\partial^\alpha \bar{P}(x,t)}{\partial t^\alpha} \end{pmatrix} = \underbrace{\begin{pmatrix} f_u & f_v \\ g_u & g_v \end{pmatrix}_{\mathcal{P}}}_{\mathbf{A}} \begin{pmatrix} \bar{N} \\ \bar{P} \end{pmatrix}. \tag{10}$$

By transforming the system to Laplace space, it is possible to rearrange it as follows:

$$\underbrace{(\lambda(s)\mathbf{I} - \mathbf{A})}_{\Delta(s)}(\mathcal{L}(\bar{N}), \mathcal{L}(\bar{P})) = (\mathcal{L}\{\bar{N}(0)\}, \mathcal{L}\{\bar{P}(0)\})s^{\alpha-1}, \tag{11}$$

where $\lambda(s) = s^\alpha$. The equilibrium point $\mathcal{P}$ of the system is stable if all the roots of the characteristic equation $\Delta(s) = 0$ have negative real part, i.e., $\mathrm{Re}(\lambda) < 0$, additionally to satisfying the usual conditions [2,23]. In the complex plane, the negativity condition means that the argument of s must be greater than $\frac{\pi}{2}$; this implies that the argument of λ must be

$$|\arg(\lambda)| > \alpha\frac{\pi}{2}, \tag{12}$$

this is called the Mantignon form for the stability criterion for the fractional case [24,25].

For the system (1) and (2), it was shown that, in the absence of diffusion, $\mu = \sin\left(\arg\left(\widehat{\lambda}\right)\right)$; condition (12) implies that $\mu > \mu_\alpha = \sin(\alpha\pi/2)$, which defines a constraint surface in the extended parameter space (μ, ℓ, α), such that, besides satisfying the condition seen above $\mu > \mu_c$, this condition must also be fulfilled to guarantee the stability of the steady state associated with the order α.

In Figures 2–4, the effect of this constraint can be seen. In Figure 2, $\mu_c(\ell)$ is plotted, so to guarantee pattern formation μ must take values above this curve. Considering different values of $alpha$, we see that for larger ell, the values of $mu_c(\ell)$ must be beyond those determined by $mu_c(\ell)$., i.e., there will be a region associated with the order α, given by $\mu_\alpha > \mu_c$, for which the parameter values that previously met the instability conditions are now discarded, and pattern formation is no longer possible.

Notably, for the extreme case $\alpha = 1$, condition (12) merely reduces to asking for $\mu > 1$ values. Although this condition does not influence the non-fractional case, it does set an upper bound on the values of μ dropped by the fractional order. This case is illustrated as a dotted line in Figure 2. The interesting point is that its intersection with the curve μ_c, which occurs at approximately $\ell_* \approx 6$, indicates the values of ℓ above from which the fractional order will have an effect, depending on the value of α. In Figures 3 and 4, the intersection of the two surfaces μ_c and μ_α in the extended parameter space is shown for each value of α. The region below the surface is just the region discarded by the fractional order of the system, while the intersection curve gives the minimum ℓ for each α.

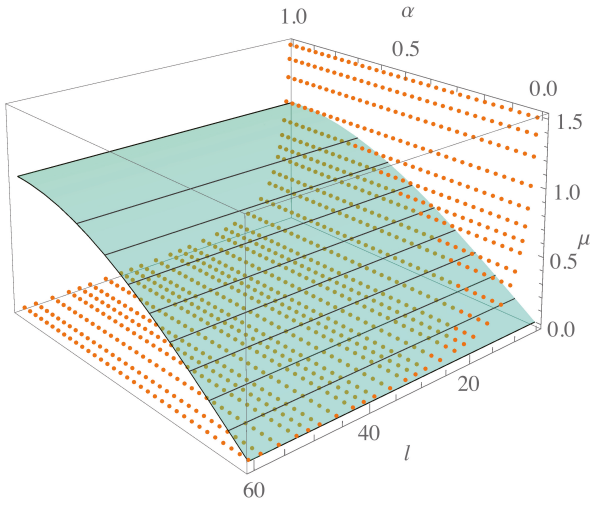

Figure 3. Intersection of the two surfaces μ_c and μ_α in the extended parameter space for $0 < \alpha < 1$.

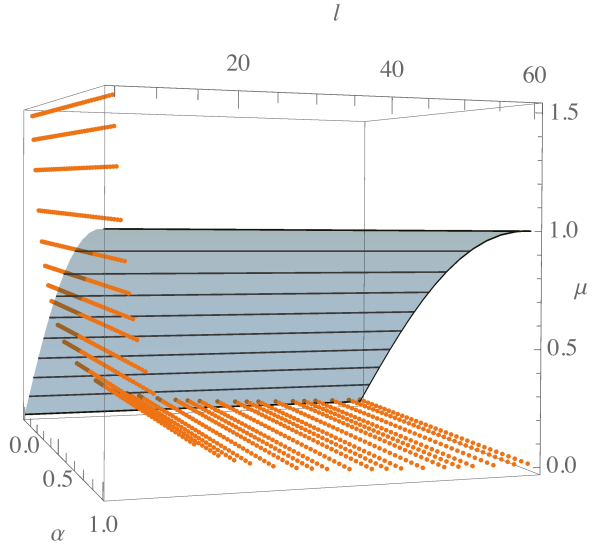

Figure 4. Alternative point of view of the intersection of the surfaces μ_c and μ_α.

4. Conclusions

Over the last few years, it has been seen that many physical, chemical, and biological systems, where memory effects cannot be neglected, are well described through reaction–diffusion equations with fractional time derivatives. This work presents the stability analysis of a reaction–diffusion system when a fractional operator replaces the time derivative.

Early analyses found that this distance is indeed one of the parameters guiding the system towards the instability that leads to pattern formation [8,9]. Later studies showed that the parameter space for studying this instability could be extended to include drift effects, as well as the large values of the characteristic length ratio and the parameter μ that is a combination of the birth and death rates of the species and the characteristic time at which they diffuse [10].

Introducing the fractional time operator to include memory effects restricts the time eigenvalue as a function of the fractional order of the derivative, in addition to the well-known conditions. Thus, on the one hand, it is necessary to extend the parameter space to include the fractional order. However, on the other hand, since several conditions must be fulfilled simultaneously, the intersections of the restriction surfaces must be found to find the corresponding critical values. In the specific case of the predator–prey system, this is reflected in the fact that for large values of the characteristic length ratio—values approximately greater than six—the value of μ must be taken above the critical value given by the Turing conditions. How large this value should be depends on the fractional order. That is, there is a region of μ values that in the usual case can form patterns but at the order α is forbidden. When the interaction lengths of the species are very different, memory effects cause the μ values that are suitable for pattern formation to be reduced.

The class of oscillations and their behavior will be analyzed in future work. The present study reinforces the importance of the influence of the anomalous order in the formation of unsteady state structures in a system where diffusivity is not the only parameter guiding instabilities.

Author Contributions: Conceptualization, G.C.-A.; formal analysis, G.C.-A. and M.N.-L.; investigation, G.C.-A. and M.N.-L.; writing—original draft preparation, G.C.-A. and M.N.-L.; writing—review and editing, G.C.-A. and M.N.-L. All authors have read and agreed to the published version of the manuscript.

Funding: This research received no external funding.

Institutional Review Board Statement: Not applicable.

Informed Consent Statement: Not applicable.

Data Availability Statement: Not applicable.

Acknowledgments: G.C.-A. acknowledges support form the grant Becas de Superación Académica Elisa Acuña 2021 from Universidad Autónoma Metropolitana. M.N.-L. also acknowledges support from Asociación Mexicana de Cultura A.C.

Conflicts of Interest: The authors declare no conflict of interest.

References

1. Brauer, F.; Castillo-Chavez, C. *Mathematical Models in Population Biology and Epidemiology*, 2nd ed.; Springer Science+Business Media, LLC: Berlin/Heidelberg, Germany, 2012.
2. Murray, J.D. *Mathematical Biology II: Spatial Models and Biomedical Applications*, 3rd ed.; Springer: Berlin/Heidelberg, Germany, 2003.
3. Kondo, S.; Miura, T. Reaction–diffusion model as a framework for understanding biological pattern formation. *Science* **2010**, *329*, 1616–1620. [CrossRef] [PubMed]
4. Bartumeus, F.; Alonso, D.; Catalan, J. Self-organized spatial structures in a ratio-dependent predator–prey model. *Physica A* **2001**, *295*, 53. [CrossRef]
5. McGehee, E.; Peacock-López, E. Turing patterns in a modified Lotka-Volterra model. *Phys. Lett. A* **2005**, *342*, 90–98. [CrossRef]
6. McGehee, E.; Schutt, N.; Vasquez, D.; Peacock-López, E. Bifurcations, and temporal and spatial patterns of a modified Lotka-Volterra model. *Int. J. Bifurc. Chaos* **2008**, *18*, 2223. [CrossRef]
7. Abrams, P.A. The Evolution of predator–prey Interactions: Theory and Evidence. *Annu. Rev. Ecol. Syst.* **2000**, *31*, 79–105. [CrossRef]
8. Brigatti, E.; Oliva, M.; Núñez-López, M.; Oliveros-Ramos, R.; Benavides, J. Pattern formation in a predator–prey system characterized by a spatial scale of interaction. *Europhys. Lett.* **2009**, *88*, 68002. [CrossRef]
9. Brigatti, E.; Núñez-López, M.; Oliva, M. Analysis of a spatial Lotka-Volterra model with a finite range predator–prey interaction. *Eur. Phys. J. B* **2011**, *81*, 321. [CrossRef]
10. Núñez-López, M.; Chacón-Acosta, G. Pattern formation in a predator–prey system with a finite interaction range in a channel-like region using the Fick–Jacobs diffusion approach. *Physica D* **2022**, *433*, 133194. [CrossRef]
11. Patnaik, S.; Hollkamp, J.P.; Semperlotti, F. Applications of variable-order fractional operators: A review. *Proc. R. Soc. A. Math. Phys. Eng. Sci.* **2020**, *476*, 20190498. [CrossRef]
12. Sun, H.; Zhang, Y.; Baleanu, D.; Chen, W.; Chen, Y. A new collection of real world applications of fractional calculus in science and engineering. *Commun. Nonlinear Sci. Numer. Simul.* **2018**, *64*, 213–231. [CrossRef]

13. Henry, B.I.; Langlands, T.A.M. Turing pattern formation in fractional activator-inhibitor systems. *Phys. Rev. E* **2005**, *72*, 026101. [CrossRef] [PubMed]
14. Carfora, M.F.; Torcicollo, I. A Fractional-in-Time Prey–Predator Model with Hunting Cooperation: Qualitative Analysis, Stability and Numerical Approximations. *Axioms* **2021**, *10*, 78. [CrossRef]
15. Ghosh, U.; Pal, S.; Banerjee, M. Memory effect on Bazykin's predator–prey model: Stability and bifurcation analysis. *Chaos Solitons Fractals* **2021**, *143*, 110531. [CrossRef]
16. Yin, H.; Wen, X. Pattern Formation through Temporal Fractional Derivatives. *Sci. Rep.* **2018**, *8*, 5070. [CrossRef]
17. Tang, B. Dynamics for a fractional-order predator–prey model with group defense. *Sci. Rep.* **2020**, *10*, 4906. [CrossRef] [PubMed]
18. Gafiychuk, V.V.; Datsko, B.Y. Pattern formation in a fractional reaction–diffusion system. *Physica A* **2006**, *365*, 300–306. [CrossRef]
19. Gafiychuk, V.V.; Datsko, B.Y. Stability analysis and oscillatory structures in time-fractional reaction–diffusion systems. *Phys. Rev. E* **2007**, *75*, 055201. [CrossRef]
20. Datsko, B.; Gafiychuk, V. Complex nonlinear dynamics in subdiffusive activator–inhibitor systems. *Commun. Nonlinear Sci. Numer. Simul.* **2012**, *17*, 1673–1680.. [CrossRef]
21. Zhang, L.; Tian, C. Turing pattern dynamics in an activator-inhibitor system with superdiffusion. *Phys. Rev. E***2014**, *90*, 062915. [CrossRef]
22. Torabi, R.; Rezaei, Z. Instability in reaction-superdiffusion systems. *Phys. Rev. E* **2016**, *94*, 052202. [CrossRef]
23. Nicolis, G. *Introduction to Nonlinear Science*, 1st ed.; Cambridge University Press: Cambridge, UK, 1995.
24. Gjurchinovski, A.; Sandev, T.; Urumov, V. Delayed feedback control of fractional-order chaotic systems. *J. Phys. A: Math. Theor.* **2010**, *43*, 445102. [CrossRef]
25. Mantignon, D. Stability results for fractional differential equations with applications to control processing. *Comput. Eng. Syst. Appl.* **1996**, *2*, 963–968.

computer sciences and mathematics forum

MDPI

Proceeding Paper

Dynamic Analysis for the Physically Correct Model of a Fractional-Order Buck-Boost Converter †

Daniel F. Zambrano-Gutierrez [1], Jorge M. Cruz-Duarte [1], Gerardo Humberto Valencia-Rivera [1], Ivan Amaya [1] and Juan Gabriel Avina-Cervantes [2,*]

[1] Tecnológico de Monterrey, Av. Eugenio Garza Sada 2501, Col. Tecnológico, Monterrey 64700, Mexico
[2] Telematics Group, Department of Electronics Engineering, University of Guanajuato, Carr. Salamanca-Valle de Santiago km 3.5 + 1.8 km, Comunidad de Palo Blanco, Salamanca 36885, Mexico
* Correspondence: avina@ugto.mx
† Presented at the 5th Mexican Workshop on Fractional Calculus (MWFC), Monterrey, Mexico, 5–7 October 2022.

Abstract: This work proposes a fractional-order mathematical model of a Buck-Boost converter performing in continuous conduction mode. To do so, we employ the average duty-cycle representation in state space, driven by the nonadimensionalize approach to avoid unit inconsistencies in the model. We also consider a Direct Current (DC) analysis through the fractional Riemann–Liouville (R-L) approach. Moreover, the fractional order Buck-Boost converter model is implemented in the Matlab/Simulink setting, which is also powered by the Fractional-order Modeling and Control (FOMCON) toolbox. When modifying the fractional model order, we identify significant variations in the dynamic converter response from this simulated scenario. Finally, we detail how to achieve a fast dynamic response without oscillations and an adequate overshoot, appropriately varying the fractional-order coefficient. The numerical results have allowed us to determine that with the decrease of the fractional order, the model presents minor oscillations, obtaining an output voltage response six times faster with a significant overshoot reduction of 67%, on average.

Keywords: fractional order Buck-Boost converter; modeling; Riemann–Liouville fractional derivative; FOMCON; steady state analysis

Citation: Zambrano-Gutierrez, D.F.; Cruz-Duarte, J.M.; Valencia-Rivera, G.H.; Iván Amaya; Avina-Cervantes, J.G. Dynamic Analysis for the Physically Correct Model of a Fractional-Order Buck-Boost Converter. *Comput. Sci. Math. Forum* **2022**, *4*, 2. https://doi.org/10.3390/cmsf2022004002

Academic Editors: Porfirio Toledo-Hernández

Published: 22 November 2022

1. Introduction

Modern power electronics techniques aim to provide an efficient way to transform electrical energy [1]. One is a Direct Current (DC–DC) voltage converter [2], which transforms an input voltage into an output voltage of a different magnitude, preserving its exact nature. The main goal is to supply a regulated voltage with a minimum ripple. DC–DC converters are switched sources that transform the input voltage to the desired output value with elements that intrinsically make the system non-linear. These converters are widely used, especially as power supplies in computer hardware and medical equipment [3]. The adequate control of the output voltage of these converters has been an essential subject of study during the last few years. Therefore, the switching operation is mainly responsible for their non-linear behavior and increasing design complexity [4,5].

The literature is prolific in studying integer-order models of DC–DC converters. Nevertheless, the capacitor and inductor could behave depending on fractional derivatives [1,6]. Therefore, fractional order models provide a more accurate description and deeper insight into physical processes [7,8]. In recent years, there has been significant study and development of fractional order systems [9,10]. Unfortunately, the inconsistency of units at the time of modeling is often overlooked when trying to model these electronic elements. There are three most used definitions of fractional calculus: Caputo Derivative (CD), Riemann–Liouville (R-L) fractional integral, and Grünwald–Letnikov (G-L) derivative [11]. Because of differences between the fractional calculus definitions,

the model results under different fractional orders may present variations related to the used fractional derivative and the occasional requirement of initial conditions.

This work analyzes the fractional order model of a Buck-Boost converter, its system is nondimensionalized, and its properties are in Continuous Conduction Mode (CCM). In doing so, we first nondimensionalized the fractional-order model of such a converter represented in the state space. Next, we consider the converter's duty cycle to achieve an average model in the state–space of fractional order. Afterward, we analyze the non-linear nature of the Buck-Boost converter fractional representation to determine the values for which the converter's performance increases.

The main contributions of the proposed Fractional-order Buck-Boost model were a decrease in the output voltage oscillations or harmonics, fast settling time, and a nondimensionalized version of the inductor current and capacitor voltage responses at a stable state.

2. Mathematical Modeling

This section describes the mathematical procedure we followed for analyzing and modeling the fractional-order Buck-Boost converter. First, we detail the most relevant aspects of the traditional converter model using classical calculus. Then, we apply the non-dimensionalization procedure to achieve a physically correct model.

2.1. DC–DC Buck-Boost Converter

The DC–DC Buck-Boost converter is derived from the combination of elementary converters such as Buck and Boost. The resulting configuration can provide an output voltage of inverse polarity, either greater or smaller than the input voltage. In this study, we replace the integer-order capacitor and inductor with fractional-order ones to transform the traditional converter model into the fractional domain. Figure 1 shows the circuit based on non-integer calculus representing the fractional-order Buck-Boost converter.

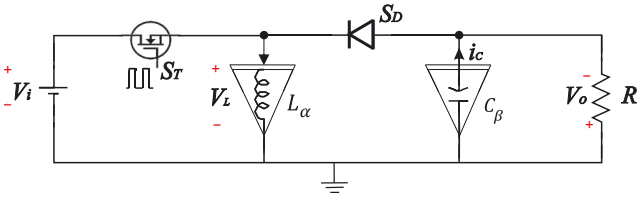

Figure 1. Fractional-order Buck-Boost converter.

In this circuit, R [Ω] corresponds to the load, Vi [V] stands for the input voltage, S_T represents an ideal switching power MOSFET, and S_D an ideal diode. In a broad sense, the converter works as follows: when it operates in CCM, it appears in two switching states defined below.

1. State 1: S_T = ON and S_D = OFF, for $nT < t \leq (n + D_c)T$.
2. State 2: S_T = OFF and S_D = ON, for $(n + D_c)T < t \leq (n + 1)T$.

In both states, n is an integer, T is the switching period, and D_c is the duty cycle of the Pulse Width Modulation (PWM) commuting S_T, which is defined as the ratio between the turn-on time of S_T and T. Hence, States 1 and 2 switch periodically in a stable state. In practice, obtaining a fractional model of the capacitor and inductor is possible based on the pioneering analysis performed by Zhang et al. [12] and Jiang and Zhang [13]. Consequently, the inductor's voltage v_L and the capacitor's current i_c can be represented using a fractional model, such as,

$$v_L(t) = L\frac{d^\alpha i_L}{dt^\alpha}, \quad i_C(t) = C\frac{d^\beta v_C}{dt^\beta}, \tag{1}$$

where α and β denote the fractional order of the derivatives for the inductor's current i_L and capacitor's voltage v_c, respectively.

This model contains two features worth noticing. The former is when $\alpha = \beta = 1$, so the inductor and the capacitor components behave as ideal electronic components of integer order derivatives. The latter is when $\{\alpha, \beta\} \in (0, 1)$ presents a fractional order.

Considering the particular case when $S_T =$ ON and $S_D =$ OFF, the fractional-order Buck-Boost converter turns into State 1.

Applying Kirchhoff's voltage law over the equivalent circuits of Figure 2, it is easy to obtain,

$$L\frac{d^{\alpha} i_L}{dt^{\alpha}} = V_i, \quad C\frac{d^{\beta} v_C}{dt^{\beta}} = -\frac{v_C}{R}. \tag{2}$$

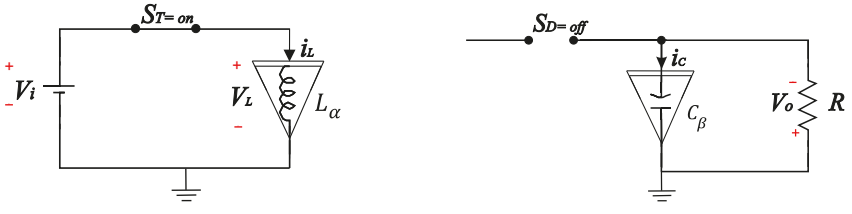

(**a**) (**b**)

Figure 2. Equivalent circuits of the Buck-Boost converter in State 1 with $S_T =$ on and $S_D =$ off. (**a**) Equivalent circuit of the Buck-Boost converter in State 1 and $S_T =$ ON. (**b**) Equivalent circuit of the Buck-Boost converter in State 1 and $S_D =$ OFF.

Meanwhile, when the $S_T =$ OFF and $S_D =$ ON, the fractional-order Buck-Boost converter is in State 2, as Figure 3 depicts.

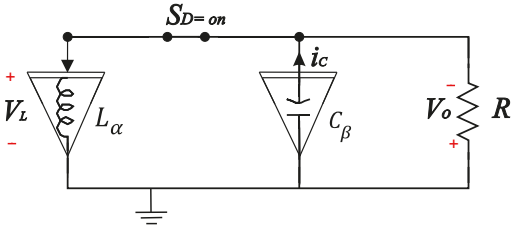

Figure 3. Equivalent circuit of the Buck-Boost converter in State 2 with $S_T =$ OFF and $S_D =$ ON.

Performing a Kirchhoff's voltage law analysis on the equivalent circuit in Figure 3, the fractional-order differential equations supporting the State 2 analysis are,

$$\begin{aligned} L\frac{d^{\alpha} i_L}{dt^{\alpha}} &= -v_C, \\ C\frac{d^{\beta} v_C}{dt^{\beta}} &= i_L - \frac{v_C}{R}. \end{aligned} \tag{3}$$

Merging (2) and (3) and implementing the state-space averaging model of the fractional-order Buck-Boost converter operating in CCM leads to the next coupled model:

$$\begin{aligned} L\frac{d^{\alpha}\langle i_L\rangle_T}{dt^{\alpha}} &= S_D\langle V_i\rangle_T - (1 - S_D)\langle v_C\rangle_T, \\ C\frac{d^{\beta}\langle v_C\rangle_T}{dt^{\beta}} &= -\frac{\langle v_C\rangle_T}{R} + (1 - S_D)\langle i_L\rangle_T. \end{aligned} \tag{4}$$

From these expressions, it is essential to recall that $\langle x \rangle_T$, for any $x(t)$, is the average value of this variable x during a switching period, and it can be numerically computed as follows,

$$\langle x \rangle_T = \frac{1}{T} \int_t^{t+T} x(t)\, dt. \tag{5}$$

2.2. Fractional-Order DC–DC Buck-Boost Converter

It is well-known that circuit variables in the converter, such as inductor's current i_L and capacitor's voltage v_c, present high-order harmonics due to the commutation sequence related to the operating principle of the Buck-Boost converter. These harmonics are eliminated by averaging the circuit variables, considering a switching period. Furthermore, when linearizing the model and obtaining the system transfer function, the averaged model of the converter is given by,

$$\begin{aligned} L\frac{d^{\alpha} i_L}{dt^{\alpha}} &= D_c\, V_i - (1 - D_c) v_c, \\ C\frac{d^{\beta} v_c}{dt^{\beta}} &= -\frac{v_c}{R} + (1 - D_c) i_L. \end{aligned} \tag{6}$$

Since a fractional-order derivative is used, such a transformation procedure generates inconsistency in the units of the model depending on the chosen operator [14]. Consequently, it is paramount to apply a nonadimensionalize procedure to render fractional-order differential equations with dimensions physically correct. Next, the characteristic parameters used to nonadimensionalize are

$$\begin{aligned} \hat{\tau} = \frac{t}{L/R} \quad &\longrightarrow \quad dt = \frac{L}{R} d\hat{\tau}, \\ \hat{\phi} = \frac{i_L}{V_i/R} \quad &\longrightarrow \quad di_L = \frac{v_i}{R} d\hat{\phi}, \\ \hat{\psi} = \frac{v_c}{V_i} \quad &\longrightarrow \quad dv_c = V_i d\hat{\psi}. \end{aligned} \tag{7}$$

Therefore, the nondimensional model is obtained by substituting (7) into (6), as follows

$$\begin{aligned} \frac{d^{\alpha} \hat{\phi}}{d\hat{\tau}^{\alpha}} &= -(1 - D_c)\hat{\psi} + D_c, \\ \frac{d^{\beta} \hat{\psi}}{d\hat{\tau}^{\beta}} &= k_{\tau}\left[-\hat{\psi} + (1 - D_c)\hat{\phi}\right], \end{aligned} \tag{8}$$

where $k_{\tau} = \frac{L/R}{RC}$ is a constant produced by nondimensionalizing (6).

As in the integer case, the fractional state–space model is defined by two equations [15]:

1. A state equation, where each state $x_i(t)$ is differentiated to a fractional-order α_i, is given in the case of a generalized state–space model. All states $x_i(t)$ are differentiated to the same fractional order α for the commensurate case.
2. An output equation depends on the internal states and the inputs, as in the integer case.

Before obtaining the fractional state–space model, we first applied the concept of fractional derivative to the classic state–space representation. In consequence, such a fractional model in the state–space domain corresponds to

$$\begin{aligned} D^{(\alpha)}(x) &= A_s x + B_s u, \\ y &= C_s x + D_s u, \end{aligned} \tag{9}$$

where $D^{(\alpha)}(x) = [D^{\alpha_1}x_1, D^{\alpha_2}x_2, \ldots, D^{\alpha_n}]^{\mathsf{T}}$, since A_s, B_s, C_s, and D_s are the state–space representation model matrices. Roughly speaking, we can obtain any model in the Laplace domain by using its transform and considering zero initial conditions,

$$G(s) = C_s\left[(s^{\alpha}I_n - A_s)^{-1}\right]B_s + D_s, \tag{10}$$

where D_s is generally null. The fractional state–space model, derived from (8), is now defined as

$$\begin{bmatrix} \frac{d^{\alpha}\hat{\phi}}{d\hat{\tau}^{\alpha}} \\ \frac{d^{\beta}\psi}{d\hat{\tau}^{\beta}} \end{bmatrix} = \underbrace{\begin{bmatrix} 0 & -(1-D_c) \\ k_{\tau}(1-D_c) & -k_{\tau} \end{bmatrix}}_{A_s}\begin{bmatrix} \hat{\phi} \\ \hat{\psi} \end{bmatrix} + \underbrace{\begin{bmatrix} D_c \\ 0 \end{bmatrix}}_{B_s}u(t), \quad y = \underbrace{\begin{bmatrix} 1 & 0 \\ 0 & 1 \end{bmatrix}}_{Cs}\begin{bmatrix} \hat{\phi} \\ \hat{\psi} \end{bmatrix}. \tag{11}$$

For the sake of simplicity, we assume that $\alpha = \beta$. Thus, the proposed transfer function is obtained from (11) as follows,

$$M = s^{\alpha}I - A_s = \begin{bmatrix} s^{\alpha} & (1-D_c) \\ -k_{\tau}(1-D_c) & s^{\alpha}+k_{\tau} \end{bmatrix}, \tag{12}$$

where the characteristic equation is given by

$$|M| = s^{2\alpha} + k_{\tau}s^{\alpha} + (1-D_c)^2 k_{\tau}, \tag{13}$$

$$G(s) = \frac{1}{s^{2\alpha} + k_{\tau}s^{\alpha} + k\tau(1-D_c)^2}\begin{bmatrix} 1 & 0 \\ 0 & 1 \end{bmatrix}\begin{bmatrix} s^{\alpha}+k_{\tau} & -(1-D_c) \\ k_{\tau}(1-D_c) & s^{\alpha} \end{bmatrix}\begin{bmatrix} D_c \\ 0 \end{bmatrix}. \tag{14}$$

$$G(S) = \begin{bmatrix} \frac{D_c(s^{\alpha}+k_{\tau})}{s^{2\alpha} + k_{\tau}s^{\alpha} + (1-D_c)^2 k_{\tau}} \\ \frac{k_{\tau}D_c(1-D_c)}{s^{2\alpha} + k_{\tau}s^{\alpha} + (1-D_c)^2 k_{\tau}} \end{bmatrix}U(S), \tag{15}$$

where $U(S) = \mathcal{L}\{u(t)\}$ is the Laplace transform of $u(t)$. Once the system of equations is nondimensionalized, we can express the output $\hat{\phi}$ and $\hat{\psi}$ as follows,

$$\hat{\phi}(s) = \frac{D_c(s^{\alpha}+k_{\tau})U(s)}{s^{2\alpha} + k_{\tau}s^{\alpha} + (1-D_c)^2 k_{\tau}}, \tag{16}$$

$$\hat{\psi}(s) = \frac{k_{\tau}\,D_c(1-D_c)\,U(s)}{s^{2\alpha} + k_{\tau}s^{\alpha} + (1-D_c)^2 k_{\tau}}. \tag{17}$$

3. Stable-State Analysis

The linearized model (6) is solved using the definition of the Riemann–Liouville derivative, defined as

$${}^{\mathrm{RL}}_{a}D^{\alpha}_{b}f(t) = \frac{1}{\Gamma(1-\alpha)}\frac{d}{dt}\int_a^b \frac{f(t)}{(t-\tau)^{\alpha}}d\tau, \tag{18}$$

where $\Gamma(\cdot)$ is the Gamma function and [a, b] is the interval of the stable-state signal.

Thereby, the fractional derivatives of the variables i_L and v_c are obtained from (18), respectively, as shown,

$$\begin{aligned} \frac{d^{\alpha}i_L}{dt^{\alpha}} &= \frac{1}{\Gamma(1-\alpha)}\frac{d}{dt}\int_{nT}^{(n+1)T}\frac{i_L}{(t-\tau)^{\alpha}}d\tau = \frac{i_L t_s^{-\alpha}}{\Gamma(1-\alpha)}, \\ \frac{d^{\beta}v_c}{dt^{\beta}} &= \frac{1}{\Gamma(1-\beta)}\frac{d}{dt}\int_{nT}^{(n+1)T}\frac{v_c}{(t-\tau)^{\beta}}d\tau = \frac{v_c t_s^{-\beta}}{\Gamma(1-\beta)}, \end{aligned} \tag{19}$$

where n is the current operating cycle of the PWM, t_s is the time needed so that the Buck-Boost converter achieves the stable state. Once the converter reaches this state, the inductor current (i_L) and capacitor voltage (v_c) are considered constant and $t_s \approx T$.

Substituting (19) in (6), the inductor current and capacitor voltage at stable state are defined as,

$$i_L = \frac{V_i D_c \left[RC t_s^{-\beta} + \Gamma(1-\beta) \right]}{\Gamma(1-\beta) R (1-D_c)^2 + \frac{L t_s^{-\alpha} \Gamma(1-\beta)}{\Gamma(1-\alpha)} + \frac{RC L t_s^{-(\beta+\alpha)}}{\Gamma(1-\alpha)}}, \tag{20}$$

$$v_c = \frac{V_i D_c (1-D_c) R \Gamma(1-\beta)\Gamma(1-\alpha)}{R\,\Gamma(1-\beta)\Gamma(1-\alpha)(1-D_c)^2 + \Gamma(1-\beta) L t_s^{-\alpha} + RLC t_s^{-(\alpha+\beta)}}. \tag{21}$$

The Buck-Boost converter voltage ratio G_v at stable state is obtained by (21) since the capacitor voltage is directly the output voltage,

$$G_v = \frac{v_c}{V_i} = \frac{D_c (1-D_c) R \Gamma(1-\beta)\Gamma(1-\alpha)}{R\,\Gamma(1-\beta)\Gamma(1-\alpha)(1-D_c)^2 + \Gamma(1-\beta) L\, t_s^{-\alpha} + RLC\, t_s^{-(\alpha+\beta)}}. \tag{22}$$

Table 1 presents the circuit parameters used in the numerical simulations and the fractional-order converter model analysis in the stable state.

Table 1. Parameters used for the simulations to obtain the Buck-Boost converter fractional model response in the stable state.

Parameter	Values
Stable–state time	$t_s = T = 4$ ms
Input voltage	$V_i = 25$ V
Inductor	$L = 3$ mH
Capacitor	$C = 150$ µF
Load	$R = 30\ \Omega$
Duty cycle	$D_c = 0.6$

Figure 4 displays the response of the Buck-Boost converter fractional model in the stable state. Plus, in Figure 4b, we fixed α, varying the value of β. Notice that the G_v response falls slowly but then recovers rapidly. Figure 4a is the opposite case. When varying β, the G_v response tends to mimic the behavior shown in Figure 4b. Additionally, Figure 4c shows the dynamic variation of the G_v with the change of the fractional order, presenting a minimum gain when $\alpha = \beta = 0.956$.

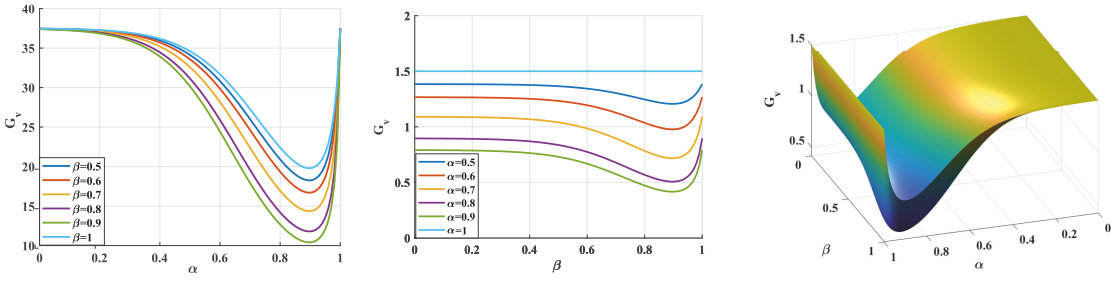

(**a**) (**b**) (**c**)

Figure 4. Visualization of α and β influence the response of G_V in stable-state. (**a**) Relationship between G_v and α. (**b**) Relationship between G_v and β. (**c**) Three-dimensional representation of α and β variations.

4. Numerical Simulation

The mathematical model of the fractional-order Buck-Boost converter driven by CCM is implemented in the Matlab/Simulink environment through the FOMCON toolbox [16]. According to the state–space model given by (11), we construct the block diagram of the system, as shown in Figure 5. It is noteworthy that $1/s^{\alpha}$ is the fractional integral unit.

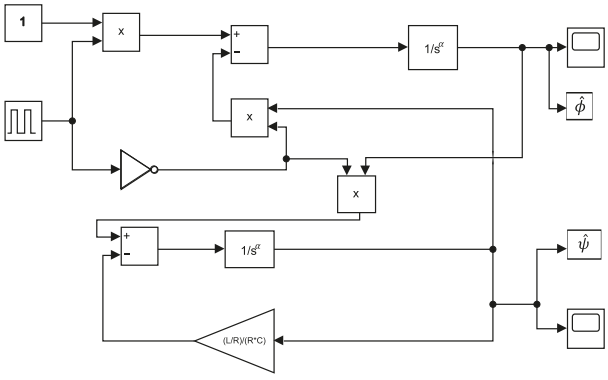

Figure 5. Numerical simulation of the fractional mathematical model by Matlab/Simulink.

The parameters for this numerical simulation were previously given in Table 1. Furthermore, Figure 6 shows the dynamic response of $\hat{\phi}$ and $\hat{\psi}$, cf. (7), which are associated with the nondimensionalized inductor current (i_L) and capacitor voltage (v_C), respectively.

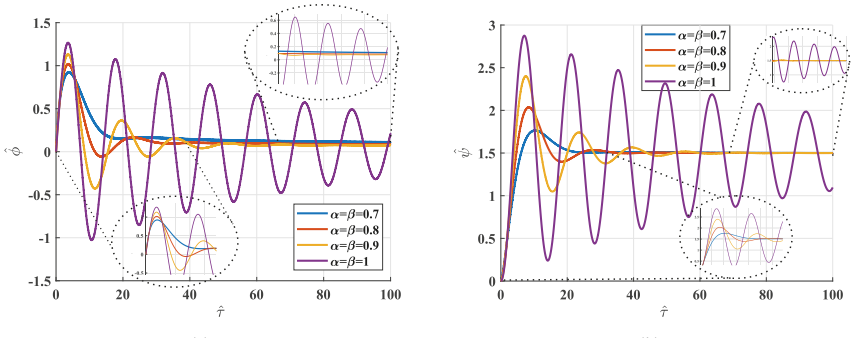

(**a**) (**b**)

Figure 6. Nondimensionalized voltage and current of the fractional-order Buck-Boost converter. (**a**) Nondimensionalized inductor's current. (**b**) Nondimensionalized capacitor's voltage.

Figure 6a displays the behavior of the nondimensionalized inductor current with different α values. It is worth commenting that when $\alpha = 0.7$, i_L achieves the desired behavior, exhibiting a lower overshoot without negative values.

Figure 6b shows the nondimensionalized capacitor voltage under different scenarios. We noticed that when the fractional order tends to unity, we obtain the traditional responses of the converter, containing a myriad of oscillations. Further, the converter must evolve for a long time to reach the desired reference. However, when α begins to decrease, this reference is tracked in a shorter time. A similar behavior occurs with the nondimensional inductor's current for the nondimensional voltage when $\alpha = 0.7$, as Figure 7 shows. The obtained output is the desired one in this type of converter: a smooth and controlled voltage rise, a lower overshoot concerning the other solutions, and a fast settling time.

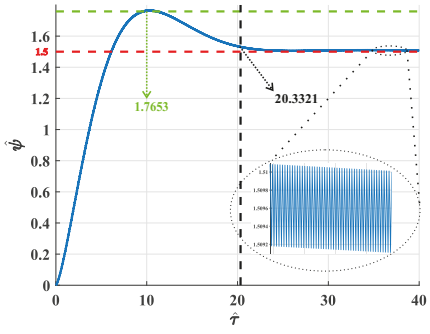

Figure 7. Nondimensionalized capacitor voltage with $\alpha = 0.7$.

The red dotted line represents the voltage reference value set in 1.5. The green dotted line represents the maximum peak reached by the converter, which has a value of 1.7653 that translates into an overshoot of 17.6854%. The black dotted line corresponds to the reached settling time by this device, which is equal to $\hat{t}_{ss} = 20.3321$, using the criterion of 5%. Note that in the lower right part of Figure 7, a zoomed version of the output voltage ripple response is located after achieving the stable state. Such an output ripple ranges between 0.5100 and 0.5092. It is noteworthy that these values are nondimensionalized, and to have the expected values with real units, we must use the reconversion described in (7).

We attribute the behavior observed in Figure 6a,b to the location of the poles of the characteristic polynomial described in (13). As one may see, the α value directly affects the imaginary part of the poles. Indeed, when α starts to decrease, the imaginary pole magnitude tends to decrease. For this reason, the converter output response changes its behavior from an under-damped system with many oscillations to an under-damped system with a single overshoot. Notwithstanding, the α value should be carefully chosen, since a small α value may provoke the converter to not work correctly and hinder the construction of the electrical elements of the fractional order circuit. Table 2 exhibits the converter performance w.r.t. the variation of α. It is observed that $\alpha = 1$ presents an overshoot of 71.8907 V, representing 91.7086%, while $\alpha = 0.7$ produces an overshoot of 17.6854%. We can observe that the position of the poles cthange.

Table 2. Electrical characteristics of the fractional-order Buck-Boost Converter while varying α.

		Nondimensionalized			**Real**		
α	**Poles**	$\hat{L}$	$\hat{t}_{ss}$	$\hat{v}_f$	L **[v]**	t_{ss} **[ms]**	v_f **[v]**
0.7	$-0.0391 \pm 0.0165i$	1.7653	20.420	1.5003	37.5075	2.0420	37.5075
0.8	$-0.0465 \pm 0.0426i$	2.0369	29.832	1.5002	50.9225	2.9832	37.5045
0.9	$-0.0457 \pm 0.0725i$	2.4010	48.5906	1.5001	60.0257	4.8590	37.5034
1	$-0.0375 \pm 0.1029i$	2.8756	318.6323	1.5020	71.8907	31.8620	37.5511

On the other hand, we employ the phase portrait approach to represent the Buck-Boost converter dynamic in the phase plane geometrically. The main idea is to identify those equilibrium points permitting the system to maintain stable states. Retracing the path of the fractional calculus concept applied to this work, the phase portraits shown in Figure 8 considered null initial conditions with different α values.

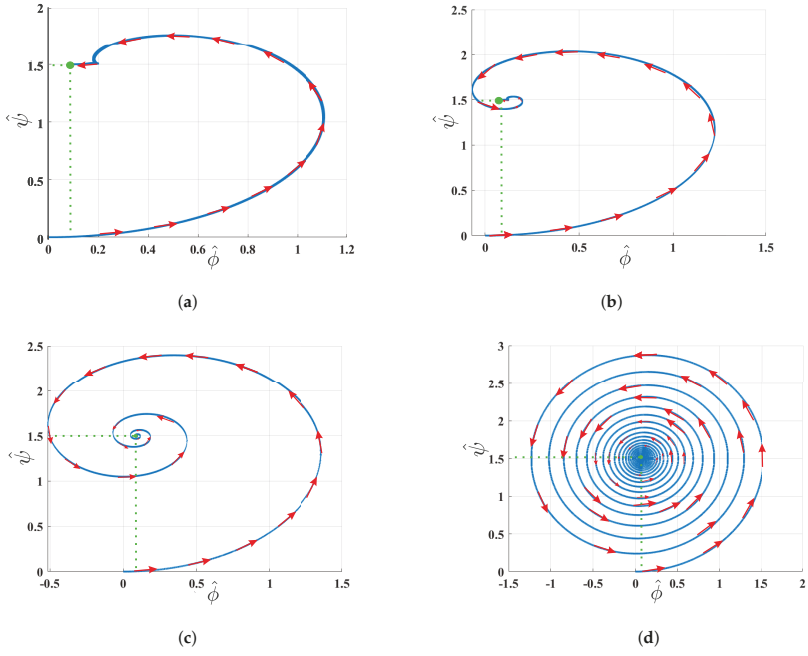

Figure 8. Phase portrait of the fractional-order Buck-Boost converter at different values of α: (**a**) $\alpha = 0.7$, (**b**) $\alpha = 0.8$, (**c**) $\alpha = 0.9$, (**d**) $\alpha = 1$.

Analyzing the obtained phase portraits, one can see that the equilibrium point $(1.54, 0.2)$ remains constant for all α values. Furthermore, we detected two significant findings regarding the α range. The first one liaises a low α value so that the trajectory toward the equilibrium point is much faster and more stable than in the other cases (cf. Figure 8a). The second one corresponds to the unit value of α, which leads to an asymptotically stable spiral point (cf. Figure 8d). With this in mind, the obtained results prove that a fractional-order Buck-Boost model yields an improved behavior and performance than an integer-order model.

5. Conclusions

In general terms, most DC–DC converters adopt the integer-order approach for representing the behavior of their electrical components. Consequently, the mathematical models of such converters do not match the reported experimental data. Therefore, the proposed fractional-order Buck-Boost converter model was nondimensionalized, and the fractional-order state–space model was deduced to avoid integer-order model inconsistencies in the analysis. To carry this out, the inductor current and capacitor voltage were determined through the fractional Riemann–Liouville definition in the stable state. Moreover, the steady-state response of the system showed variations while the order of the derivative changed. Some models demonstrated a remarkable performance over the integer-order model. This phenomenon happened for α values of 0.7. Therefore, we consider that decreasing below this value makes building the model very difficult. The proposed nondimensionalized model was tested using the Simulink and FOMCOM. It is worth mentioning that the parameter α directly impacts the capacitor voltage and inductor current responses. Additionally, we determined that the converter reaches the desired behavior when $\alpha = 0.7$. According to the obtained results, the fractional-order concept used in this work seems feasible for achieving more realistic models of DC–DC

converters. Finally, the experimental tests led to the design of a Buck-Boost converter with fractional-order electrical components that do not require complex control schemes.

Author Contributions: Conceptualization, D.F.Z.-G.; formal analysis, J.M.C.-D. and J.G.A.-C.; investigation, D.F.Z.-G., J.M.C.-D., G.H.V.-R., I.A., and J.G.A.-C.; methodology, D.F.Z.-G., J.M.C.-D., and J.G.A.-C.; validation, J.M.C.-D. and J.G.A.-C.; writing—original draft, D.F.Z.-G., G.H.V.-R., I.A., and J.G.A.-C.; writing—review and editing, D.F.Z.-G. and J.M.C.-D. All authors read and agreed to the published version of the manuscript.

Funding: This project was funded by the Mexican National Council of Science and Technology CONACyT grant 1046000, under Grant Number and the University of Guanajuato Grant 171/2022. Tecnológico de Monterrey under Grant Number A008356756.

Institutional Review Board Statement: Not required for this study.

Informed Consent Statement: No formal written consent was required for this study.

Data Availability Statement: Data available under a formal demand.

Acknowledgments: This research was supported by the Tecnológico de Monterrey project A008356756 and the University of Guanajuato project CIIC 171/2022.

Conflicts of Interest: All authors declare no conflicts of interest in this paper.

References

1. Yu, W.; Qian, H.; Lai, J.S. Design of High-Efficiency Bidirectional DC–DC Converter and High-Precision Efficiency Measurement. *IEEE Trans. Power Electron.* **2010**, *25*, 650–658. [CrossRef]
2. Masri, S.; Chan, P.W. Design and development of a DC-DC boost converter with constant output voltage. In Proceedings of the 2010 International Conference on Intelligent and Advanced Systems, Kuala Lumpur, Malaysia, 15–17 June 2010; pp. 1–4. [CrossRef]
3. Forouzesh, M.; Siwakoti, Y.P.; Gorji, S.A.; Blaabjerg, F.; Lehman, B. Step-Up DC–DC Converters: A Comprehensive Review of Voltage-Boosting Techniques, Topologies, and Applications. *IEEE Trans. Power Electron.* **2017**, *32*, 9143–9178. [CrossRef]
4. Mumtaz, F.; Zaihar Yahaya, N.; Tanzim Meraj, S.; Singh, B.; Kannan, R.; Ibrahim, O. Review on non-isolated DC-DC converters and their control techniques for renewable energy applications. *Ain Shams Eng. J.* **2021**, *12*, 3747–3763. [CrossRef]
5. Rojas-Dueñas, G.; Roger Riba, J.; Moreno-Eguilaz, M. Modeling of a DC-DC Bidirectional Converter used in Mild Hybrid Electric Vehicles from Measurements. *Measurement* **2021**, *183*, 109838. [CrossRef]
6. Westerlund, S. Dead matter has memory! *Phys. Scr.* **1991**, *43*, 174–179. [CrossRef]
7. Patnaik, S.; Hollkamp, J.P.; Semperlotti, F. Applications of variable-order fractional operators: A review. *Proc. R. Soc. A* **2020**, *476*, 20190498. [CrossRef] [PubMed]
8. Zhou, P.; Ma, J.; Tang, J. Clarify the physical process for fractional dynamical systems. *Nonlinear Dyn.* **2020**, *100*, 2353–2364. [CrossRef]
9. Muresan, C.I.; Birs, I.; Ionescu, C.; Dulf, E.H.; De Keyser, R. A Review of Recent Developments in Autotuning Methods for Fractional-Order Controllers. *Fractal Fract.* **2022**, *6*, 37. [CrossRef]
10. Naifar, O.; Makhlouf, A.B. *Fractional Order Systems-Control Theory and Applications*; Studies in Systems, Decision and Control (SSDC); Springer: Berlin/Heidelberg, Germany, 2022; Volume 364.
11. Wang, Y.; Liu, Y.; Hou, C. New concepts of fractional Hahn'sq, ω q, ω-derivative of Riemann–Liouville type and Caputo type and applications. *Adv. Differ. Equ.* **2018**, *2018*, 8262860. [CrossRef]
12. Zhang, L.; Kartci, A.; Elwakil, A.; Bagci, H.; Salama, K.N. Fractional-Order Inductor: Design, Simulation, and Implementation. *IEEE Access* **2021**, *9*, 73695–73702. [CrossRef]
13. Jiang, Y.; Zhang, B. Comparative Study of Riemann–Liouville and Caputo Derivative Definitions in Time-Domain Analysis of Fractional-Order Capacitor. *IEEE Trans. Circuits Syst. II Express Briefs* **2020**, *67*, 2184–2188. [CrossRef]
14. Cruz-Duarte, J.M.; Guía-Calderón, M.; Rosales-García, J.J.; Correa, R. Determination of a physically correct fractional-order model for electrolytic computer-grade capacitors. *Math. Methods Appl. Sci.* **2021**, *44*, 4366–4380. [CrossRef]
15. Djamah, T.; Djennoune, S.; Bettayeb, M. Identification of diffusion processes using fractional non commensurate order models. In Proceedings of the 2008 5th International Multi-Conference on Systems, Signals and Devices, Amman, Jordan, 20–22 July 2008; pp. 1–6. [CrossRef]
16. Tepljakov, A.; Vunder, V.; Petlenkov, E.; Nakshatharan, S.S.; Punning, A.; Kaparin, V.; Belikov, J.; Aabloo, A. Fractional-order modeling and control of ionic polymer-metal composite actuator. *Smart Mater. Struct.* **2019**, *28*, 084008. [CrossRef]

computer sciences and mathematics forum

MDPI

Proceeding Paper

Fractional Approach to the Study of Damped Traveling Disturbances in a Vibrating Medium †

Fernando Olivar-Romero

Tecnológico de Monterrey, School of Engineering and Sciences, Atizapán de Zaragoza 52926, Mexico; folivar@tec.mx

† Presented at the 5th Mexican Workshop on Fractional Calculus (MWFC), Monterrey, Mexico, 5–7 October 2022.

Abstract: The Cauchy problem of a time–space fractional partial differential equation which has as a particular case the damped wave equation is solved for the Dirac delta initial condition. The solution is obtained in terms of H-Fox functions and models the travel of a disturbance in a vibrating medium.

Keywords: fractional partial differential equation; Cauchy problem; H-Fox functions

Citation: Olivar-Romero, F. Fractional Approach to the Study of Damped Traveling Disturbances in a Vibrating Medium. *Comput. Sci. Math. Forum* **2022**, *4*, 1. https://doi.org/10.3390/cmsf2022004001

Academic Editors: Jorge M. Cruz-Duarte and Porfirio Toledo-Hernández

Published: 22 November 2022

1. Introduction

In previous works [1–3], the fractional space–time partial linear differential equation $D_t^{\alpha} u(x,t) = v_{\alpha,\beta}^2 \mathbb{D}_x^{\beta} u(x,t)$ has been solved. In such an expression, D_t^{α} indicates the time fractional derivative in the sense that Caputo (see Ref. [4]), $\mathbb{D}_x^{\beta}$ represents the space fractional operator in the sense of Riesz (see Ref. [5]) and $v_{\alpha,\beta}$ is a constant such that $[v_{\alpha,\beta}] = [L]^{\beta/2}[T]^{-\alpha/2}$, where $[L]$ and $[T]$ stand for the units of length and time, respectively. This equation includes as particular cases the heat equation [6] for $(\alpha,\beta) = (1,2)$, for which $v_{1,2}^2 = k$, where k stands for the thermometric conductivity, and the wave equation [7–10], for $(\alpha,\beta) = (2,2)$, for which $v_{2,2} = v$, where v represents the velocity of propagation of the wave. The Cauchy problem of such an equation with the Dirac delta initial condition is solved by means of Laplace and Fourier methods in Refs. [1–3]. In Ref. [1], the equation was solved in terms of generalized Wright functions [11]. The solution has different representations depending on which of the three cases $\alpha > \beta$, $\alpha = \beta$ or $\alpha < \beta$ is fulfilled. In Ref. [2], a unified representation of the solution was obtained for all possible combinations of α and β by solving the problem in terms of H-Fox functions. Furthermore, in Ref. [2], a Gaussian initial condition was also considered, leading to a series of H-Fox functions as a solution, where, in the appropriate limit, the solution for the Dirac delta initial condition is recovered. In Ref. [3], attention is paid to the particular case $\alpha = \beta$. The solution is obtained in terms of the well-known sine and cosine trigonometric functions. In the first two cases (Refs. [1,2]), the solution depends on the parameters α and β. Its solution enables on to recover the heat and wave equation solutions for $(\alpha,\beta) = (1,2)$ and $(\alpha,\beta) = (2,2)$, respectively. In the last case, (Ref. [3]), the main results depend on α and enable one to recover the wave equation solution for $\alpha = 2$. In addition, the integro-differential equations of integer order arise as particular cases of the mentioned equation: the first is obtained for $(\alpha,\beta) = (1,1)$ (see Refs. [1,2]) and the second for $(\alpha,\beta) = (2,1)$ (see Ref. [2]). The last is introduced in Ref. [2] as a complementary equation, a broader analysis of an such equation is made in Ref. [12].

In a recent work [13], the Cauchy problem of the more general fractional differential expression $[D_t^{\alpha} + a^{\alpha}]u(x,t) = v_{\alpha,\beta}^2 \mathbb{D}_x^{\beta} u(x,t)$ $(a > 0)$ that includes as a particular case the Klein–Gordon equation [14] (for its classical applications see, e.g., [15]), is solved in terms of a series of H-Fox functions. The solution is reduced to that of the equation $D_t^{\alpha} u(x,t) = v_{\alpha,\beta}^2 \mathbb{D}_x^{\beta} u(x,t)$ in the limit $a = 0$.

Numerical techniques to solve space–time fractional differential equations were proposed in Refs. [16–19]. In [16], they aimed to solve the equations of the wave type and

in Ref. [17], they aimed to solve the equations of the telegraph form, in both cases with constant coefficients. In Ref. [18], they aimed to solve equations of the Klein–Gordon-type and in Ref. [19], of a more general form, in these two last cases with variable coefficients.

Motivated by those previous works, we consider now the study of a fractional differential equation that includes as a limit case the damped wave equation. Such an equation has the form $[D_t^{\alpha} + \gamma^{\frac{\alpha}{2}} D_t^{\frac{\alpha}{2}}]u(x,t) = v_{\alpha,\beta}^2 \mathbb{D}_x^{\beta} u(x,t)$ with $\gamma > 0$. This work is addressed to solve the Cauchy problem of such a fractional differential equation for Dirac delta initial condition.

2. Problem Formulation

Let us consider the one-dimensional damped wave equation

$$\left[\frac{\partial^2}{\partial t^2} + \gamma \frac{\partial}{\partial t}\right] u(x,t) = v^2 \frac{\partial^2}{\partial x^2} u(x,t). \tag{1}$$

In Equation (1), $\gamma > 0$ represents the damping parameter and the constant v the velocity of the damped wave. By replacing the time derivative operators $\frac{\partial^2}{\partial t^2}$ and $\frac{\partial}{\partial t}$ in Equation (1) with the Caputo fractional derivative operators D_t^{α} and $D_t^{\frac{\alpha}{2}}$, respectively, (see its definition in Appendix A). We obtain the equation

$$\left[D_t^{\alpha} + \gamma^{\frac{\alpha}{2}} D_t^{\frac{\alpha}{2}}\right] u(x,t) = v_{\alpha}^2 \frac{\partial^2}{\partial x^2} u(x,t). \tag{2}$$

In Equation (2), $\alpha \in [1,2]$ and the constant v_{α} fulfills $[v_{\alpha}] = [L][T]^{-\frac{\alpha}{2}}$.

A more general expression of Equation (2) can be obtained by replacing the space-derivative operator $\frac{\partial^2}{\partial x^2}$ in Equation (2) with the Riesz fractional operator $\mathbb{D}_x^{\beta}$ (see its definition in Appendix A). We arrive at the expression

$$\left[D_t^{\alpha} + \gamma^{\frac{\alpha}{2}} D_t^{\frac{\alpha}{2}}\right] u(x,t) = v_{\alpha,\beta}^2 \mathbb{D}_x^{\beta} u(x,t). \tag{3}$$

In Equation (3), $\beta \in [1,2]$ and the constant $v_{\alpha,\beta}$ fulfills $[v_{\alpha,\beta}] = [L]^{\frac{\beta}{2}}[T]^{-\frac{\alpha}{2}}$. Additionally, $v_{\alpha,2} = v_{\alpha}$ and $v_{2,2} = v_2 = v$.

Let us consider a fractional η-order differential equation with $1 \leq \eta \leq 2$, derivatives defined in the sense of Caputo and solution $y(t)$. The Caputo fractional derivative is reduced to the first and second derivative operators for $\eta = 1$ and $\eta = 2$, respectively; this permits the equation to transit from a first-order differential equation for $\eta = 1$ to a second-order one for $\eta = 2$. For $1 < \eta \leq 2$, this equation requires two initial conditions to have a completely determined solution. For $\eta = 1$, the equation requires one initial condition for such purposes. To obtain a solution that permits to transit between the solution to the fractional differential equation for $\eta = 1$ to that of $\eta = 2$ through the parameter η, we may impose the initial condition $\frac{dy}{dt}|_{t=0} = 0$ for $1 < \eta \leq 2$. Taking into account the last considerations, we may impose the following initial conditions into Equation (3)

$$u(x,0) = \varphi(x), \qquad \frac{\partial u}{\partial t}(x,t)|_{t=0} = 0. \tag{4}$$

Equations (3) and (4) constitute the Cauchy problem to be solved. In this work, we consider the Dirac delta initial condition $u(x,0) = \varphi(x) = \mu\delta(x)$ and no boundary conditions.

3. Solution of the Problem

The Laplace transform $\mathcal{L}$ of Equation (3) is

$$(s^{\alpha} + \gamma^{\frac{\alpha}{2}} s^{\frac{\alpha}{2}}) U(x,s) - (s^{\alpha-1} + \gamma^{\frac{\alpha}{2}} s^{\frac{\alpha}{2}-1})\varphi(x) = v_{\alpha,\beta}^2 \mathbb{D}_x^{\beta} U(x,s). \tag{5}$$

In the above equation, $U(x,s) = \mathcal{L}[u(x,t)]$. The Fourier transform $\mathcal{F}$ of Equation (5) is

$$(s^{\alpha}+\gamma^{\frac{\alpha}{2}}s^{\frac{\alpha}{2}})\overline{U}(k,s)-(s^{\alpha-1}+\gamma^{\frac{\alpha}{2}}s^{\frac{\alpha}{2}-1})\phi(k)=-v_{\alpha,\beta}^{2}|k|^{\beta}\overline{U}(k,s), \tag{6}$$

where $\overline{U}(k,s)=\mathcal{F}[\mathcal{L}[u(x,t)]]$ and $\mathcal{F}[\varphi(x)]=\phi(k)$. The algebraic expression (6) is solved by

$$\overline{U}(k,s)=\frac{(s^{\alpha-1}+\gamma^{\frac{\alpha}{2}}s^{\frac{\alpha}{2}-1})\phi(k)}{s^{\alpha}+\gamma^{\frac{\alpha}{2}}s^{\frac{\alpha}{2}}+v_{\alpha,\beta}^{2}|k|^{\beta}}. \tag{7}$$

To obtain the solution $u(x,t)$, we first recover $U(x,s)$ by taking the inverse Fourier transform $\mathcal{F}^{-1}$ of $\overline{U}(k,s)$. From the definition of inverse Fourier transform, we have

$$U(x,s)=\frac{1}{\sqrt{2\pi}}\int_{-\infty}^{\infty}\frac{(s^{\alpha-1}+\gamma^{\frac{\alpha}{2}}s^{\frac{\alpha}{2}-1})\phi(k)e^{ikx}dk}{s^{\alpha}+\gamma^{\frac{\alpha}{2}}s^{\frac{\alpha}{2}}+v_{\alpha,\beta}^{2}|k|^{\beta}}. \tag{8}$$

Setting the initial condition $\varphi(x)=\mu\delta(x)$ into Equation (8) gives

$$U(x,s)=\frac{\mu\lambda^{\beta}}{2\pi s}\int_{-\infty}^{\infty}\frac{e^{ikx}dk}{\lambda^{\beta}+|k|^{\beta}},\qquad \lambda=\left(\frac{s^{\alpha}+\gamma^{\frac{\alpha}{2}}s^{\frac{\alpha}{2}}}{v_{\alpha,\beta}^{2}}\right)^{\frac{1}{\beta}}. \tag{9}$$

In Ref. [20], the integral in Equation (9) was calculated (as can also be seen in Ref. [2]), and the result leads to the following expression for $U(x,s)$

$$U(x,s)=\frac{\mu\lambda}{\beta s}H_{2,3}^{2,1}\left[\lambda|x|\,\middle|\,\begin{matrix}\left(1-\frac{1}{\beta},\frac{1}{\beta}\right),\left(\frac{1}{2},\frac{1}{2}\right)\\(0,1),\left(1-\frac{1}{\beta},\frac{1}{\beta}\right),\left(\frac{1}{2},\frac{1}{2}\right)\end{matrix}\right], \tag{10}$$

where $H_{p,q}^{m,n}[x|-]$ is the H-Fox function [21,22] (as can also be seen in Appendix A). The inverse Laplace transform $\mathcal{L}^{-1}$ of $U(x,s)$ is calculated in the Appendix B and gives the solution $u(x,t)$ as follows

$$u(x,t)=\frac{\mu}{\beta t^{\frac{\alpha}{\beta}}v_{\alpha,\beta}^{\frac{2}{\beta}}}\sum_{n=0}^{\infty}(\gamma t)^{\frac{\alpha n}{2}}\Theta_{n}(x,t;\alpha,\beta), \tag{11}$$

where

$$\Theta_{n}(x,t;\alpha,\beta)=H_{4,4}^{2,2}\left[\frac{|x|}{t^{\frac{\alpha}{\beta}}v_{\alpha,\beta}^{\frac{2}{\beta}}}\,\middle|\,\begin{matrix}\left(1-\frac{1}{\beta},\frac{1}{\beta}\right),\left(-\frac{1}{\beta},\frac{1}{\beta}\right),\left(\frac{1}{2},\frac{1}{2}\right),\left(1-\frac{\alpha}{\beta}+\frac{\alpha n}{2},\frac{\alpha}{\beta}\right)\\(0,1),\left(1-\frac{1}{\beta},\frac{1}{\beta}\right),\left(\frac{1}{2},\frac{1}{2}\right),\left(-\frac{1}{\beta}+n,\frac{1}{\beta}\right)\end{matrix}\right]. \tag{12}$$

4. Discussion of Results

In Figure 1, the graphic representation of the solution is depicted in Equations (11) and (12) for some combinations of (α,β). According to the graphics contained in the panel, the solution to Equation (3) can be studied in terms of a disturbance propagating in a vibrating medium. In all the cases presented herein, a mixture of diffusive and wave-like behavior can be observed in the traveling disturbances. As α becomes smaller, the diffusive behavior becomes more predominant. As α approaches 2, the wave-like behavior is predominant over the diffusive one and the effects of the reduction in the parameter β become notorious, as can be observed in the third column with the change in the shape in the center of the traveling disturbances, in contrast to the first and second columns where such changes are not evident. Such a phenomenon may be associated with the presence of jump processes (as can be seen in [23–25]) into the traveling disturbance; as β is reduced, its effects become more significant.

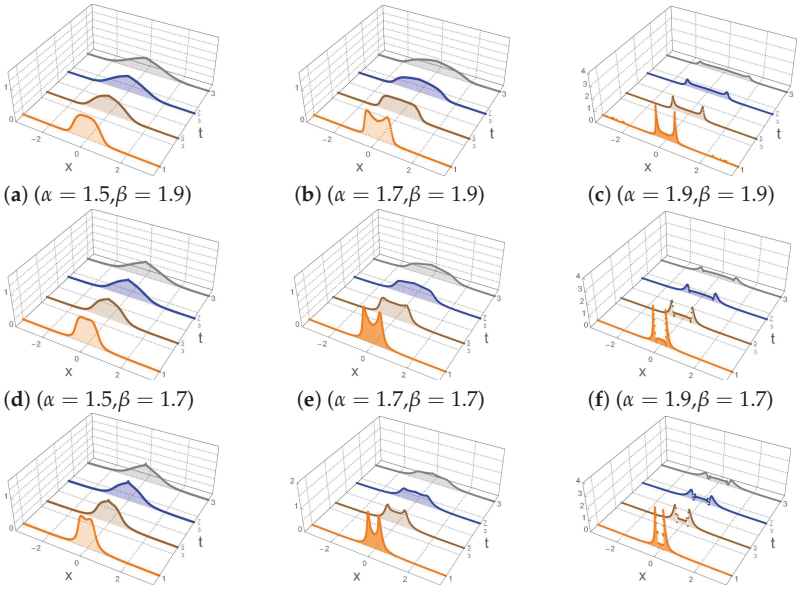

(**a**) ($\alpha = 1.5, \beta = 1.9$) (**b**) ($\alpha = 1.7, \beta = 1.9$) (**c**) ($\alpha = 1.9, \beta = 1.9$)

(**d**) ($\alpha = 1.5, \beta = 1.7$) (**e**) ($\alpha = 1.7, \beta = 1.7$) (**f**) ($\alpha = 1.9, \beta = 1.7$)

(**g**) ($\alpha = 1.5, \beta = 1.5$) (**h**) ($\alpha = 1.7, \beta = 1.5$) (**i**) ($\alpha = 1.9, \beta = 1.5$)

Figure 1. Time evolution of the disturbances described by the solution $u(x,t)$ in Equations (11) and (12) ($\mu = v_{\alpha\beta} = \gamma = 1$). The orange line stands for $u(x, t = 1)$, the brown for $u(x, t = 5/3)$, the blue for $u(x, t = 7/3)$, and the gray for $u(x, t = 3)$.

5. Conclusions

The Cauchy problem for a fractional differential equation with the damped wave equation as a particular case was solved with the Dirac delta initial condition, and its solution was obtained in terms of series of H-Fox functions. According to the graphic representation of the solution, the fractional differential equation models traveling disturbances, where a mixture of wave-like and diffusive behavior is observed. Future work is addressed to the study of a fractional differential equation with the telegrapher equation as a particular case. Such an equation also contains the fractional expressions $[D^{\alpha} + a^{\alpha}]u(x,t) = v_{\alpha,\beta}^2 \mathbb{D}^{\beta} u(x,t)$ and $\left[D^{\alpha} + \gamma^{\frac{\alpha}{2}} D^{\frac{\alpha}{2}}\right] u(x,t) = v_{\alpha,\beta}^2 \mathbb{D}^{\beta} u(x,t)$ as limit cases, which are the second object of study in this work. Work in this direction is in progress and will be reported elsewhere.

Funding: This research has been funded by Consejo Nacional de Ciencia y Tecnología (CONACYT), Mexico, Grant Number A1-S-24569.

Institutional Review Board Statement: Not applicable.

Informed Consent Statement: Not applicable.

Data Availability Statement: Not applicable.

Acknowledgments: The author is grateful to O. Rosas-Ortiz and L.M. Nieto for useful comments.

Conflicts of Interest: The author declares no conflict of interest.

Appendix A. Some Useful Definitions

Let $\alpha > 0$, $f \in C^n(\mathbb{R}^+)$ and $n = \lceil \alpha \rceil$. The α-order *Caputo's fractional derivative* with respect to t ${}_t D_t^{\alpha}$ of a function f is defined as

$$D_t^{\alpha} f(t) = \frac{1}{\Gamma(n-\alpha)} \int_0^t (t-t')^{n-\alpha-1} \left(\frac{d^n f}{dt'^n}\right) dt'. \tag{A1}$$

Let $1 < \beta < 2$. The β-order Riesz fractional derivative with respect to x $\mathbb{D}_x^\beta$ of a function f is defined as

$$\mathbb{D}_x^\beta f(x) = -\frac{1}{\sqrt{2\pi}} \int_{-\infty}^{\infty} e^{ikx} |k|^\beta \mathcal{F}[f](k) dk, \tag{A2}$$

where $\mathcal{F}[f]$ is the Fourier transform of the function f.

The Mellin-Barnes integral $I_{\mathcal{M}}$ of a function f is defined as follows

$$[I_{\mathcal{M}} f](x) = \int_{c-i\infty}^{c+i\infty} f_{\mathcal{M}}(s) x^{-s} ds. \tag{A3}$$

Let $m, n, p, q \in \mathbb{N}$ such that $0 \le m \le q$ and $0 \le n \le p$, $A_i, B_j \in (0, \infty)$ and $a_i, b_j \in \mathbb{C}$ $(i = 1, \ldots, p; j = 1, \ldots q)$. The H-Fox function is defined via the next Mellin–Barnes integral

$$H_{p,q}^{m,n}\left[z \middle| \begin{array}{c} (a_1, A_1), \ldots, (a_p, A_p) \\ (b_1, B_1), \ldots, (b_q, B_q) \end{array} \right] = \int_L \frac{\prod_{j=1}^m \Gamma(b_j + B_j s) \prod_{i=1}^n \Gamma(1 - a_i - A_i s) z^{-s} ds}{\prod_{i=n+1}^p \Gamma(a_i + A_i s) \prod_{j=m+1}^q \Gamma(1 - b_j - B_j s)}. \tag{A4}$$

The path of integration L separates the poles of $\Gamma(b_j + B_j s)$ to the left and the poles of $\Gamma(1 - a_i - A_i s)$ to the right of L.

Appendix B. Derivation of Expressions (11) and (12)

According to the definition of the H-Fox function provided in (A4), one can express the Equation (10) in its Mellin–Barnes representation as follows

$$U(x, s) = \frac{\mu}{\beta} \frac{1}{2\pi i} \int_L \frac{\lambda^{1-z}}{s} \frac{\Gamma(z)\Gamma(1 - \frac{1}{\beta} + \frac{z}{\beta})\Gamma(\frac{1}{\beta} - \frac{z}{\beta}) x^{-z} dz}{\Gamma\left(\frac{1}{2} - \frac{z}{2}\right)\Gamma\left(\frac{1}{2} + \frac{z}{2}\right)}, \tag{A5}$$

where

$$\lambda = \left(\frac{s^\alpha + \gamma^{\frac{\alpha}{2}} s^{\frac{\alpha}{2}}}{v_{\alpha,\beta}^2} \right)^{\frac{1}{\beta}}. \tag{A6}$$

The inverse Laplace transform operator $\mathcal{L}^{-1}$ acts on the complex variable s, then $\mathcal{L}^{-1} U(x, s)$ can be expressed as follows

$$\mathcal{L}^{-1} U(x, s) = \frac{\mu}{\beta} \frac{1}{2\pi i} \int_L \mathcal{L}^{-1}\left[\frac{\lambda^{1-z}}{s} \right] \frac{\Gamma(z)\Gamma(1 - \frac{1}{\beta} + \frac{z}{\beta})\Gamma(\frac{1}{\beta} - \frac{z}{\beta}) x^{-z} dz}{\Gamma\left(\frac{1}{2} - \frac{z}{2}\right)\Gamma\left(\frac{1}{2} + \frac{z}{2}\right)}. \tag{A7}$$

The series expansion

$$\frac{\lambda^{1-z}}{s} = \frac{1}{v_{\alpha,\beta}^{\frac{2(1-z)}{\beta}}} \sum_{n=0}^{\infty} \frac{\Gamma\left(1 + \frac{1}{\beta} - \frac{z}{\beta}\right) \gamma^{\frac{\alpha n}{2}}}{n! \Gamma\left(1 + \frac{1}{\beta} - n - \frac{z}{\beta}\right) s^{1 - \frac{\alpha}{\beta} + \frac{\alpha n}{2} + \frac{\alpha z}{\beta}}}, \tag{A8}$$

together with the inverse Laplace transform formula

$$\mathcal{L}^{-1}\left[\frac{1}{s^{1 - \frac{\alpha}{\beta} + \frac{\alpha n}{2} + \frac{\alpha z}{\beta}}} \right] = \frac{t^{-\frac{\alpha}{\beta} + \frac{\alpha n}{2} + \frac{\alpha z}{\beta}}}{\Gamma\left(1 - \frac{\alpha}{\beta} + \frac{\alpha n}{2} + \frac{\alpha z}{\beta}\right)}, \qquad 1 - \frac{\alpha}{\beta} + \frac{\alpha n}{2} + \frac{\alpha z}{\beta} > 0, \tag{A9}$$

leads to

$$\mathcal{L}^{-1}\left[\frac{\lambda^{1-z}}{s} \right] = \frac{\Gamma\left(1 + \frac{1}{\beta} - \frac{z}{\beta}\right) t^{-\frac{\alpha}{\beta} + \frac{\alpha z}{\beta}}}{v_{\alpha,\beta}^{\frac{2(1-z)}{\beta}}} \sum_{n=0}^{\infty} \frac{(\gamma t)^{\frac{\alpha n}{2}}}{n! \Gamma\left(1 + \frac{1}{\beta} - n - \frac{z}{\beta}\right) \Gamma\left(1 - \frac{\alpha}{\beta} + \frac{\alpha n}{2} + \frac{\alpha z}{\beta}\right)}. \tag{A10}$$

From (A7) and (A10), we have

$$\mathcal{L}^{-1}U(x,s) = \frac{\mu}{\beta t^{\frac{\alpha}{\beta}} v_{\alpha,\beta}^{\frac{2}{\beta}}} \sum_{n=0}^{\infty} (\gamma t)^{\frac{\alpha n}{2}} \Theta_n(x,t;\alpha,\beta) \tag{A11}$$

where

$$\Theta_n(x,t;\alpha,\beta) = \frac{1}{2\pi i}\int_L \frac{\Gamma(z)\Gamma(1-\frac{1}{\beta}+\frac{z}{\beta})\Gamma(\frac{1}{\beta}-\frac{z}{\beta})\Gamma\left(1+\frac{1}{\beta}-\frac{z}{\beta}\right)}{\Gamma\left(\frac{1}{2}-\frac{z}{2}\right)\Gamma\left(1+\frac{1}{\beta}-n-\frac{z}{\beta}\right)\Gamma\left(\frac{1}{2}+\frac{z}{2}\right)\Gamma(1-\frac{\alpha}{\beta}+\frac{\alpha n}{2}+\frac{\alpha z}{\beta})} \left(\frac{|x|}{t^{\frac{\alpha}{\beta}} v_{\alpha,\beta}^{\frac{2}{\beta}}}\right)^{-z} dz. \tag{A12}$$

From the definition of the H-function, one may write the expression (A12) as follows

$$\Theta_n(x,t;\alpha,\beta) = H_{4,4}^{2,2}\left[\frac{|x|}{t^{\frac{\alpha}{\beta}} v_{\alpha,\beta}^{\frac{2}{\beta}}}\middle| \begin{matrix}(1-\frac{1}{\beta},\frac{1}{\beta}),(-\frac{1}{\beta},\frac{1}{\beta}),(\frac{1}{2},\frac{1}{2}),(1-\frac{\alpha}{\beta}+\frac{\alpha n}{2},\frac{\alpha}{\beta})\\ (0,1),(1-\frac{1}{\beta},\frac{1}{\beta}),(\frac{1}{2},\frac{1}{2}),(-\frac{1}{\beta}+n,\frac{1}{\beta})\end{matrix}\right]. \tag{A13}$$

The results (A11)–(A13) are included in Section 3, as are the solutions to Equations (11) and (12).

References

1. Gorenflo, R.; Iskenderov, A.; Luchko, Y. Mapping between solutions of fractional diffusion wave equations. *Fract. Calc. Appl. Anal.* **2000**, *3*, 75.
2. Olivar-Romero, F.; Rosas-Ortiz, O. Transition from the Wave Equation to Either the Heat or the Transport Equations through Fractional Differential Expressions. *Symmetry* **2018**, *10*, 524. [CrossRef]
3. Luchko, Y.J. Fractional wave equation and damped waves. *Math. Phys.* **2013**, *54*, 031505. [CrossRef]
4. Podlubny, I. *Fractional Differential Equations*; Academic Press: London, UK, 1999.
5. Umarov, S. *Introduction to Fractional and Pseudo-Differential Equations with Singular Symbols*; Springer: Basel, Switzerland, 2015.
6. Widder, D.V. *The Heat Equation*; Academic Press: New York, NY, USA, 1975.
7. Tikhonov, A.N.; Samarskii, A.A. *Equations of Mathematical Physics*; Pergamon Press: New York, NY, USA, 1963.
8. Gustafson, K.E. *Introduction to Partial Differential Equations and Hilbert Space Methods*; Dover: New York, NY, USA, 1999.
9. Duffy, D.G. *Green's Functions with Applications*; CRC Press: Boca Raton, FL, USA, 2015.
10. Borthwick, D. *Introduction to Partial Differential Equations*; Springer: Basel, Switzerland, 2018.
11. Luchko, Y. The Wright function and its applications. In *Handbook of Fractional Calculus with Applications. Volume 1: Basic Theory*; De Gruyte: Berlin, Germany; Boston, MA, USA, 2019; Chapter 10, pp. 241–268.
12. Olivar-Romero, F.; Rosas-Ortiz, O. An integro-differential Equation of the Fractional Form: Cauchy Problem and Solution. In *Integrability, Supersymmetry and Coherent States*; A Volume in Honour of Professor Véronique Hussin, CRM Series in Mathematical Physics; Kuru, S., Negro, J., Nieto, L.M., Eds.; Springer: Berlin, Germany, 2019; Chapter 18, pp. 387–393.
13. Olivar-Romero, F. Fractional Approach to the Study of Some Partial Differential and Integro-Differential Equations. *J. Phys. Conf. Ser.* 2022, *accepted*.
14. Srednicki, M. *Quantum Field Theory*; Cambridge University Press: Cambridge, UK, 2007.
15. Gravel, P.; Gauthier, C. Classical applications of the Klein-Gordon equation. *Am. J. Phys.* **2011**, *79*, 447. [CrossRef]
16. Bansu, H.; Kumar, S. Meshless method for the numerical solution of space and time fractional wave equation. In Proceedings of the International Workshop Numerical Solution of Fractional Differential Equations and Applications, Sozopol, Bulgaria, 8–13 June 2020; pp. 11–14.
17. Bansu, H.; Kumar, S. Numerical Solution of Space and Time Fractional Telegraph Equation: A Meshless Approach. *Int. J. Nonlinear Sci. Num. Simul.* **2019**, *20*, 325. [CrossRef]
18. Bansu, H.; Kumar, S. Numerical Solution of Space-Time Fractional Klein-Gordon Equation by Radial Basis Functions and Chebyshev Polynomials. *Int. J. Appl. Comput. Math.* **2021**, *7*, 201. [CrossRef]
19. Kumar, S.; Piret, C. Numerical solution of space-time fractional PDEs using RBF-QR and Chebyshev polynomials. *Appl. Numer. Math.* **2019**, *143*, 300. [CrossRef]
20. Capelas de Oliveira, E.; Costa, F.; Vaz, J. The fractional Schrödinger equation for delta potentials. *J. Math. Phys.* **2010**, *51*, 123517. [CrossRef]
21. Kilbas, A.A. *H-Transforms: Theory and Applications*; CRC Press: New York, NY, USA, 2004.
22. Mathai, A.M.; Saxena, R.K.; Haubold, H.J. *The H-Function*; Springer: New York, NY, USA, 2010.
23. Saichev, A.; Zazlavsk, G. Fractional kinetic equations: Solutions and applications. *Chaos* **1997**, *7*, 753. [CrossRef] [PubMed]
24. Gorenflo, E.; Mainardi, F. Random walk models for space-fractional diffusion processes. *Fract. Calc. Appl. Anal.* **1998**, *1*, 167.
25. Gorenflo, R.; Mainardi, F. Approximation to Lévy-Feller diffusion by random walk. *Z. Anal. Anwend.* **1999**, *18*, 231. [CrossRef]

computer sciences and mathematics forum

MDPI

Proceeding Paper

Analyzing All the Instances of a Chaotic Map to Generate Random Numbers †

Luis Gerardo de la Fraga

Cinvestav, Computer Science Deparment, Av. IPN 2508, Mexico City 07360, Mexico; fraga@cs.cinvestav.mx

† Presented at the 5th Mexican Workshop on Fractional Calculus (MWFC), Monterrey, Mexico, 5–7 October 2022.

Abstract: All possible configurations of a chaotic map without fixed points, called "nfp1", in its implementation in fixed-point arithmetic are analyzed. As the multiplication on the computer does not follow the associative property, we analyze the number of forms in which the multiplications can be performed in this chaotic map. As chaos enhanced the small perturbations produced in the multiplications, it is possible to built different pseudorandom number generators using the same chaotic map.

Keywords: chaotic map; fixed-point arithmetic; PRNG; chaos sensitivity

Citation: de la Fraga, L.G. Analyzing All the Instances of a Chaotic Map to Generate Random Numbers. *Comput. Sci. Math. Forum* **2022**, *4*, 6. https://doi.org/10.3390/cmsf2022004006

Academic Editors: Jorge M. Cruz-Duarte and Porfirio Toledo-Hernández

Published: 18 January 2023

1. Introduction

The multiplication inside a computer does not follow the associative property, that is, for the three different numbers a, b, and c, $a(bc) \neq (ab)c \neq (ac)b$. This fact is produced because of using fixed-point arithmetic; the multiplication of two numbers, $i.f$, with i bits in the integer part and f bits in the factional part, produces a number $(2i+1).2f$. This resulted number must be returned to the same used representation, then the result is shifted f bits to the right. Moreover, to avoid the increasing size of the bits in the integer part, the number of bits in this part is chosen large enough to keep all the results of the multiplications within i bits. Fixed-point arithmetic is mostly used in the hardware implementation of chaotic circuits because of its simplicity [1–3].

The dynamics of a chaotic system are highly sensitive to small changes in its initial conditions. In this work, a map without fixed points to generate pseudorandom numbers by changing the order in the multiplications is studied, which also produces small changes that are increased by the chaos. In [4], the authors study the sensitivity of a chaotic system more as a problem. In this work, the sensitivity of a chaotic map is taken as an advantage to generate more maps by changing the order in the multiplications of the map terms.

Random numbers are very important in simulations [5], video games, in Monte Carlo methods, in cryptography [6], and in evolutionary algorithms [7] as the genetic algorithms, because these kind of algorithms can be considered a guided (intelligent) random search.

In the next Section 2, the chaotic map used and the generation of random sequences are described. In Section 3, the process to generate new sequences by changing the order of the multiplication is described. In this section, it is also shown that generated sequences are uncorrelated and random. Finally, in Section 4, the conclusion of this work is given.

2. Chaotic Map

The map nfp1 in [8] is used in this work. This map is defined as

$$\begin{aligned} x(i+1) &= a\left[y^2(i)-1\right]x(i)+c, \\ y(i+1) &= x(i)+y(i), \end{aligned} \tag{1}$$

with parameters values $a = 1.78$ and $c = 0.001$. These parameters values are the suggested in [8].

The domain of attraction for Equation (1) is shown in Figure 1. The gray zone in Figure 1 represents where the initial values take the shown values on the x and y axes, and the maps converge to the behavior shown as the black points. The white zone in Figure 1 represents where, with the shown initial values, the map's dynamic behavior is destroyed. Thus, from this figure, it is possible to choose the initial values for $x(0)$ and $y(0)$ within the interval $[-0.5, 0.5]$. Moreover, from Figure 1, it possible to see that the range of values for $x(i+1)$ is the interval $[-2, 2]$ and $[-1, 1]$ for $y(i+1)$, then 2 bits in the integer part are necessary for the calculations. For the fractional part, we decided to use 61 bits, plus the sign bit, then numbers of 64 bits are used. Then, the initial values can be expressed as the interval $[-0.5 + u, -0.5 + v]$, where $u, v \in [0, 1)$, and $1 = 2^{61}$ with the used representation. Thus, the possible values for the initial values are $(2^{61})^2 = 2^{122}$. These values can also be seen as the different possible values for the seed of the pseudorandom number generator (PRNG). A PRNG gives the same output sequence if the same seed is used. A PRNG is a deterministic process that generates a sequence of binary numbers that looks random.

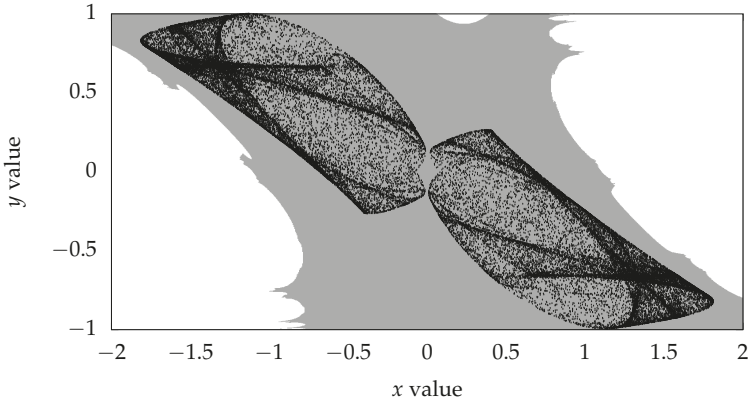

Figure 1. The domain of attraction of the map in Equation (1). This domain was obtained in floating point arithmetic. Moreover, 40,000 points obtained with initial conditions $(x(0), y(0)) = (-0.5, 0.4)$ are shown.

An output binary sequence of 16 bits can be generated by concatenating two iterations of

$$b[i+1] = x[i+1] \bmod 256, \tag{2}$$

that is, the last 8 bits of the value of x variable are consider random. The value of the y variable cannot be used because it can be obtained easily from the previous values. In Equation (2) brackets are used due the sequences now being discrete binary values. This same technique was applied in [9] using a 2D map.

3. Analysis of the Map

The Equation (1), for the calculation of the $x(i+1)$ term can be expressed as

$$x(i+1) = ay^2(i)x(i) - ax(i) + c, \tag{3}$$

where the first term in the right part can be also expressed as the calculation of three terms: $(ay)(y)(x)$ or as $(a)(y^2)(x)$. Each one of these two triplets of terms can be multiplied in three forms as $(t_1t_2)t_3$, $t_1(t_2t_3)$, or $(t_1t_3)t_2$; therefore, with the map in Equation (1), $3 \times 3 = 9$ different forms of multiplying the terms to obtain $x(i+1)$ in Equation (3) are possible. This can be seen as, if three more bits are added to the possible initial values, then now $(2^3 + 1) \times 2^{122} = 2^{125} + 2^{122}$ different initial values could be possible.

As a test of this idea, eight sequences are generated, four sequences with the values shown in Table 1, and another four sequences with the codes 10, 10, 11, and 12 named as sequences s_5, s_6, s_7, and s_8. The first number in the code selects between the terms $(ay)(y)(x)$ or $(a)(y^2)(x)$. The second number in the code selects among the three possible forms of multiplying the three previous terms: 0 for $(t_1t_2)t_3$, 1 for $t_1(t_2t_3)$, and 2 for $(t_1t_3)t_2$.

Table 1. Initial values and codes for the first four generated sequences.

Seq. Name	$x(0)$	$y(0)$	Code
s_1	-0.5	-0.5	00
s_2	-0.5	$-0.5+2^{-61}$	00
s_3	-0.5	-0.5	01
s_4	-0.5	-0.5	02

The correlations between the pair of sequences (s_1, s_2), (s_1, s_3), and (s_1, s_4) are show in the graph of Figure 2a; the correlations between the sequences (s_5, s_6), (s_5, s_7), and (s_5, s_8) are show in the graph of Figure 2b. The correlation is calculated with the overlapped pairs of five samples of the sequences. The values of the each of the four nibbles ranging from the most significant to the least significant at the output of the PRNG are used as the samples values.

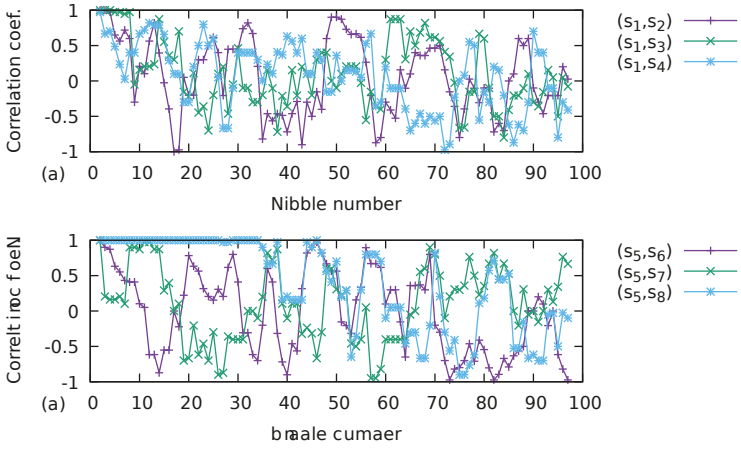

Figure 2. In (**a**) is shown the three correlations between the sequences (s_1, s_2), (s_1, s_3), and (s_1, s_4), and in (**b**), between sequences (s_5, s_6), (s_5, s_7), and (s_5, s_8).

From Figure 2, it is possible to see that sequences are uncorrelated if the initial values are change in a single bit (as sequences s_2 and s_6 are generated) or by changing the order of the multiplication around the nibble 10, or 40 bits, except for the correlation of sequences (s_5, s_8). This last case, in which the sequence s_8 is calculated with the code 12, is when the term $(a)(y^2)(x)$ is calculated as $(ax)y^2$. If the value of the constant a in Equation (1) is changed from 1.78 to 1.7777777, or as 0x38e38e38e38e38e3 in hexadecimal, the correlations change, as shown in Figure 3.

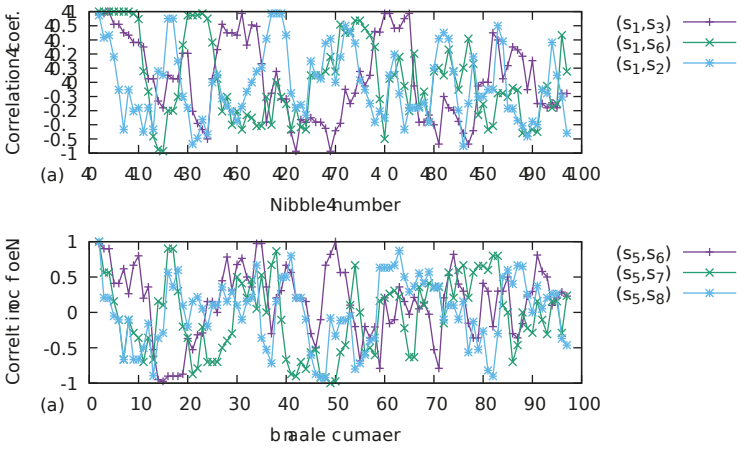

Figure 3. In (**a**) is shown the three correlations between the sequences (s_1, s_2), (s_1, s_3), and (s_1, s_4), and in (**b**), between sequences (s_5, s_6), (s_5, s_7), and (s_5, s_8); by now, the value of a in Equation (1) is changed to 1.7777777.

From Figure 3, the first 40 bits of each sequence must be discharged to consider them as uncorrelated sequences when the order in the multiplications in the map is changed.

To demonstrate that the generated sequences are random, three tests of TestU01 suite, Rabbit, Alphabit, and BlockAlphabit are applied on 100 sequences of 10^6 bits. These tests were designed for bits stored in a file (or a physical device). Rabbit and Alphabit apply 40 and 17 different statistical tests, respectively. BlockAlphabit applies the Alphabit battery of tests repeatedly to a binary file after reordering the bits by blocks of different sizes (with sizes of 2, 4, 8, 16, and 32 bits) [10]. Applying the TestU01 to the eight generated sequences from s_1 to s_8 gives the results shown in Table 2. All the sequences passed the tests, except the sequence s_7. This sequence is generated as the multiplication of the terms $a(y^2 x)$. It looks as though multiplication by the constant a does not give enough variability to generate a random sequence by obtaining the last 8 bits of each iteration on the map calculation.

Table 2. Results of applying the TestU01 to the generated sequences.

	Test Name	**Seqs.** s_1, s_2, s_3, s_4, s_5, s_6, s_8	**Seqs.** s_7
1	Rabbit	All 40 tests passed	17/40
2	Alphabit	All 17 tests passed	1/17
3	Block Alphabit	All 6 repetitions of Alphabit tests passed	8/102

As a configuration does not give random sequences, the number of possible initial values is $2^3 \times 2^{122} = 2^{125}$.

Discussing the number of bits used in the number representation, the number of bits in the integer part is clear: they are necessary to perform the calculations of Equation (1). The number of bits for the fractional part is not so clear: they must be necessary to maintain the map behavior shown in Figure 1 and to keep a random behavior in the eight less significant bits. The used representation of 64 bits is more precise than real numbers (doubles in C programming language) that have around 52 bits of precision. Lesser bits in the fractional part could keep the map behavior but, at the same time, stop the random behavior of the less significant bits.

4. Conclusions

A map without a fixed point was used to generate random numbers by changing the association in the multiplication of a term with three variables. Fixed-point arithmetic was used with numbers with 2 bits for the integer part and 61 bits for the fractional part. The value of a constant used by the map was changed slightly (from 1.78 to 1.7777777) to generate uncorrelated sequences. One of the configuration multiplies the constant values by the other terms; this configuration does not generate random sequences. With the used numbers, 2^{122} values can be used as the seed for the random number generator. With the different association in the multiplication, three bits can be added to the seed values, given a total of 2^{125} possible values for the seed. An efficient design in hardware can be proposed in a future work, as well as the search for more applications for the studied configuration.

Funding: This research received no external funding.

Institutional Review Board Statement: Not applicable.

Data Availability Statement: Not applicable.

Conflicts of Interest: The author declare no conflict of interest.

References

1. Garcia-Bosque, M.; Pérez-Resa, A.; Sánchez-Azqueta, C.; Aldea, C.; Celma, S. Chaos-Based Bitwise Dynamical Pseudorandom Number Generator On FPGA. *IEEE Trans. Instrum. Meas.* **2019**, *68*, 291–293. [CrossRef]
2. Elmanfaloty, R.; Abou-Bakr, E. Random property enhancement of a 1D chaotic PRNG with finite precision implementation. *Chaos Solitons Fractals* **2019**, *118*, 134–144. [CrossRef]
3. Tuna, M. A novel secure chaos-based pseudo random number generator based on ANN-based chaotic and ring oscillator: Design and its FPGA implementation. *Analog. Integr. Circ. Sig. Process.* **2020**, *105*, 167–181. [CrossRef]
4. Sayed, W.; Radwan, A.; Fahmy, H.; El-Sedeek, A. Software and Hardware Implementation Sensitivity of Chaotic Systems and Impact on Encryption Applications. *Circuits Syst. Signal Process.* **2020**, *39*, 5638–5655. [CrossRef]
5. Nazaré, T.; Nepomuceno, E.; Martins, S.; Butusov, D. A Note on the Reproducibility of Chaos Simulation. *Entropy* **2020**, *22*, 953. [CrossRef] [PubMed]
6. Rezk, A.A.; Madian, A.H.; Radwan, A.G.; Soliman, A.M. Multiplierless chaotic Pseudo random number generators. *AEU—Int. J. Electron. Commun.* **2020**, *113*, 152947. [CrossRef]
7. Coello, C.; Lamont, G.; Van Veldhuizen, D. *Evolutionary Algorithms for Solving Multi-Objective Problems*; Springer: New York, NY, USA, 2007.
8. Ramadoss, J.; Ouannas, A.; Tamba, V.K.; Grassi, G.; Momani, S.; Pham, V.T. Constructing non-fixed-point maps with memristors. *Eur. Phys. J. Plus* **2022**, *137*, 211. [CrossRef]
9. De la Fraga, L.; Mancillas-López, C.; Tlelo-Cuautle, E. Designing an authenticated Hash function with a 2D chaotic map. *Nonlinear Dyn.* **2021**, *104*, 4569–4580. [CrossRef]
10. Ecuyer, L.; Simard, R. TestU01: A C Library for Empirical Testing of Random Number Generators. *ACM Trans. Math. Softw.* **2007**, *33*, 22. Available online: http://simul.iro.umontreal.ca/testu01/tu01.html (accessed on 1 January 2020). [CrossRef]

computer sciences and mathematics forum

MDPI

Proceeding Paper

Abelian Groups of Fractional Operators †

Anthony Torres-Hernandez [1,2,*], Fernando Brambila-Paz [3] and Rafael Ramirez-Melendez [2]

[1] Department of Physics, Faculty of Science, Universidad Nacional Autónoma de México, Mexico City 04510, Mexico
[2] Music and Machine Learning Lab, Department of Information and Communication Technologies, Universitat Pompeu Fabra, 08018 Barcelona, Spain
[3] Department of Mathematics, Faculty of Science, Universidad Nacional Autónoma de México, Mexico City 04510, Mexico
* Correspondence: anthony.torres@ciencias.unam.mx
† Presented at the 5th Mexican Workshop on Fractional Calculus, Tecnológico de Monterrey (TEC), Monterrey, Mexico, 5–7 October 2022.

Abstract: Taking into count the large number of fractional operators that have been generated over the years, and considering that their number is unlikely to stop increasing at the time of writing this paper due to the recent boom of fractional calculus, everything seems to indicate that an alternative that allows to fully characterize some elements of fractional calculus is through the use of sets. Therefore, this paper presents a recapitulation of some fractional derivatives, fractional integrals, and local fractional operators that may be found in the literature, as well as a summary of how to define sets of fractional operators that allow to fully characterize some elements of fractional calculus, such as the Taylor series expansion of a scalar function in multi-index notation. In addition, it is presented a way to define finite and infinite Abelian groups of fractional operators through a family of sets of fractional operators and two different internal operations. Finally, using the above results, it is shown one way to define commutative and unitary rings of fractional operators.

Keywords: fractional operators; set theory; group theory; fractional calculus of sets

Citation: Torres-Hernandez, A.; Brambila-Paz, F.; Ramirez-Melendez, R. Abelian Groups of Fractional Operators. *Comput. Sci. Math. Forum* **2022**, *4*, 4. https://doi.org/10.3390/cmsf2022004004

Academic Editors: Jorge M. Cruz-Duarte and Porfirio Toledo-Hernández

Published: 19 December 2022

1. Introduction

Fractional calculus is a branch of mathematics that uses derivatives of non-integer order that originated around the same time as conventional calculus due to Leibniz's notation for derivatives of integer order

$$\frac{d^n}{dx^n}.$$

Therefore, thanks to this notation, L'Hopital could ask in a letter to Leibniz about the interpretation of taking $n = 1/2$ in a derivative. Since at that moment Leibniz could not give a physical or geometrical interpretation of this question, he simply answered to L'Hopital in a letter, "... is an apparent paradox of which, one day, useful consequences will be drawn" [1]. The name of fractional calculus comes from a historical question since, in this branch of mathematical analysis, the derivatives and integrals of a certain order α are studied, with $\alpha \in \mathbb{R}$. Currently, fractional calculus does not have a unified definition of what is considered a fractional derivative. As a consequence, when it is not necessary to explicitly specify the form of a fractional derivative, it is usually denoted as follows

$$\frac{d^\alpha}{dx^\alpha}.$$

The fractional operators have many representations, but one of their fundamental properties is that they allow retrieving the results of conventional calculus when $\alpha \to n$.

For example, let $f : \Omega \subset \mathbb{R} \to \mathbb{R}$ be a function such that $f \in L^1_{loc}(a,b)$, where $L^1_{loc}(a,b)$ denotes the space of locally integrable functions on the open interval $(a,b) \subset \Omega$. One of the fundamental operators of fractional calculus is the operator Riemann–Liouville fractional integral, which is defined as follows [2,3]:

$$ {}_aI_x^{\alpha} f(x) := \frac{1}{\Gamma(\alpha)} \int_a^x (x-t)^{\alpha-1} f(t) dt, \tag{1} $$

where Γ denotes the Gamma function. It is worth mentioning that the above operator is a fundamental piece to construct the operator Riemann-Liouville fractional derivative, which is defined as follows [2,4]:

$$ {}_aD_x^{\alpha} f(x) := \begin{cases} {}_aI_x^{-\alpha} f(x), & \text{if } \alpha < 0 \\ \dfrac{d^n}{dx^n}\left({}_aI_x^{n-\alpha} f(x)\right), & \text{if } \alpha \geq 0 \end{cases}, \tag{2} $$

where $n = \lceil \alpha \rceil$ and ${}_aI_x^0 f(x) := f(x)$. On the other hand, let $f : \Omega \subset \mathbb{R} \to \mathbb{R}$ be a function n-times differentiable such that $f, f^{(n)} \in L^1_{loc}(a,b)$. Then, the Riemann–Liouville fractional integral also allows constructing the operator Caputo fractional derivative, which is defined as follows [2,4]:

$$ {}_a^{C}D_x^{\alpha} f(x) := \begin{cases} {}_aI_x^{-\alpha} f(x), & \text{if } \alpha < 0 \\ {}_aI_x^{n-\alpha} f^{(n)}(x), & \text{if } \alpha \geq 0 \end{cases}, \tag{3} $$

where $n = \lceil \alpha \rceil$ and ${}_aI_x^0 f^{(n)}(x) := f^{(n)}(x)$. Furthermore, if the function f fulfills that $f^{(k)}(a) = 0 \; \forall k \in \{0, 1, \cdots, n-1\}$, the Riemann–Liouville fractional derivative coincides with the Caputo fractional derivative, that is,

$$ {}_aD_x^{\alpha} f(x) = {}_a^{C}D_x^{\alpha} f(x). \tag{4} $$

Therefore, applying the operator (2) with $a = 0$ to the function x^{μ}, with $\mu > -1$, we obtain the following result:

$$ {}_0D_x^{\alpha} x^{\mu} = \frac{\Gamma(\mu+1)}{\Gamma(\mu-\alpha+1)} x^{\mu-\alpha}, \quad \alpha \in \mathbb{R} \setminus \mathbb{Z}, \tag{5} $$

where if $1 \leq \lceil \alpha \rceil \leq \mu$, it is fulfilled that ${}_0D_x^{\alpha} x^{\mu} = {}_0^{C}D_x^{\alpha} x^{\mu}$. To illustrate a bit the diversity of representations that fractional operators may have, we proceed to present a recapitulation of some fractional derivatives, fractional integrals, and local fractional operators that may be found in the literature [5–7]:

1. Grünwald-Letnikov fractional derivative:

$$ {}_a^{GL}D_x^{\alpha} f(x) = \lim_{h \to 0} \frac{1}{h^{\alpha}} \sum_{k=0}^{n} \frac{(-1)^k \Gamma(\alpha+1)}{\Gamma(k+1)\Gamma(\alpha-k+1)} f(x-kh), \quad n = \lfloor (x-a)/h \rfloor. $$

2. Marchaud fractional derivative:

$$ {}_{-\infty}^{Ma}D_x^{\alpha} f(x) = \frac{\alpha}{\Gamma(1-\alpha)} \int_{-\infty}^{x} (x-t)^{-\alpha-1} (f(x) - f(t)) dt, \quad 0 < \alpha < 1. $$

3. Hadamard fractional derivative:

$$ {}_a^{Ha}D_x^{\alpha} f(x) = \frac{x}{\Gamma(1-\alpha)} \frac{d}{dx} \int_a^x (\ln(x) - \ln(t))^{2-\alpha} \frac{f(t)}{t} dt, \quad 0 < \alpha < 1. $$

4. Chen fractional derivative:

$$ {}_{a}^{Ch}D_{x}^{\alpha}f(x) = \frac{1}{\Gamma(1-\alpha)}\frac{d}{dx}\int_{a}^{x}(x-t)^{-\alpha}f(t)dt, \quad 0<\alpha<1. $$

5. Caputo-Fabrizio fractional derivative:

$$ {}_{a}^{CF}D_{x}^{\alpha}f(x) = \frac{M(\alpha)}{1-\alpha}\int_{a}^{x}\exp\left(-\frac{\alpha}{1-\alpha}(x-t)\right)f^{(1)}(t)dt, \quad 0<\alpha<1, \quad M(0)=M(1)=1. $$

6. Atangana-Baleanu-Caputo fractional derivative:

$$ {}_{a}^{ABC}D_{x}^{\alpha}f(x) = \frac{M(\alpha)}{1-\alpha}\int_{a}^{x}E_{\alpha}\left(-\frac{\alpha}{1-\alpha}(x-t)^{\alpha}\right)f^{(1)}(t)dt, \quad 0<\alpha<1, \quad M(0)=M(1)=1. $$

7. Canavati fractional derivative:

$$ {}_{a}^{Ca}D_{x}^{\alpha}f(x) = \frac{1}{\Gamma(1+\alpha-n)}\frac{d}{dx}\int_{a}^{x}(x-t)^{n-\alpha}\frac{d^{n}}{dt^{n}}f(t)dt, \quad n=\lfloor\alpha\rfloor. $$

8. Jumarie fractional derivative:

$$ {}_{a}^{Ju}D_{x}^{\alpha}f(x) = \frac{1}{\Gamma(n-\alpha)}\frac{d^{n}}{dx^{n}}\int_{a}^{x}(x-t)^{n-\alpha-1}(f(t)-f(a))dt, \quad n=\lceil\alpha\rceil. $$

9. Hadamard fractional integral:

$$ {}_{a}^{Ha}I_{x}^{\alpha}f(x) = \frac{1}{\Gamma(\alpha)}\int_{a}^{x}(\ln(t)-\ln(x))^{\alpha-1}\frac{f(t)}{t}dt. $$

10. Weyl fractional integral:

$$ {}_{x}W_{\infty}^{\alpha}f(x) = \frac{1}{\Gamma(\alpha)}\int_{x}^{\infty}(t-x)^{\alpha-1}f(t)dt. $$

11. Conformable fractional operator:

$$ T_{\alpha}f(x) = \lim_{h\to 0}\frac{f\left(x+hx^{1-\alpha}\right)-f(x)}{h}. $$

12. Katugampola fractional operator:

$$ D^{\alpha}f(x) = \lim_{h\to 0}\frac{f(x\exp(hx^{-\alpha}))-f(x)}{h}. $$

13. Deformable fractional operator:

$$ \mathcal{D}^{\alpha}f(x) = \lim_{h\to 0}\frac{(1+h\beta)f(x+h\alpha)-f(x)}{h}, \quad \alpha+\beta=1. $$

Before continuing, it is worth mentioning that the applications of fractional operators have spread to different fields of science, such as finance [8,9], economics [10,11], number theory through the Riemann zeta function [12,13], in engineering with the study for the manufacture of hybrid solar receivers [14,15], and in physics and mathematics to solve nonlinear algebraic equation systems [16–25], which is a classical problem in mathematics,

physics and engineering that consists of finding the set of zeros of a function $f : \Omega \subset \mathbb{R}^n \to \mathbb{R}^n$, that is,

$$\{\xi \in \Omega \ : \ \|f(\xi)\| = 0\},$$

where $\|\cdot\| : \mathbb{R}^n \to \mathbb{R}$ denotes any vector norm, or equivalently,

$$\{\xi \in \Omega \ : \ [f]_k(\xi) = 0 \ \forall k \geq 1\},$$

where $[f]_k : \mathbb{R}^n \to \mathbb{R}$ denotes the k-th component of the function f.

2. Sets of Fractional Operators

Before continuing, it is worth mentioning that due to the large number of fractional operators that exist [5–7,26–41], it seems that the most natural way to fully characterize the elements of the fractional calculus is by using sets, which is the main idea behind of the methodology known as fractional calculus of sets [42,43]. Therefore, considering a scalar function $h : \mathbb{R}^m \to \mathbb{R}$ and the canonical basis of $\mathbb{R}^m$ denoted by $\{\hat{e}_k\}_{k\geq 1}$, it is feasible to define the following fractional operator of order α using Einstein's notation

$$o_x^\alpha h(x) := \hat{e}_k o_k^\alpha h(x). \tag{6}$$

Therefore, denoting by ∂_k^n the partial derivative of order n applied with respect to the k-th component of the vector x, using the previous operator, it is feasible to define the following set of fractional operators

$$\mathrm{O}_{x,\alpha}^n(h) := \left\{ o_x^\alpha \ : \ \exists o_k^\alpha h(x) \ \text{ and } \ \lim_{\alpha \to n} o_k^\alpha h(x) = \partial_k^n h(x) \ \forall k \geq 1 \right\}, \tag{7}$$

which corresponds to a nonempty set since it contains the following sets of fractional operators

$$\mathrm{O}_{0,x,\alpha}^n(h) := \left\{ o_x^\alpha \ : \ \exists o_k^\alpha h(x) = (\partial_k^n + \mu(\alpha)\partial_k^\alpha)h(x) \ \text{ and } \ \lim_{\alpha \to n} \mu(\alpha)\partial_k^\alpha h(x) = 0 \ \forall k \geq 1 \right\}. \tag{8}$$

As a consequence, it is feasible to obtain the following result:

$$\text{If } \ o_{i,x}^\alpha, o_{j,x}^\alpha \in \mathrm{O}_{x,\alpha}^n(h) \ \text{ with } \ i \neq j \ \Rightarrow \ \exists o_{k,x}^\alpha = \frac{1}{2}\left(o_{i,x}^\alpha + o_{j,x}^\alpha\right) \in \mathrm{O}_{x,\alpha}^n(h). \tag{9}$$

On the other hand, the complement of the set (7) may be defined as follows

$$\mathrm{O}_{x,\alpha}^{n,c}(h) := \left\{ o_x^\alpha \ : \ \exists o_k^\alpha h(x) \ \forall k \geq 1 \ \text{ and } \ \lim_{\alpha \to n} o_k^\alpha h(x) \neq \partial_k^n h(x) \ \text{ in at least one value } k \geq 1 \right\}, \tag{10}$$

with which it is feasible to obtain the following result:

$$\text{If } \ o_{i,x}^\alpha = \hat{e}_k o_{i,k}^\alpha \in \mathrm{O}_{x,\alpha}^n(h) \ \Rightarrow \ \exists o_{j,x}^\alpha = \hat{e}_k o_{i,\sigma_j(k)}^\alpha \in \mathrm{O}_{x,\alpha}^{n,c}(h), \tag{11}$$

where $\sigma_j : \{1, 2, \cdots, m\} \to \{1, 2, \cdots, m\}$ denotes any permutation different from the identity. Before continuing, it is necessary to mention that set (7) allows generalizing elements of conventional calculus. For example, let $\mathbb{N}_0$ be the set $\mathbb{N} \cup \{0\}$. If $\gamma \in \mathbb{N}_0^m$ and $x \in \mathbb{R}^m$, then it is feasible to define the following multi-index notation:

$$\left\{ \begin{array}{c} \gamma! := \displaystyle\prod_{k=1}^m [\gamma]_k!, \quad |\gamma| := \sum_{k=1}^m [\gamma]_k, \quad x^\gamma := \prod_{k=1}^m [x]_k^{[\gamma]_k} \\ \dfrac{\partial^\gamma}{\partial x^\gamma} := \dfrac{\partial^{[\gamma]_1}}{\partial [x]_1^{[\gamma]_1}} \dfrac{\partial^{[\gamma]_2}}{\partial [x]_2^{[\gamma]_2}} \cdots \dfrac{\partial^{[\gamma]_m}}{\partial [x]_m^{[\gamma]_m}} \end{array} \right. . \tag{12}$$

Therefore, considering a function $h:\Omega\subset\mathbb{R}^m\to\mathbb{R}$ and the fractional operator

$$s_x^{\alpha\gamma}(o_x^\alpha):=o_1^{\alpha[\gamma]_1}o_2^{\alpha[\gamma]_2}\cdots o_m^{\alpha[\gamma]_m},\tag{13}$$

it is feasible to define the following set of fractional operators

$$\mathrm{S}^{n,\gamma}_{x,\alpha}(h):=\left\{s_x^{\alpha\gamma}=s_x^{\alpha\gamma}(o_x^\alpha)\ :\ \exists s_x^{\alpha\gamma}h(x)\ \text{ with }\ o_x^\alpha\in\mathrm{O}^s_{x,\alpha}(h)\ \forall s\leq n^2\ \text{ and }\ \lim_{\alpha\to k}s_x^{\alpha\gamma}h(x)=\frac{\partial^{k\gamma}}{\partial x^{k\gamma}}h(x)\ \ \forall\alpha,|\gamma|\leq n\right\},\tag{14}$$

from which it is feasible to obtain the following results:

$$\text{If } s_x^{\alpha\gamma}\in\mathrm{S}^{n,\gamma}_{x,\alpha}(h)\ \Rightarrow\ \begin{cases}\lim\limits_{\alpha\to0}s_x^{\alpha\gamma}h(x)=o_1^0o_2^0\cdots o_m^0h(x)=h(x)\\ \lim\limits_{\alpha\to1}s_x^{\alpha\gamma}h(x)=o_1^{[\gamma]_1}o_2^{[\gamma]_2}\cdots o_m^{[\gamma]_m}h(x)=\dfrac{\partial^\gamma}{\partial x^\gamma}h(x)\ \ \forall|\gamma|\leq n\\ \lim\limits_{\alpha\to q}s_x^{\alpha\gamma}h(x)=o_1^{q[\gamma]_1}o_2^{q[\gamma]_2}\cdots o_m^{q[\gamma]_m}h(x)=\dfrac{\partial^{q\gamma}}{\partial x^{q\gamma}}h(x)\ \ \forall q|\gamma|\leq qn\\ \lim\limits_{\alpha\to n}s_x^{\alpha\gamma}h(x)=o_1^{n[\gamma]_1}o_2^{n[\gamma]_2}\cdots o_m^{n[\gamma]_m}h(x)=\dfrac{\partial^{n\gamma}}{\partial x^{n\gamma}}h(x)\ \ \forall n|\gamma|\leq n^2\end{cases}.\tag{15}$$

On the other hand, using little-o notation, it is feasible to obtain the following result:

$$\text{If } x\in B(a;\delta)\ \Rightarrow\ \lim_{x\to a}\frac{o((x-a)^\gamma)}{(x-a)^\gamma}\to0\ \ \forall|\gamma|\geq1,\tag{16}$$

with which it is feasible to define the following set of functions

$$R^n_{\alpha\gamma}(a):=\left\{r^n_{\alpha\gamma}\ :\ \lim_{x\to a}\left\|r^n_{\alpha\gamma}(x)\right\|=0\ \forall|\gamma|\geq n\ \text{ and }\ \left\|r^n_{\alpha\gamma}(x)\right\|\leq o\big(\|x-a\|^n\big)\ \forall x\in B(a;\delta)\right\},\tag{17}$$

where $r^n_{\alpha\gamma}:B(a;\delta)\subset\Omega\to\mathbb{R}$. Therefore, considering the previous set and some $B(a;\delta)\subset\Omega$, it is feasible to define the following sets of fractional operators

$$\mathrm{T}^{n,q,\gamma}_{x,\alpha,p}(a,h):=\left\{t_x^{\alpha,p}=t_x^{\alpha,p}\big(s_x^{\alpha\gamma}\big)\ :\ s_x^{\alpha\gamma}\in\mathrm{S}^{M,\gamma}_{x,\alpha}(h)\ \text{ and }\ t_x^{\alpha,p}h(x):=\sum_{|\gamma|=0}^{p}\frac{1}{\gamma!}s_x^{\alpha\gamma}h(a)(x-a)^\gamma+r^p_{\alpha\gamma}(x)\ \begin{matrix}\forall\alpha\leq n\\ \forall p\leq q\end{matrix}\right\},\tag{18}$$

$$\mathrm{T}^{\infty,\gamma}_{x,\alpha}(a,h):=\left\{t_x^{\alpha,\infty}=t_x^{\alpha,\infty}\big(s_x^{\alpha\gamma}\big)\ :\ s_x^{\alpha\gamma}\in\mathrm{S}^{\infty,\gamma}_{x,\alpha}(h)\ \text{ and }\ t_x^{\alpha,\infty}h(x):=\sum_{|\gamma|=0}^{\infty}\frac{1}{\gamma!}s_x^{\alpha\gamma}h(a)(x-a)^\gamma\right\},\tag{19}$$

which allow generalizing the Taylor series expansion of a scalar function in multi-index notation [22], where $M=\max\{n,q\}$. As a consequence, it is feasible to obtain the following results:

$$\text{If } t_x^{\alpha,p}\in\mathrm{T}^{1,q,\gamma}_{x,\alpha,p}(a,h)\text{ and }\alpha\to1\ \Rightarrow\ t_x^{1,p}h(x)=h(a)+\sum_{|\gamma|=1}^{p}\frac{1}{\gamma!}\frac{\partial^\gamma}{\partial x^\gamma}h(a)(x-a)^\gamma+r^p_\gamma(x),\tag{20}$$

$$\text{If } t_x^{\alpha,p}\in\mathrm{T}^{n,1,\gamma}_{x,\alpha,p}(a,h)\text{ and }p\to1\ \Rightarrow\ t_x^{\alpha,1}h(x)=h(a)+\sum_{k=1}^{m}o_k^\alpha h(a)[(x-a)]_k+r^1_{\alpha\gamma}(x).\tag{21}$$

Finally, it is worth mentioning that the set (7) may be considered as a generating set of sets of fractional tensor operators. For example, considering $\alpha,n\in\mathbb{R}^d$ with $\alpha=\hat{e}_k[\alpha]_k$ and $n=\hat{e}_k[n]_k$, it is feasible to define the following set of fractional tensor operators

$$\mathrm{O}^n_{x,\alpha}(h):=\left\{o_x^\alpha\ :\ \exists o_x^\alpha h(x)\ \text{ and }\ o_x^\alpha\in\mathrm{O}^{[n]_1}_{x,[\alpha]_1}(h)\times\mathrm{O}^{[n]_2}_{x,[\alpha]_2}(h)\times\cdots\times\mathrm{O}^{[n]_d}_{x,[\alpha]_d}(h)\right\}.\tag{22}$$

3. Groups of Fractional Operators

Considering a function $h : \Omega \subset \mathbb{R}^m \to \mathbb{R}^m$, it is feasible to define sets of fractional operators for a vector function in the following way:

$$ {}_m\,\mathrm{O}^{n}_{x,\alpha}(h) := \left\{ o^{\alpha}_{x} \ : \ o^{\alpha}_{x} \in \mathrm{O}^{n}_{x,\alpha}([h]_k) \ \forall k \leq m \right\}, \tag{23} $$

$$ {}_m\,\mathrm{O}^{n,c}_{x,\alpha}(h) := \left\{ o^{\alpha}_{x} \ : \ o^{\alpha}_{x} \in \mathrm{O}^{n,c}_{x,\alpha}([h]_k) \ \forall k \leq m \right\}, \tag{24} $$

$$ {}_m\,\mathrm{O}^{n,u}_{x,\alpha}(h) := {}_m\,\mathrm{O}^{n}_{x,\alpha}(h) \cup {}_m\,\mathrm{O}^{n,c}_{x,\alpha}(h), \tag{25} $$

where $[h]_k : \Omega \subset \mathbb{R}^m \to \mathbb{R}$ denotes the k-th component of the function h. Therefore, using the above sets, it is feasible to construct the following family of fractional operators

$$ {}_m\,\mathrm{MO}^{\infty,u}_{x,\alpha}(h) := \bigcap_{k \in \mathbb{Z}} {}_m\,\mathrm{O}^{k,u}_{x,\alpha}(h). \tag{26} $$

Before continuing, it should be noted that the above family of fractional operators fulfills the following property with respect to the classical Hadamar product:

$$ o^{0}_{x} \circ h(x) := h(x) \ \ \forall o^{\alpha}_{x} \in {}_m\,\mathrm{MO}^{\infty,u}_{x,\alpha}(h). \tag{27} $$

Furthermore, for each operator $o^{\alpha}_{x} \in {}_m\,\mathrm{MO}^{\infty,u}_{x,\alpha}(h)$, it is feasible to define the following fractional matrix operator [44]:

$$ A_{\alpha}(o^{\alpha}_{x}) = \left([A_{\alpha}(o^{\alpha}_{x})]_{jk} \right) := (o^{\alpha}_{k}). \tag{28} $$

On the other hand, defining the following modified Hadamard product [42]:

$$ o^{p\alpha}_{i,x} \circ o^{q\alpha}_{j,x} := \begin{cases} o^{p\alpha}_{i,x} \circ o^{q\alpha}_{j,x}, & \text{if } i \neq j \ \text{ (Hadamard product of type horizontal)} \\ o^{(p+q)\alpha}_{i,x}, & \text{if } i = j \ \text{ (Hadamard product of type vertical)} \end{cases}, \tag{29} $$

for each operator $o^{\alpha}_{x} \in {}_m\,\mathrm{MO}^{\infty,u}_{x,\alpha}(h)$, it is feasible to define an Abelian group of fractional operators isomorphic to the group of integers under the addition, as shown by the following theorem [43,44]:

Theorem 1. *Let o^{α}_{x} be a fractional operator such that $o^{\alpha}_{x} \in {}_m\,\mathrm{MO}^{\infty,u}_{x,\alpha}(h)$ and let $(\mathbb{Z}, +)$ be the group of integers under the addition. Therefore, considering the modified Hadamard product given by (29), it is feasible to define the following set of fractional matrix operators*

$$ {}_m\,\mathrm{G}(A_{\alpha}(o^{\alpha}_{x})) := \left\{ A^{\circ r}_{\alpha} = A_{\alpha}(o^{r\alpha}_{x}) \ : \ r \in \mathbb{Z} \ \text{ and } \ A^{\circ r}_{\alpha} = \left([A^{\circ r}_{\alpha}]_{jk} \right) := (o^{r\alpha}_{k}) \right\}, \tag{30} $$

which corresponds to the Abelian group generated by the operator $A_{\alpha}(o^{\alpha}_{x})$ isomorphic to the group $(\mathbb{Z}, +)$, that is,

$$ {}_m\,\mathrm{G}(A_{\alpha}(o^{\alpha}_{x})) \cong (\mathbb{Z}, +). \tag{31} $$

Proof. It should be noted that due to the way the set (30) is defined, just the Hadamard product of type vertical is applied among its elements. So, $\forall A^{\circ p}_{\alpha}, A^{\circ q}_{\alpha} \in {}_m\,\mathrm{G}(A_{\alpha}(o^{\alpha}_{x}))$ it is fulfilled that

$$ A^{\circ p}_{\alpha} \circ A^{\circ q}_{\alpha} = \left([A^{\circ p}_{\alpha}]_{jk} \right) \circ \left([A^{\circ q}_{\alpha}]_{jk} \right) = \left(o^{(p+q)\alpha}_{k} \right) = \left([A^{\circ (p+q)}_{\alpha}]_{jk} \right) = A^{\circ (p+q)}_{\alpha}. \tag{32} $$

So, from the previous result, it is feasible to prove that the set ${}_m\,\mathrm{G}(A_{\alpha}(o^{\alpha}_{x}))$ is a semigroup since it fulfills the following property:

$$ \forall A^{\circ p}_{\alpha}, A^{\circ q}_{\alpha}, A^{\circ r}_{\alpha} \in {}_m\,\mathrm{G}(A_{\alpha}(o^{\alpha}_{x})) \ \text{ it is fulfilled that } \ \left(A^{\circ p}_{\alpha} \circ A^{\circ q}_{\alpha} \right) \circ A^{\circ r}_{\alpha} = A^{\circ p}_{\alpha} \circ \left(A^{\circ q}_{\alpha} \circ A^{\circ r}_{\alpha} \right). \tag{33} $$

Furthermore, it follows from the definition of the set (30) that it contains a neutral element, with which it is feasible to prove from the previous result that the set ${}_m\mathrm{G}(A_\alpha(o_x^\alpha))$ is also a monoid since it fulfills the following property:

$$\exists A_\alpha^{\circ 0} \in {}_m\mathrm{G}(A_\alpha(o_x^\alpha)) \text{ such that } \forall A_\alpha^{\circ p} \in {}_m\mathrm{G}(A_\alpha(o_x^\alpha)) \text{ it is fulfilled that } A_\alpha^{\circ 0} \circ A_\alpha^{\circ p} = A_\alpha^{\circ p}. \tag{34}$$

It should be noted that due to the way in which the set (30) is defined, for each element contained in the set its symmetric element is also defined, with which from the previous result the set ${}_m\mathrm{G}(A_\alpha(o_x^\alpha))$ is also a group since it fulfills the following property:

$$\forall A_\alpha^{\circ p} \in {}_m\mathrm{G}(A_\alpha(o_x^\alpha)) \; \exists A_\alpha^{\circ -p} \in {}_m\mathrm{G}(A_\alpha(o_x^\alpha)) \text{ such that } A_\alpha^{\circ p} \circ A_\alpha^{\circ -p} = A_\alpha^{\circ 0}. \tag{35}$$

Finally, observing that the order in which the elements of the sets are operated does not influence the final result, it is obtained that the set ${}_m\mathrm{G}(A_\alpha(o_x^\alpha))$ is also an Abelian group since it fulfills the following property:

$$\forall A_\alpha^{\circ p}, A_\alpha^{\circ q} \in {}_m\mathrm{G}(A_\alpha(o_x^\alpha)) \text{ it is fulfilled that } A_\alpha^{\circ p} \circ A_\alpha^{\circ q} = A_\alpha^{\circ q} \circ A_\alpha^{\circ p}. \tag{36}$$

Once proven that the set (30) defines an Abelian group, to finish the proof of the theorem it is enough to define a bijective homomorphism between the sets ${}_m\mathrm{G}(A_\alpha(o_x^\alpha))$ and $(\mathbb{Z},+)$. So, defining the following functions

$$\begin{array}{c} \psi : {}_m\mathrm{G}(A_\alpha(o_x^\alpha)) \to (\mathbb{Z},+) \\ \psi(A_\alpha^{\circ r}) = r \end{array} \quad \text{and} \quad \begin{array}{c} \psi^{-1} : (\mathbb{Z},+) \to {}_m\mathrm{G}(A_\alpha(o_x^\alpha)) \\ \psi^{-1}(r) = A_\alpha^{\circ r} \end{array}, \tag{37}$$

it is feasible to prove that the function ψ defines a homeomorphism between the sets ${}_m\mathrm{G}(A_\alpha(o_x^\alpha))$ and $(\mathbb{Z},+)$ through the following result:

$$\forall A_\alpha^{\circ p}, A_\alpha^{\circ q} \in {}_m\mathrm{G}(A_\alpha(o_x^\alpha)) \text{ it is fulfilled that } \psi\left(A_\alpha^{\circ p} \circ A_\alpha^{\circ q}\right) = \psi\left(A_\alpha^{\circ (p+q)}\right) = p+q = \psi\left(A_\alpha^{\circ p}\right) + \psi\left(A_\alpha^{\circ q}\right), \tag{38}$$

and analogously it is proved that the function ψ^{-1} defines a homeomorphism between the sets $(\mathbb{Z},+)$ and ${}_m\mathrm{G}(A_\alpha(o_x^\alpha))$ through the following result:

$$\forall p,q \in (\mathbb{Z},+) \text{ it is fulfilled that } \psi^{-1}(p+q) = A_\alpha^{\circ (p+q)} = A_\alpha^{\circ p} \circ A_\alpha^{\circ q} = \psi^{-1}(p) \circ \psi^{-1}(q). \tag{39}$$

Therefore, from the previous results, it follows that the function ψ defines an isomorphism between the sets ${}_m\mathrm{G}(A_\alpha(o_x^\alpha))$ and $(\mathbb{Z},+)$. □

Therefore, from the previous theorem, it is feasible to obtain the following corollary:

Corollary 1. *Let o_x^α be a fractional operator such that $o_x^\alpha \in {}_m\mathrm{MO}_{x,\alpha}^{\infty,u}(h)$ and let $(\mathbb{Z},+)$ be the group of integers under the addition. Therefore, considering the modified Hadamard product given by (29) and some subgroup $\mathbb{H}$ of the group $(\mathbb{Z},+)$, it is feasible to define the following set of fractional matrix operators*

$${}_m\mathrm{G}(A_\alpha(o_x^\alpha),\mathbb{H}) := \left\{ A_\alpha^{\circ r} = A_\alpha(o_x^{r\alpha}) \; : \; r \in \mathbb{H} \text{ and } A_\alpha^{\circ r} = \left([A_\alpha^{\circ r}]_{jk} \right) := (o_k^{r\alpha}) \right\}, \tag{40}$$

which corresponds to a subgroup of the group generated by the operator $A_\alpha(o_x^\alpha)$, that is,

$${}_m\mathrm{G}(A_\alpha(o_x^\alpha),\mathbb{H}) \leq {}_m\mathrm{G}(A_\alpha(o_x^\alpha)). \tag{41}$$

Example 1. *Let $\mathbb{Z}_n$ be the set of residual classes less than a positive integer n. Therefore, considering a fractional operator $o_x^\alpha \in {}_m\mathrm{MO}_{x,\alpha}^{\infty,u}(h)$ and the set $\mathbb{Z}_{14}$, it is feasible to define, under the modified Hadamard product given by (29), the following Abelian group of fractional matrix operators*

$${}_m\mathrm{G}(A_\alpha(o_x^\alpha),\mathbb{Z}_{14}) = \left\{ A_\alpha^{\circ 0}, A_\alpha^{\circ 1}, A_\alpha^{\circ 2}, A_\alpha^{\circ 3}, A_\alpha^{\circ 4}, A_\alpha^{\circ 5}, A_\alpha^{\circ 6}, A_\alpha^{\circ 7}, A_\alpha^{\circ 8}, A_\alpha^{\circ 9}, A_\alpha^{\circ 10}, A_\alpha^{\circ 11}, A_\alpha^{\circ 12}, A_\alpha^{\circ 13} \right\}. \tag{42}$$

Furthermore, all possible combinations of the elements of the group are summarized in the following Cayley table:

$\circ$	$A_\alpha^{\circ 0}$	$A_\alpha^{\circ 1}$	$A_\alpha^{\circ 2}$	$A_\alpha^{\circ 3}$	$A_\alpha^{\circ 4}$	$A_\alpha^{\circ 5}$	$A_\alpha^{\circ 6}$	$A_\alpha^{\circ 7}$	$A_\alpha^{\circ 8}$	$A_\alpha^{\circ 9}$	$A_\alpha^{\circ 10}$	$A_\alpha^{\circ 11}$	$A_\alpha^{\circ 12}$	$A_\alpha^{\circ 13}$
$A_\alpha^{\circ 0}$	$A_\alpha^{\circ 0}$	$A_\alpha^{\circ 1}$	$A_\alpha^{\circ 2}$	$A_\alpha^{\circ 3}$	$A_\alpha^{\circ 4}$	$A_\alpha^{\circ 5}$	$A_\alpha^{\circ 6}$	$A_\alpha^{\circ 7}$	$A_\alpha^{\circ 8}$	$A_\alpha^{\circ 9}$	$A_\alpha^{\circ 10}$	$A_\alpha^{\circ 11}$	$A_\alpha^{\circ 12}$	$A_\alpha^{\circ 13}$
$A_\alpha^{\circ 1}$	$A_\alpha^{\circ 1}$	$A_\alpha^{\circ 2}$	$A_\alpha^{\circ 3}$	$A_\alpha^{\circ 4}$	$A_\alpha^{\circ 5}$	$A_\alpha^{\circ 6}$	$A_\alpha^{\circ 7}$	$A_\alpha^{\circ 8}$	$A_\alpha^{\circ 9}$	$A_\alpha^{\circ 10}$	$A_\alpha^{\circ 11}$	$A_\alpha^{\circ 12}$	$A_\alpha^{\circ 13}$	$A_\alpha^{\circ 0}$
$A_\alpha^{\circ 2}$	$A_\alpha^{\circ 2}$	$A_\alpha^{\circ 3}$	$A_\alpha^{\circ 4}$	$A_\alpha^{\circ 5}$	$A_\alpha^{\circ 6}$	$A_\alpha^{\circ 7}$	$A_\alpha^{\circ 8}$	$A_\alpha^{\circ 9}$	$A_\alpha^{\circ 10}$	$A_\alpha^{\circ 11}$	$A_\alpha^{\circ 12}$	$A_\alpha^{\circ 13}$	$A_\alpha^{\circ 0}$	$A_\alpha^{\circ 1}$
$A_\alpha^{\circ 3}$	$A_\alpha^{\circ 3}$	$A_\alpha^{\circ 4}$	$A_\alpha^{\circ 5}$	$A_\alpha^{\circ 6}$	$A_\alpha^{\circ 7}$	$A_\alpha^{\circ 8}$	$A_\alpha^{\circ 9}$	$A_\alpha^{\circ 10}$	$A_\alpha^{\circ 11}$	$A_\alpha^{\circ 12}$	$A_\alpha^{\circ 13}$	$A_\alpha^{\circ 0}$	$A_\alpha^{\circ 1}$	$A_\alpha^{\circ 2}$
$A_\alpha^{\circ 4}$	$A_\alpha^{\circ 4}$	$A_\alpha^{\circ 5}$	$A_\alpha^{\circ 6}$	$A_\alpha^{\circ 7}$	$A_\alpha^{\circ 8}$	$A_\alpha^{\circ 9}$	$A_\alpha^{\circ 10}$	$A_\alpha^{\circ 11}$	$A_\alpha^{\circ 12}$	$A_\alpha^{\circ 13}$	$A_\alpha^{\circ 0}$	$A_\alpha^{\circ 1}$	$A_\alpha^{\circ 2}$	$A_\alpha^{\circ 3}$
$A_\alpha^{\circ 5}$	$A_\alpha^{\circ 5}$	$A_\alpha^{\circ 6}$	$A_\alpha^{\circ 7}$	$A_\alpha^{\circ 8}$	$A_\alpha^{\circ 9}$	$A_\alpha^{\circ 10}$	$A_\alpha^{\circ 11}$	$A_\alpha^{\circ 12}$	$A_\alpha^{\circ 13}$	$A_\alpha^{\circ 0}$	$A_\alpha^{\circ 1}$	$A_\alpha^{\circ 2}$	$A_\alpha^{\circ 3}$	$A_\alpha^{\circ 4}$
$A_\alpha^{\circ 6}$	$A_\alpha^{\circ 6}$	$A_\alpha^{\circ 7}$	$A_\alpha^{\circ 8}$	$A_\alpha^{\circ 9}$	$A_\alpha^{\circ 10}$	$A_\alpha^{\circ 11}$	$A_\alpha^{\circ 12}$	$A_\alpha^{\circ 13}$	$A_\alpha^{\circ 0}$	$A_\alpha^{\circ 1}$	$A_\alpha^{\circ 2}$	$A_\alpha^{\circ 3}$	$A_\alpha^{\circ 4}$	$A_\alpha^{\circ 5}$
$A_\alpha^{\circ 7}$	$A_\alpha^{\circ 7}$	$A_\alpha^{\circ 8}$	$A_\alpha^{\circ 9}$	$A_\alpha^{\circ 10}$	$A_\alpha^{\circ 11}$	$A_\alpha^{\circ 12}$	$A_\alpha^{\circ 13}$	$A_\alpha^{\circ 0}$	$A_\alpha^{\circ 1}$	$A_\alpha^{\circ 2}$	$A_\alpha^{\circ 3}$	$A_\alpha^{\circ 4}$	$A_\alpha^{\circ 5}$	$A_\alpha^{\circ 6}$
$A_\alpha^{\circ 8}$	$A_\alpha^{\circ 8}$	$A_\alpha^{\circ 9}$	$A_\alpha^{\circ 10}$	$A_\alpha^{\circ 11}$	$A_\alpha^{\circ 12}$	$A_\alpha^{\circ 13}$	$A_\alpha^{\circ 0}$	$A_\alpha^{\circ 1}$	$A_\alpha^{\circ 2}$	$A_\alpha^{\circ 3}$	$A_\alpha^{\circ 4}$	$A_\alpha^{\circ 5}$	$A_\alpha^{\circ 6}$	$A_\alpha^{\circ 7}$
$A_\alpha^{\circ 9}$	$A_\alpha^{\circ 9}$	$A_\alpha^{\circ 10}$	$A_\alpha^{\circ 11}$	$A_\alpha^{\circ 12}$	$A_\alpha^{\circ 13}$	$A_\alpha^{\circ 0}$	$A_\alpha^{\circ 1}$	$A_\alpha^{\circ 2}$	$A_\alpha^{\circ 3}$	$A_\alpha^{\circ 4}$	$A_\alpha^{\circ 5}$	$A_\alpha^{\circ 6}$	$A_\alpha^{\circ 7}$	$A_\alpha^{\circ 8}$
$A_\alpha^{\circ 10}$	$A_\alpha^{\circ 10}$	$A_\alpha^{\circ 11}$	$A_\alpha^{\circ 12}$	$A_\alpha^{\circ 13}$	$A_\alpha^{\circ 0}$	$A_\alpha^{\circ 1}$	$A_\alpha^{\circ 2}$	$A_\alpha^{\circ 3}$	$A_\alpha^{\circ 4}$	$A_\alpha^{\circ 5}$	$A_\alpha^{\circ 6}$	$A_\alpha^{\circ 7}$	$A_\alpha^{\circ 8}$	$A_\alpha^{\circ 9}$
$A_\alpha^{\circ 11}$	$A_\alpha^{\circ 11}$	$A_\alpha^{\circ 12}$	$A_\alpha^{\circ 13}$	$A_\alpha^{\circ 0}$	$A_\alpha^{\circ 1}$	$A_\alpha^{\circ 2}$	$A_\alpha^{\circ 3}$	$A_\alpha^{\circ 4}$	$A_\alpha^{\circ 5}$	$A_\alpha^{\circ 6}$	$A_\alpha^{\circ 7}$	$A_\alpha^{\circ 8}$	$A_\alpha^{\circ 9}$	$A_\alpha^{\circ 10}$
$A_\alpha^{\circ 12}$	$A_\alpha^{\circ 12}$	$A_\alpha^{\circ 13}$	$A_\alpha^{\circ 0}$	$A_\alpha^{\circ 1}$	$A_\alpha^{\circ 2}$	$A_\alpha^{\circ 3}$	$A_\alpha^{\circ 4}$	$A_\alpha^{\circ 5}$	$A_\alpha^{\circ 6}$	$A_\alpha^{\circ 7}$	$A_\alpha^{\circ 8}$	$A_\alpha^{\circ 9}$	$A_\alpha^{\circ 10}$	$A_\alpha^{\circ 11}$
$A_\alpha^{\circ 13}$	$A_\alpha^{\circ 13}$	$A_\alpha^{\circ 0}$	$A_\alpha^{\circ 1}$	$A_\alpha^{\circ 2}$	$A_\alpha^{\circ 3}$	$A_\alpha^{\circ 4}$	$A_\alpha^{\circ 5}$	$A_\alpha^{\circ 6}$	$A_\alpha^{\circ 7}$	$A_\alpha^{\circ 8}$	$A_\alpha^{\circ 9}$	$A_\alpha^{\circ 10}$	$A_\alpha^{\circ 11}$	$A_\alpha^{\circ 12}$

It is worth mentioning that the Corollary 1 allows generating groups of fractional operators under other operations. For example, considering the following operation

$$A_\alpha^{\circ r} * A_\alpha^{\circ s} = A_\alpha^{\circ rs}, \tag{43}$$

it is feasible to obtain the following corollaries:

Corollary 2. *Let $\mathbb{M}_n$ be the set of positive residual classes corresponding to the coprimes less than a positive integer n. Therefore, for each fractional operator $o_x^\alpha \in {}_m\mathrm{MO}_{x,\alpha}^{\infty,u}(h)$, it is feasible to define the following Abelian group of fractional matrix operators under the operation (43):*

$${}_m\mathrm{G}^*(A_\alpha(o_x^\alpha), \mathbb{M}_n) := \left\{ A_\alpha^{\circ r} = A_\alpha(o_x^{r\alpha}) \,:\, r \in \mathbb{M}_n \;\; and \;\; A_\alpha^{\circ r} = \left([A_\alpha^{\circ r}]_{jk} \right) := (o_k^{r\alpha}) \right\}. \tag{44}$$

Example 2. *Let o_x^α be a fractional operator such that $o_x^\alpha \in {}_m\mathrm{MO}_{x,\alpha}^{\infty,u}(h)$. Therefore, considering the set $\mathbb{M}_{14}$, it is feasible to define, under the operation (43), the following Abelian group of fractional matrix operators*

$${}_m\mathrm{G}^*(A_\alpha(o_x^\alpha), \mathbb{M}_{14}) = \left\{ A_\alpha^{\circ 1}, A_\alpha^{\circ 3}, A_\alpha^{\circ 5}, A_\alpha^{\circ 9}, A_\alpha^{\circ 11}, A_\alpha^{\circ 13} \right\}. \tag{45}$$

Furthermore, all possible combinations of the elements of the group are summarized in the following Cayley table:

$*$	$A_\alpha^{\circ 1}$	$A_\alpha^{\circ 3}$	$A_\alpha^{\circ 5}$	$A_\alpha^{\circ 9}$	$A_\alpha^{\circ 11}$	$A_\alpha^{\circ 13}$
$A_\alpha^{\circ 1}$	$A_\alpha^{\circ 1}$	$A_\alpha^{\circ 3}$	$A_\alpha^{\circ 5}$	$A_\alpha^{\circ 9}$	$A_\alpha^{\circ 11}$	$A_\alpha^{\circ 13}$
$A_\alpha^{\circ 3}$	$A_\alpha^{\circ 3}$	$A_\alpha^{\circ 9}$	$A_\alpha^{\circ 1}$	$A_\alpha^{\circ 13}$	$A_\alpha^{\circ 5}$	$A_\alpha^{\circ 11}$
$A_\alpha^{\circ 5}$	$A_\alpha^{\circ 5}$	$A_\alpha^{\circ 1}$	$A_\alpha^{\circ 11}$	$A_\alpha^{\circ 3}$	$A_\alpha^{\circ 13}$	$A_\alpha^{\circ 9}$
$A_\alpha^{\circ 9}$	$A_\alpha^{\circ 9}$	$A_\alpha^{\circ 13}$	$A_\alpha^{\circ 3}$	$A_\alpha^{\circ 11}$	$A_\alpha^{\circ 1}$	$A_\alpha^{\circ 5}$
$A_\alpha^{\circ 11}$	$A_\alpha^{\circ 11}$	$A_\alpha^{\circ 5}$	$A_\alpha^{\circ 13}$	$A_\alpha^{\circ 1}$	$A_\alpha^{\circ 9}$	$A_\alpha^{\circ 3}$
$A_\alpha^{\circ 13}$	$A_\alpha^{\circ 13}$	$A_\alpha^{\circ 11}$	$A_\alpha^{\circ 9}$	$A_\alpha^{\circ 5}$	$A_\alpha^{\circ 3}$	$A_\alpha^{\circ 1}$

Corollary 3. *Let $\mathbb{Z}_p^+$ be the set of positive residual classes less than p, with p a prime number. Therefore, for each fractional operator $o_x^\alpha \in {}_m\mathrm{MO}_{x,\alpha}^{\infty,u}(h)$, it is feasible to define the following Abelian group of fractional matrix operators under the operation (43):*

$$ {}_m\mathrm{G}^*\left(A_\alpha(o_x^\alpha), \mathbb{Z}_p^+\right) := \left\{ A_\alpha^{\circ r} = A_\alpha(o_x^{r\alpha}) \ : \ r \in \mathbb{Z}_p^+ \ \text{ and } \ A_\alpha^{\circ r} = \left([A_\alpha^{\circ r}]_{jk} \right) := (o_k^{r\alpha}) \right\}. \quad (46) $$

Example 3. *Let o_x^α be a fractional operator such that $o_x^\alpha \in {}_m\mathrm{MO}_{x,\alpha}^{\infty,u}(h)$. Therefore, considering the set $\mathbb{Z}_{13}^+$, it is feasible to define, under the operation (43), the following Abelian group of fractional matrix operators*

$$ {}_m\mathrm{G}^*\left(A_\alpha(o_x^\alpha), \mathbb{Z}_{13}^+\right) = \left\{ A_\alpha^{\circ 1}, A_\alpha^{\circ 2}, A_\alpha^{\circ 3}, A_\alpha^{\circ 4}, A_\alpha^{\circ 5}, A_\alpha^{\circ 6}, A_\alpha^{\circ 7}, A_\alpha^{\circ 8}, A_\alpha^{\circ 9}, A_\alpha^{\circ 10}, A_\alpha^{\circ 11}, A_\alpha^{\circ 12} \right\}. \quad (47) $$

Furthermore, all possible combinations of the elements of the group are summarized in the following Cayley table:

$*$	$A_\alpha^{\circ 1}$	$A_\alpha^{\circ 2}$	$A_\alpha^{\circ 3}$	$A_\alpha^{\circ 4}$	$A_\alpha^{\circ 5}$	$A_\alpha^{\circ 6}$	$A_\alpha^{\circ 7}$	$A_\alpha^{\circ 8}$	$A_\alpha^{\circ 9}$	$A_\alpha^{\circ 10}$	$A_\alpha^{\circ 11}$	$A_\alpha^{\circ 12}$
$A_\alpha^{\circ 1}$	$A_\alpha^{\circ 1}$	$A_\alpha^{\circ 2}$	$A_\alpha^{\circ 3}$	$A_\alpha^{\circ 4}$	$A_\alpha^{\circ 5}$	$A_\alpha^{\circ 6}$	$A_\alpha^{\circ 7}$	$A_\alpha^{\circ 8}$	$A_\alpha^{\circ 9}$	$A_\alpha^{\circ 10}$	$A_\alpha^{\circ 11}$	$A_\alpha^{\circ 12}$
$A_\alpha^{\circ 2}$	$A_\alpha^{\circ 2}$	$A_\alpha^{\circ 4}$	$A_\alpha^{\circ 6}$	$A_\alpha^{\circ 8}$	$A_\alpha^{\circ 10}$	$A_\alpha^{\circ 12}$	$A_\alpha^{\circ 1}$	$A_\alpha^{\circ 3}$	$A_\alpha^{\circ 5}$	$A_\alpha^{\circ 7}$	$A_\alpha^{\circ 9}$	$A_\alpha^{\circ 11}$
$A_\alpha^{\circ 3}$	$A_\alpha^{\circ 3}$	$A_\alpha^{\circ 6}$	$A_\alpha^{\circ 9}$	$A_\alpha^{\circ 12}$	$A_\alpha^{\circ 2}$	$A_\alpha^{\circ 5}$	$A_\alpha^{\circ 8}$	$A_\alpha^{\circ 11}$	$A_\alpha^{\circ 1}$	$A_\alpha^{\circ 4}$	$A_\alpha^{\circ 7}$	$A_\alpha^{\circ 10}$
$A_\alpha^{\circ 4}$	$A_\alpha^{\circ 4}$	$A_\alpha^{\circ 8}$	$A_\alpha^{\circ 12}$	$A_\alpha^{\circ 3}$	$A_\alpha^{\circ 7}$	$A_\alpha^{\circ 11}$	$A_\alpha^{\circ 2}$	$A_\alpha^{\circ 6}$	$A_\alpha^{\circ 10}$	$A_\alpha^{\circ 1}$	$A_\alpha^{\circ 5}$	$A_\alpha^{\circ 9}$
$A_\alpha^{\circ 5}$	$A_\alpha^{\circ 5}$	$A_\alpha^{\circ 10}$	$A_\alpha^{\circ 2}$	$A_\alpha^{\circ 7}$	$A_\alpha^{\circ 12}$	$A_\alpha^{\circ 4}$	$A_\alpha^{\circ 9}$	$A_\alpha^{\circ 1}$	$A_\alpha^{\circ 6}$	$A_\alpha^{\circ 11}$	$A_\alpha^{\circ 3}$	$A_\alpha^{\circ 8}$
$A_\alpha^{\circ 6}$	$A_\alpha^{\circ 6}$	$A_\alpha^{\circ 12}$	$A_\alpha^{\circ 5}$	$A_\alpha^{\circ 11}$	$A_\alpha^{\circ 4}$	$A_\alpha^{\circ 10}$	$A_\alpha^{\circ 3}$	$A_\alpha^{\circ 9}$	$A_\alpha^{\circ 2}$	$A_\alpha^{\circ 8}$	$A_\alpha^{\circ 1}$	$A_\alpha^{\circ 7}$
$A_\alpha^{\circ 7}$	$A_\alpha^{\circ 7}$	$A_\alpha^{\circ 1}$	$A_\alpha^{\circ 8}$	$A_\alpha^{\circ 2}$	$A_\alpha^{\circ 9}$	$A_\alpha^{\circ 3}$	$A_\alpha^{\circ 10}$	$A_\alpha^{\circ 4}$	$A_\alpha^{\circ 11}$	$A_\alpha^{\circ 5}$	$A_\alpha^{\circ 12}$	$A_\alpha^{\circ 6}$
$A_\alpha^{\circ 8}$	$A_\alpha^{\circ 8}$	$A_\alpha^{\circ 3}$	$A_\alpha^{\circ 11}$	$A_\alpha^{\circ 6}$	$A_\alpha^{\circ 1}$	$A_\alpha^{\circ 9}$	$A_\alpha^{\circ 4}$	$A_\alpha^{\circ 12}$	$A_\alpha^{\circ 7}$	$A_\alpha^{\circ 2}$	$A_\alpha^{\circ 10}$	$A_\alpha^{\circ 5}$
$A_\alpha^{\circ 9}$	$A_\alpha^{\circ 9}$	$A_\alpha^{\circ 5}$	$A_\alpha^{\circ 1}$	$A_\alpha^{\circ 10}$	$A_\alpha^{\circ 6}$	$A_\alpha^{\circ 2}$	$A_\alpha^{\circ 11}$	$A_\alpha^{\circ 7}$	$A_\alpha^{\circ 3}$	$A_\alpha^{\circ 12}$	$A_\alpha^{\circ 8}$	$A_\alpha^{\circ 4}$
$A_\alpha^{\circ 10}$	$A_\alpha^{\circ 10}$	$A_\alpha^{\circ 7}$	$A_\alpha^{\circ 4}$	$A_\alpha^{\circ 1}$	$A_\alpha^{\circ 11}$	$A_\alpha^{\circ 8}$	$A_\alpha^{\circ 5}$	$A_\alpha^{\circ 2}$	$A_\alpha^{\circ 12}$	$A_\alpha^{\circ 9}$	$A_\alpha^{\circ 6}$	$A_\alpha^{\circ 3}$
$A_\alpha^{\circ 11}$	$A_\alpha^{\circ 11}$	$A_\alpha^{\circ 9}$	$A_\alpha^{\circ 7}$	$A_\alpha^{\circ 5}$	$A_\alpha^{\circ 3}$	$A_\alpha^{\circ 1}$	$A_\alpha^{\circ 12}$	$A_\alpha^{\circ 10}$	$A_\alpha^{\circ 8}$	$A_\alpha^{\circ 6}$	$A_\alpha^{\circ 4}$	$A_\alpha^{\circ 2}$
$A_\alpha^{\circ 12}$	$A_\alpha^{\circ 12}$	$A_\alpha^{\circ 11}$	$A_\alpha^{\circ 10}$	$A_\alpha^{\circ 9}$	$A_\alpha^{\circ 8}$	$A_\alpha^{\circ 7}$	$A_\alpha^{\circ 6}$	$A_\alpha^{\circ 5}$	$A_\alpha^{\circ 4}$	$A_\alpha^{\circ 3}$	$A_\alpha^{\circ 2}$	$A_\alpha^{\circ 1}$

Finally, it should be noted that when n is a prime number, the following result is obtained:

$$ {}_m\mathrm{G}^*(A_\alpha(o_x^\alpha), \mathbb{M}_n) = {}_m\mathrm{G}^*\left(A_\alpha(o_x^\alpha), \mathbb{Z}_n^+\right). \quad (48) $$

4. Conclusions

Although this article presents one way to define groups of fractional operators using sets related to the set of integer numbers, it would be feasible to extend the results using

other sets of numbers that allow defining Abelian groups, as is the case of the set of rational numbers and the set of real numbers, being feasible to define the following groups:

$$ {}_{m}\mathrm{G}(A_{\alpha}(o_{x}^{\alpha}),\mathbb{Q}) \quad \text{and} \quad {}_{m}\mathrm{G}(A_{\alpha}(o_{x}^{\alpha}),\mathbb{R}). \tag{49} $$

Furthermore, from the groups generated by the equation (30), it is feasible define the following group of fractional matrix operators [42,44]:

$$ {}_{m}\mathrm{G}_{FIM}(\alpha) := \bigcup_{o_{x}^{\alpha}\in_{m}\mathrm{MO}_{x,\alpha}^{\circ_{0},\mu}(h)} {}_{m}\mathrm{G}(A_{\alpha}(o_{x}^{\alpha})), \tag{50} $$

in which it is assumed that through combinations of the horizontal and vertical type of the modified Hadamard product given by the equation (29), the fractional operators are reduced to their minimum expression, allowing to obtain $\forall A_{i,\alpha}^{\circ p}, A_{j,\alpha}^{\circ q}, A_{j,\alpha}^{\circ r} \in {}_{m}\mathrm{G}_{FIM}(\alpha)$, with $i \neq j$, the following result:

$$ \left(A_{i,\alpha}^{\circ p}\circ A_{j,\alpha}^{\circ q}\right)\circ A_{j,\alpha}^{\circ r} = A_{i,\alpha}^{\circ p}\circ\left(A_{j,\alpha}^{\circ q}\circ A_{j,\alpha}^{\circ r}\right) = A_{k,\alpha}^{\circ 1} := A_{k,\alpha}\left(o_{i,x}^{p\alpha}\circ o_{j,x}^{(q+r)\alpha}\right), \quad p,q,r\in\mathbb{Z}\setminus\{0\}. \tag{51} $$

As a consequence, the following result is obtained:

$$ \forall A_{k,\alpha}^{\circ 1}\in {}_{m}\mathrm{G}_{FIM}(\alpha) \text{ such that } A_{k,\alpha}\left(o_{k,x}^{\alpha}\right) = A_{k,\alpha}\left(o_{i,x}^{p\alpha}\circ o_{j,x}^{q\alpha}\right) \exists A_{k,\alpha}^{\circ r} = A_{k,\alpha}^{\circ(r-1)}\circ A_{k,\alpha}^{\circ 1} = A_{k,\alpha}\left(o_{i,x}^{rp\alpha}\circ o_{j,x}^{rq\alpha}\right). \tag{52} $$

Therefore, if Φ_{FIM} denotes the iteration function of some fractional iterative method [43,44], it is feasible to obtain the following result:

$$ \text{Let } \alpha_{0}\in\mathbb{R}\setminus\mathbb{Z} \Rightarrow \forall A_{\alpha_{0}}^{\circ 1}\in {}_{m}\mathrm{G}_{FIM}(\alpha) \ \exists\Phi_{FIM}=\Phi_{FIM}(A_{\alpha_{0}}) \ \therefore \ \forall A_{\alpha_{0}} \ \exists\{\Phi_{FIM}(A_{\alpha}) \ : \ \alpha\in\mathbb{R}\setminus\mathbb{Z}\}. \tag{53} $$

Finally, it is worth mentioning that it is feasible to develop more complex algebraic structures of fractional operators using the presented results. For example, without loss of generality, considering the modified Hadamard product (29) and the operation (43), a commutative and unitary ring of fractional operators may be defined as follows

$$ {}_{m}\mathrm{R}(A_{\alpha}(o_{x}^{\alpha}),\mathbb{R}) := ({}_{m}\mathrm{G}(A_{\alpha}(o_{x}^{\alpha}),\mathbb{R}),\circ,*), \tag{54} $$

in which it is not difficult to verify the following properties:

1. The pair $({}_{m}\mathrm{G}(A_{\alpha}(o_{x}^{\alpha}),\mathbb{R}),\circ)$ is an Abelian group.
2. The pair $({}_{m}\mathrm{G}(A_{\alpha}(o_{x}^{\alpha}),\mathbb{R}),*)$ is a commutative monoid.
3. $\forall A_{\alpha}^{\circ p}, A_{\alpha}^{\circ q}, A_{\alpha}^{\circ r}\in {}_{m}\mathrm{R}(A_{\alpha}(o_{x}^{\alpha}),\mathbb{R})$, the operation $*$ is distributive with respect to the operation $\circ$, that is,

$$ \begin{cases} A_{\alpha}^{\circ p} * \left(A_{\alpha}^{\circ q}\circ A_{\alpha}^{\circ r}\right) = \left(A_{\alpha}^{\circ p} * A_{\alpha}^{\circ q}\right)\circ\left(A_{\alpha}^{\circ p} * A_{\alpha}^{\circ r}\right) \\ \left(A_{\alpha}^{\circ p}\circ A_{\alpha}^{\circ q}\right) * A_{\alpha}^{\circ r} = \left(A_{\alpha}^{\circ p} * A_{\alpha}^{\circ r}\right)\circ\left(A_{\alpha}^{\circ q} * A_{\alpha}^{\circ r}\right) \end{cases}. \tag{55} $$

Author Contributions: Conceptualization, Methodology, Formal Analysis, Investigation, Writing—Original Draft Preparation, Writing—Review and Editing, A.T.-H.; Formal Analysis, Validation, Supervision, Project Administration, F.B.-P. and R.R.-M. All authors have read and agreed to the published version of the manuscript.

Funding: This research received no external funding.

Conflicts of Interest: The authors declare no conflict of interest.

References

1. Miller, K.S.; Ross, B. *An Introduction to the Fractional Calculus and Fractional Differential Equations*; Wiley-Interscience: Hoboken, NJ, USA, 1993; pp. 1–125.
2. Hilfer, R. *Applications of Fractional Calculus in Physics*; World Scientific Publishing Co. Pte. Ltd.: Singapore, 2000; pp. 3–73.
3. Oldham, K.; Spanier, J. *The Fractional Calculus Theory and Applications of Differentiation and Integration to Arbitrary Order*; Elsevier: Amsterdam, The Netherlands, 1974; Volume 111, pp. 25–121.
4. Kilbas, A.; Srivastava, H.; Trujillo, J. *Theory and Applications of Fractional Differential Equations*; Elsevier: Amsterdam, The Netherlands, 2006; pp. 69–132.
5. De Oliveira, E.C.; Tenreiro Machado, J.A. A review of definitions for fractional derivatives and integral. *Math. Probl. Eng.* **2014**, *2014*, 238459. [CrossRef]
6. Teodoro, G.S.; Machado, J.T.; De Oliveira, E.C. A review of definitions of fractional derivatives and other operators. *J. Comput. Phys.* **2019**, *388*, 195–208. [CrossRef]
7. Valério, D.; Ortigueira, M.D.; Lopes, A.M. How Many Fractional Derivatives Are There? *Mathematics* **2022**, *10*, 737. [CrossRef]
8. Safdari-Vaighani, A.; Heryudono, A.; Larsson, E. A radial basis function partition of unity collocation method for convection–diffusion equations arising in financial applications. *J. Sci. Comput.* **2015**, *64*, 341–367. [CrossRef]
9. Torres-Hernandez, A.; Brambila-Paz, F.; Torres-Martínez, C. Numerical solution using radial basis functions for multidimensional fractional partial differential equations of type Black–Scholes. *Comput. Appl. Math.* **2021**, *40*, 245. [CrossRef]
10. Traore, A.; Sene, N. Model of economic growth in the context of fractional derivative. *Alex. Eng. J.* **2020**, *59*, 4843–4850. [CrossRef]
11. Tejado, I.; Pérez, E.; Valério, D. Fractional calculus in economic growth modelling of the group of seven. *Fract. Calc. Appl. Anal.* **2019**, *22*, 139–157. [CrossRef]
12. Guariglia, E. Fractional calculus, zeta functions and Shannon entropy. *Open Math.* **2021**, *19*, 87–100. [CrossRef]
13. Torres-Henandez, A.; Brambila-Paz, F. An Approximation to Zeros of the Riemann Zeta Function Using Fractional Calculus. *Math. Stat.* **2021**, *9*, 309–318. [CrossRef]
14. De-la Vega, E.; Torres-Hernandez, A.; Rodrigo, P.M.; Brambila-Paz, F. Fractional derivative-based performance analysis of hybrid thermoelectric generator-concentrator photovoltaic system. *Appl. Therm. Eng.* **2021**, *193*, 116984. [CrossRef]
15. Torres-Hernandez, A.; Brambila-Paz, F.; Rodrigo, P.M.; De-la-Vega, E. Reduction of a nonlinear system and its numerical solution using a fractional iterative method. *J. Math. Stat. Sci.* **2020**, *6*, 285–299.
16. Erfanifar, R.; Sayevand, K.; Esmaeili, H. On modified two-step iterative method in the fractional sense: Some applications in real world phenomena. *Int. J. Comput. Math.* **2020**, *97*, 2109–2141. [CrossRef]
17. Cordero, A.; Girona, I.; Torregrosa, J.R. A variant of chebyshev's method with 3αth-order of convergence by using fractional derivatives. *Symmetry* **2019**, *11*, 1017. [CrossRef]
18. Gdawiec, K.; Kotarski, W.; Lisowska, A. Newton's method with fractional derivatives and various iteration processes via visual analysis. *Numer. Algorithms* **2021**, *86*, 953–1010. [CrossRef]
19. Gdawiec, K.; Kotarski, W.; Lisowska, A. Visual analysis of the Newton's method with fractional order derivatives. *Symmetry* **2019**, *11*, 1143. [CrossRef]
20. Akgül, A.; Cordero, A.; Torregrosa, J.R. A fractional Newton method with 2αth-order of convergence and its stability. *Appl. Math. Lett.* **2019**, *98*, 344–351. [CrossRef]
21. Torres-Hernandez, A.; Brambila-Paz, F. Fractional Newton-Raphson Method. *Appl. Math. Sci. Int. J. (MathSJ)* **2021**, *8*, 1–13. [CrossRef]
22. Torres-Hernandez, A.; Brambila-Paz, F.; Iturrarán-Viveros, U.; Caballero-Cruz, R. Fractional Newton-Raphson Method Accelerated with Aitken's Method. *Axioms* **2021**, *10*, 47. [CrossRef]
23. Torres-Hernandez, A.; Brambila-Paz, F.; De-la-Vega, E. Fractional Newton-Raphson Method and Some Variants for the Solution of Nonlinear Systems. *Appl. Math. Sci. Int. J. (MathSJ)* **2020**, *7*, 13–27. [CrossRef]
24. Candelario, G.; Cordero, A.; Torregrosa, J.R. Multipoint Fractional Iterative Methods with (2α+ 1) th-Order of Convergence for Solving Nonlinear Problems. *Mathematics* **2020**, *8*, 452. [CrossRef]
25. Candelario, G.; Cordero, A.; Torregrosa, J.R.; Vassileva, M.P. An optimal and low computational cost fractional Newton-type method for solving nonlinear equations. *Appl. Math. Lett.* **2022**, *124*, 107650. [CrossRef]
26. Osler, T.J. Leibniz rule for fractional derivatives generalized and an application to infinite series. *SIAM J. Appl. Math.* **1970**, *18*, 658–674. [CrossRef]
27. Almeida, R. A Caputo fractional derivative of a function with respect to another function. *Commun. Nonlinear Sci. Numer. Simul.* **2017**, *44*, 460–481. [CrossRef]
28. Fu, H.; Wu, G.C.; Yang, G.; Huang, L.L. Continuous time random walk to a general fractional Fokker–Planck equation on fractal media. *Eur. Phys. J. Spec. Top.* **2021**, *230*, 3927–3933. [CrossRef]
29. Fan, Q.; Wu, G.C.; Fu, H. A note on function space and boundedness of the general fractional integral in continuous time random walk. *J. Nonlinear Math. Phys.* **2022**, *29*, 95–102. [CrossRef]
30. Abu-Shady, M.; Kaabar, M.K. A Generalized Definition of the Fractional Derivative with Applications. *Math. Probl. Eng.* **2021**, *2021*, 9444803. [CrossRef]
31. Saad, K.M. New fractional derivative with non-singular kernel for deriving Legendre spectral collocation method. *Alex. Eng. J.* **2020**, *59*, 1909–1917. [CrossRef]

32. Rahmat, M.R.S. A new definition of conformable fractional derivative on arbitrary time scales. *Adv. Differ. Equ.* **2019**, *2019*, 354. [CrossRef]
33. Sousa, J.V.d.C.; De Oliveira, E.C. On the ψ-Hilfer fractional derivative. *Commun. Nonlinear Sci. Numer. Simul.* **2018**, *60*, 72–91. [CrossRef]
34. Jarad, F.; Uğurlu, E.; Abdeljawad, T.; Baleanu, D. On a new class of fractional operators. *Adv. Differ. Equ.* **2017**, *2017*, 247. [CrossRef]
35. Atangana, A.; Gómez-Aguilar, J. A new derivative with normal distribution kernel: Theory, methods and applications. *Phys. A Stat. Mech. Appl.* **2017**, *476*, 1–14. [CrossRef]
36. Yavuz, M.; Özdemir, N. Comparing the new fractional derivative operators involving exponential and Mittag-Leffler kernel. *Discret. Contin. Dyn. Syst.-S* **2020**, *13*, 995. [CrossRef]
37. Liu, J.G.; Yang, X.J.; Feng, Y.Y.; Cui, P. New fractional derivative with sigmoid function as the kernel and its models. *Chin. J. Phys.* **2020**, *68*, 533–541. [CrossRef]
38. Yang, X.J.; Machado, J.T. A new fractional operator of variable order: Application in the description of anomalous diffusion. *Phys. A Stat. Mech. Its Appl.* **2017**, *481*, 276–283. [CrossRef]
39. Atangana, A. On the new fractional derivative and application to nonlinear Fisher's reaction–diffusion equation. *Appl. Math. Comput.* **2016**, *273*, 948–956. [CrossRef]
40. He, J.H.; Li, Z.B.; Wang, Q.L. A new fractional derivative and its application to explanation of polar bear hairs. *J. King Saud Univ.-Sci.* **2016**, *28*, 190–192. [CrossRef]
41. Sene, N. Fractional diffusion equation with new fractional operator. *Alex. Eng. J.* **2020**, *59*, 2921–2926. [CrossRef]
42. Torres-Hernandez, A.; Brambila-Paz, F. Sets of Fractional Operators and Numerical Estimation of the Order of Convergence of a Family of Fractional Fixed-Point Methods. *Fractal Fract.* **2021**, *5*, 240. [CrossRef]
43. Torres-Hernandez, A.; Brambila-Paz, F.; Montufar-Chaveznava, R. Acceleration of the order of convergence of a family of fractional fixed point methods and its implementation in the solution of a nonlinear algebraic system related to hybrid solar receivers. *Appl. Math. Comput.* **2022**, *429*, 127231. [CrossRef]
44. Torres-Hernandez, A. Code of a multidimensional fractional quasi-Newton method with an order of convergence at least quadratic using recursive programming. *Appl. Math. Sci. Int. J. (MathSJ)* **2022**, *9*, 17–24. [CrossRef]

MDPI
St. Alban-Anlage 66
4052 Basel
Switzerland
Tel. +41 61 683 77 34
Fax +41 61 302 89 18
www.mdpi.com

Computer Sciences & Mathematics Forum Editorial Office
E-mail: csmf@mdpi.com
www.mdpi.com/journal/csmf

MDPI
St. Alban-Anlage 66
4052 Basel
Switzerland

Tel: +41 61 683 77 34

www.mdpi.com

ISBN 978-3-0365-6695-5